JET PROPULSION LABORATORY
CALIFORNIA INSTITUTE OF TECHNOLOGY
PASADENA, CALIFORNIA

SE/68-009(2)

RESEARCH DEVELOPMENT & MANAGEMENT CONSULTANTS

UNSYMMETRICAL LARGE DEFLECTIONS OF EXPULSION DEVICES

Tasks 1 and 2

FINAL REPORT

FEBRUARY 1970

PREPARED FOR:

NATIONAL AERONAUTICS AND SPACE ADMINISTRATION
NASA PASADENA OFFICE
PASADENA, CALIFORNIA

PREPARED BY:

SYSTEMS EXPLORATION, INCORPORATED
3687 VOLTAIRE STREET
SAN DIEGO, CALIFORNIA 92106

SYSTEMS EXPLORATION, INC.

Report No. SE/68-D009(2)

UNSYMMETRICAL LARGE DEFLECTIONS OF EXPULSION DEVICES

TASKS 1 AND 2 REPORT

February 1970

G. A. Hegemier

S. Menat-Nasser

Prepared For

National Aeronautics and Space Administration
NASA Pasadena Office
Pasadena, California

Prepared By

SYSTEMS EXPLORATION, INC.
3687 Voltaire Street
San Diego, California 92106

TABLE OF CONTENTS

PREFACE

The work to be described herein constitutes the final report on NASA Contract NAS7-712 entitled: "Unsymmetrical Large Deflections of Expulsion Devices." The purpose of this effort was to 1) provide a qualitative assessment of various bladder-type propellant expulsion devices of current design and 2) to indicate the proper course for future studies leading to an improvement of the fatigue life and efficiency of such devices.

The text of this report is divided into four chapters. The basic problem definition, evaluation of current solution methods, conclusions and recommendations are included in Chapter I which is primarily descriptive. Detailed analytical calculation, deemed inecessary to support many of the statements in Chapter I, are included in Chapter II through IV.

As a program-management aid, a flow chart describing the major research phases considered under the present contract, as well as recommended future research, is included as Fig. P.1.

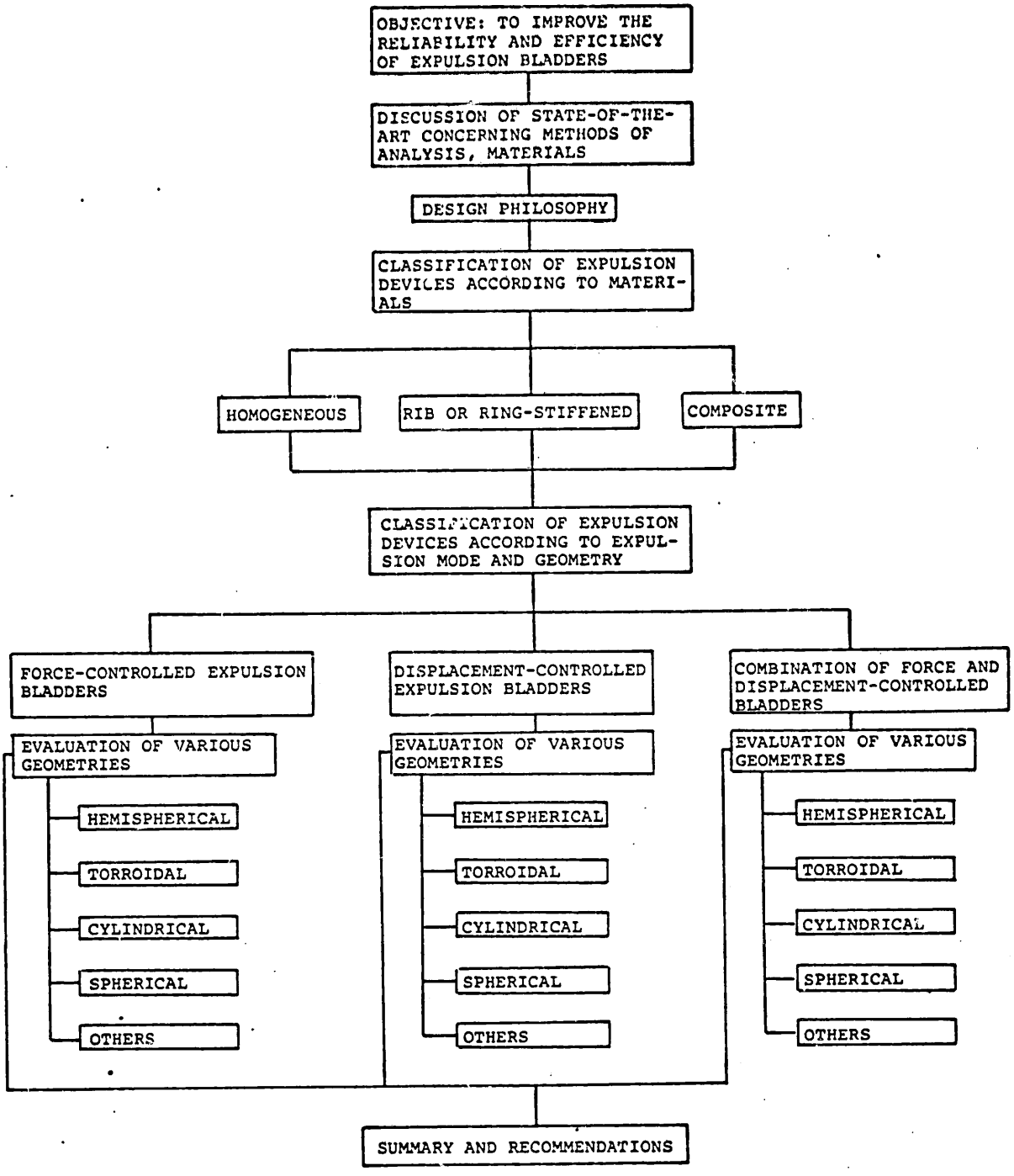

Figure P.1 Research Flow Chart for the Study of Expulsion Bladders

CHAPTER I

GENERAL DISCUSSION AND RECOMMENDATIONS

1.1 Discussion of the State-of-the-Art

The problem of designing a bladder expulsion device may be stated as follows: to maximize the "efficiency" of the device subject to such constraints as a required fatigue or cycle life, chemical inertness to the propellant, permeability of the bladder to the propellant and pressurant, storability under service conditions, and stability under flight and launch environments. The present study focuses attention on the structural aspects of this design problem, namely the fatigue or cycle life of bladder expulsion devices.

An accurate assessment of the cycle life of a bladder depends, in turn, upon the accuracy of the calculated strains and stresses of the bladder at each material point. The prediction of the topology of a collapsing bladder, however, constitutes one of the most difficult problems in Applied Mechanics. Therefore, let us review briefly what can be expected in terms of a dependable analysis of bladder deformation.

1.1.1 Analysis of Single Folds

The analysis of single folds is certainly within the present state-of-the-art. Both analytical and numerical approaches are applicable to certain classes of problems. In this connection the results obtained by Rocketdyne [1] are representative of the

strains and stresses due to an initial single folding. For a complete analysis of a single fold, one must consider: a) folding, b) unfolding, c) pure bi-axial extension, and finally d) refolding. Analytical study of such a deformation-cycle is certainly possible and should be undertaken. Such a study must include the strain hardening phenomenon for metallic bladders. The analysis presented by Rocketdyne [1], while relevant and useful, involves only the initial folding part of the complete deformation-cycle mentioned above.

To be of practical relevance, such a theoretical study should be accompanied by appropriate experiments on flat sheets, consisting of the proposed bladder materials, subject to the above mentioned deformation-cycles.

1.1.2 Double Folds and Pointing

It appears that all bladder deformations can be classified into a) single folds, b) multi-legged* folds without pointing, c) multi-legged folds with pointing (this will be referred to as "pointing"), and d) double folds. While, in a collapsing bladder,

* This refers to the case of two or more single folds intersecting at a point.

the first two types of folds occur by necessity, the occurrence of the last two types should be minimized by a judicious design.

The analysis of the double fold and/or pointing represents a problem of enormous proportions. The complications arise from a number of sources. First, since plastic deformations generally accompany pointing and double folding in metallic bladders, the strains in the material at any instant are functions of the previous strain history as well as the given load. Second, the topology of a nonsymmetrically collapsing bladder depends, to a large extent, on small irregularities in the initial (unloaded) geometry of the bladder. Since such irregularities are random in character--especially after the first cycle of deformation has taken place--the position or history of a given point or double fold may, for all practical purposes, be indeterminable. Third, double folding is usually accompanied by an instability or dramatic wrinkling of the inner surface of the fold, the result of which is an effective inner radius which may be of a much smaller order than the thickness of the bladder. In this respect the problem is a three-dimensional one, i.e., conventional shell theory is not applicable to regions in the vicinity of the fold. The magnitude of the problem can be better appreciated by recalling that the buckling and post buckling behavior of such a seemingly simple

geometry as a circular cylindrical shell dates back to Fairbairnes (1850), yet today the post buckling behavior of a cylinder cannot be adequately predicted [2].

In view of the foregoing difficulties, it should be absolutely clear that any expectation of a rigorous analysis of the nonsymmetric deformation of a collapsing bladder, with pointing and/or double folds, by either analytical or numerical means is entirely unrealistic.

In passing, it should be noted that the isometric mappings of the ASTRO Research Corporation [3] and Rocketdyne [1] appear quite useless in terms of both qualitative and quantitative information, since the equations governing isometric mappings of most bladder geometries are nonlinear and do not admit unique solutions! Moreover, the double fold analysis presented in [1] is not reliable in view of the many ad-hoc assumptions and approximations upon which it is based, and also the dubious fatigue data that is employed.

Finally, since a rigorous analysis of double folds does not appear to be within the state-of-the-art, recourse must be made to experimental investigations of this phenomena. There are relatively easy and inexpensive tests which may be superior and more informative than ad-hoc theories. One such test may be described as follows: a flat sheet of the proposed bladder material (e.g., laminated polymer-metal composite) is subjected to a) a single fold, b) a double fold, c) unfolding, and d) bi-axial extension. The folding process and the

radii of the folds may be controlled by the use of rigid cylinders upon which sheets of each specimen are folded. The objective of such tests would be a design which involves minimum plastic deformation due to folding of the metallic part of the composite.

1.2 Design Philosophy

The topology of a collapsing bladder is such that, even under seemingly idealistic conditions of geometry and environment, one cannot, in general, obtain a design which is completely void of double folds and/or pointing. One must therefore accept the consequences of their occurrence. In view of the inability to accurately predict stresses and strains at double folds, however, it is clear that one should design to minimize their occurrence and/or their undesirable effects. In the subsequent sections, the latter point is discussed with respect to the selection of bladder materials and geometry.

1.3 Classification of Expulsion Devices According to Materials

1.3.1 Homogeneous Materials

1.3.1.1 Metals: In view of the permeability problem, it is natural to select metals as bladder materials. The consequence of double folds and/or pointing, however, are extremely serious with respect to all metals, due to the large strains experienced and the extremely low fatigue life of metals under such large strains. Further, the occurrence of double folds and/or pointing is maximized with respect to a homogeneous metal. The use of a homogeneous metallic bladder is therefore not recommended.

1.3.1.2 Non-metals: Some non-metals may be ideal with respect to fatigue life under the large strains induced by folding or pointing. As examples we note Teflon and Kel-F. The Teflon produced by E. I. du Pont de Nemours & Company (tetrafluro ethylene) has a tensile strength up to 3,500 psi, elongation of 250 to 350%, melting point 594°F, and is highly chemical-resistant. Kel-F, of the Minnesota Mining and Manufacturing Company (trifluorochloro ethylene), has a tensile strength of 5,000 psi, and is also highly chemical-resistant. Some rubbers, on the other hand, may be applicable. For example, fluorocarbon rubber

(this is a saturated fluorocarbon polymer containing 50% fluorine and is produced by the Minnesota Mining and Manufacturing Company) has a tensile strength of 3,000 psi, elongation of 600%, is heat resistant to 400°F, and is highly chemical resistant. Unfortunately, permeability can be a problem with respect to homogeneous non-metals. In this connection homogeneous materials do not appear suitable unless the permeability of such polymers as Teflon can be either tolerated or improved. Also, it should be noted that the mechanical properties of many non-metals are highly temperature-dependent.

1.3.2 Composite Materials

Composite materials consisting of suitable metals and polymers or elastomers appear to offer a possible solution to the bladder material problem. Assuming the manufacturing processes can be worked out, one particular promising candidate consists of two layers of a polymer or elastomer bonded to a very thin inner layer of metal. Here the metallic layer lies on the neutral axis of the composite, thus minimizing the strains due to folding or pointing deformations. The metallic inner layer serves a dual purpose: first, it reduces permeability, and second, it adds effective tensile strength to the bladder in resisting pure membrane-type stress. The non-metal, on the other hand, absorbs the large strains off the neutral axis. It should be noted that, in

a composite, a non-metal portion of sufficient thicknesses and flexibility should 1) reduce the occurrence of double folds, and 2) reduce the magnitude of the maximum curvatures experienced at double folds. The latter leads to a reduced strain in the metal and hence to a longer fatigue life of the bladder.

One composite which can be manufactured consists of a laminated structure (in the following sequence) of $\approx 1 \times 10^{-2}$ in. TFE (tetra fluro ethylene), $\approx .5 - 1 \times 10^{-2}$ in. FEP (fluorinated ethylene-propylene), $\approx 1 - 2 \times 10^{-3}$ aluminum foil, and $\approx 1 \times 10^{-2}$ in. FEP. An optimum design would be to add another layer of TFE into the FEP, however, in view of the necessary curing sequence and the degradation of FEP at the temperatures required to process TFE, this may prove to be a formidable manufacturing task. Means of constructing "optimal" composites should be seriously explored.

An important additional feature of the foregoing composite should be carefully noted. Following a single fold, a sandwich-type structure develops that has a very high bending resistance in comparison with that of the unfolded portion of the bladder and thus is partially "double fold-proof." For example, consider a composite consisting of two layers of polymer, each of thickness h and modulus E', bonded to a central layer of metal of thickness t and

elastic modulus E. If one assumes that t/h is small (e.g., $t/h \leq 10^{-1}$), the bending stiffness per unit length of a sheet of this composite is approximately equal to

$$E' I_1 = \frac{2}{3} E' h^3$$

(Poisson's effect is neglected). On the other hand, the bending stiffness per unit length of the same composite, now once folded, is approximately equal to

$$E' I_2 = \frac{2}{3} E' h^3 \left[8 + \left(\frac{3E}{E'}\right)\left(\frac{t}{h}\right) \right] .$$

Hence, the ratio of the bending stiffnesses of a singly folded and an unfolded sheet is

$$r = \frac{E' I_2}{E' I_1} = 8 + 3 \left(\frac{E}{E'}\right)\left(\frac{t}{h}\right) .$$

For typical composites, it can be expected that the second term on the right-hand side of the above relation will be of the same order as, or much greater than the first term.

1.3.3 Rib or Ring Stiffenners

Partial deformation control can be achieved with rib- or ring-type stiffenners. For example, as has been found in previous JPL tests, nearly axisymmetric deformation of spherical-type

bladders can be attained over a limited range of deflections by a proper choice of reinforcing rings (further remarks will be made regarding this example in Section 1.4.1.1). It should be noted, however, that whereas a suitable rib-reinforcement may minimize the occurrence of double folds and pointing, it will not appreciably affect the stress-state at a double fold. Folding and pointing are local phenomena, i.e., they may occur between the reinforcing ribs. Hence, a design which is based solely upon rib-reinforcement for completely preventing folding and pointing may not be reliable. It appears that the optimum bladder material, both from the structural and permeability points of view, may be a rib-reinforced composite of metal and polymer or elastomer.

1.4 Classification of Expulsion Devices According to Expulsion Mode and Geometry

Expulsion modes may be classified as force-controlled, displacement-controlled, and a combination of force and displacement-controlled. The advantages and the disadvantages of the first two classes are briefly discussed below.

1.4.1 Force-Controlled Expulsion Bladders

Here the deformation is governed by the material composition, geometry, and a judicious use of rib-reinforcements. A common device of this type is the hemispherical bladder. Since much attention has been devoted to this geometry in the past (e.g., the Rocketdyne report [1] and numerous JPL laboratory tests), let us consider this example in more detail.

The Spherical Bladder -- What's Wrong With it. How can it be Improved? As an illustration, let us consider the gold-reinforced spherical bladder shown in Figs.1.1. Figure 1.1a shows that the collapse pattern of such a device, within limits, be constrained to an axisymmetric state. Hence, up to the instant that the Fig. 1.1a photograph was taken, double folds and points were largely non-existent. Notice also that the inverted part of the shell (Fig.1.1a) constitutes a shallow spherical cap. In Fig.1.1b the deformation has progressed somewhat further.

Small but definite asymmetric deformations can now be observed around the ridge of the inverted part of the structure. Notice that the undeformed section of the shell now resembles a cylinder whose characteristic buckled pattern (with or without reinforcing ribs) is diamond-like, involving considerable pointing. This pattern is seen to develop in Figs. 1.1c, d. Figures 1.1e, f illustrate the remaining portion of the collapse-cycle. Figure 1.1g shows the beginning of the inflation-cycle. Notice now the very irregular geometry, i.e., the many large and small imperfections. Figure 1.1h indicates that folding and pointing are numerous at the beginning of the second cycle due to the imperfections. Figures 1.1i,k show the collapsing part of the second cycle.

What's wrong with this design? In terms of the geometry, the flaw in the design may be explained as follows: even with rib-reinforcements, one may expect axisymmetric deformations only as long as the undeformed portion of the shell is reasonably shallow. In other words, had the shell been cut and supported along the ridge shown in Fig. 1.1b, the test quite probably would have been a success, at least for the first few cycles. A proper design, however, would be a spherical cap of optimum depth, or a modified spherical cap as illustrated in Fig. 1.2, consisting of a rib-reinforced composite of metal and polymer or elastomer. The selection of the optimum geometry, depth of the shell, spacing of the rib-reinforcements, and

finally the composite material and design constitutes a problem which should be carefully studied. The type of composite that one should use clearly depends on the geometry as well as the expulsion-mode of the bladder. For example if a hemispherical bladder is to be completely inverted, little advantage is gained by employing a composite that consists of a layer of metal placed on one side of a layer of polymer or elastomer; clearly enough, the composite should not consist of two metal layers placed one on each side of a polymer layer. In this example, a metal layer placed at the neutral axis, i.e., between two layers of polymers, appears to be a suitable design, although it may present a formidable manufacturing task. Hence, it appears that, with a judicious choice of the bladder geometry, composite material, and rib-reinforcements, a "highly double-fold-resistant" bladder may very well be a realistic design objective.

1.4.2. Displacement-Controlled Expulsion Bladder

Current thinking, in this connection centers around a displacement-controlled device which utilizes the concept of a piston-type collapsing process which may be employed in conjunction with a rib-reinforced torus, or rib-reinforced deep spherical cap. The basic idea may be described in connection with the latter geometry (spherical cap) as follows: The spheri-

cal cap is collapsed by means of a relatively rigid indentor of a suitable profile (for example, parabolic). The deformation begins at the apex of the shell, where the indentor first comes in contact with the bladder, Fig. 1.3. Subject to a distributed compressive force applied at the vicinity of the shell's apex, only a local buckling, in the form of a symmetric dimple, initiates at the apex and progresses to the other parts of the shell. By a suitable spacing of rib-reinforcements, and judicious choice of composite material, one may affect a deformation-controlled device which may quite possibly be void of double folds. In this case, the composite material mentioned at the end of Section 1.4.1 may prove to be a good design. However, the usefulness of any device of this kind should be established experimentally.

A basic disadvantage of these kinds of expulsion devices is the additional weight that is required for the supporting equipment.

1.5 A Promising Design - Analytical Considerations

It is evident that an optimal bladder design is one for which 1) the bladder geometry is selected to minimize the occurrence of double folding or pointing and 2) the material is selected to minimize the adverse effects of double folding or pointing should they occur. Regarding item 1), an important question is the following: can an axisymmetric bladder or diaphram (shell of revolution) be designed such that, under effective external pressure, it undergoes only axisymmetric deformation. By definition, such a mode of deformation would be void if double folds and pointing. It is clear that a device of this type must be rib-reinforced, and further that the ribs must be rings having the axis of symmetry of the shell as their common axis.

The proper design of the above mentioned bladder necessitates a numerical code designed to solve the following problem: predict 1) a shape of the meridional midsurface of the shell, 2) a spacing and stiffness distribution of the rings, 3) a shell thickness distribution and 4) the material properties (structural) of the composite comprising the shell, such that the shell would deform symmetrically and sequentially from ring to ring. In addition, once 1) through 4) have been accomplished, the numerical code must be capable of 5) predicting the strain history of the subsequent single folds with sufficient accuracy that an assessment of fatigue or cycle life could be made.

The construction of a numerical code to provide the information discussed above is indeed a difficult task, and the following questions immediately arise: 1) is the construction of such a code within the present state-of-the-art? ; 2) if yes, what analytical and numerical procedures should be followed? In an effort to provide sound judgements concerning the answer to questions 1), 2) above, it was found necessary to embark upon an exploratory analytical/numerical research program which was, however, outside the original scope of the present task. This research included 1) the analysis of nonlinear axisymmetric deformation of shells of revolution, and the stability of this state with respect to nonaxisymmetric perturbation; 2) the analysis of single folds in composite polymer-metallic sandwich-type materials; and 3) the derivation of differential equations for rib-reinforcements. The details of there investigations can be found in chapters II, III, and IV. Below we present our findings within the context of the posed problem.

1.5.1 General Analytical Sequence

A seemingly tractable analytical sequence for the construction of the above code is as follows:

(1) A suitable nonlinear shell theory is first selected to represent the bladder in the unbuckled (symmetric) state and states adjacent to this. External pressure is applied and the axisymmetric deformation of the baldder is obtained.

(2) The foregoing axisymmetric deformation is now given a general axisymmetric and non-axisymmetric perturbation and the equations governing these perturbations are derived from the original nonlinear shell equations. The static stability of the perturbation equations are then investigated.

Let the rings be numbered sequentially from the apex of the shell to the base. Let that section of the shell between the apex and the first ring be denoted as #1, that between the first and second rings as #2, etc. Then, according to the results of the eigen-value problem stated in item (1) above, one of the following events may take place: a) no buckling (symmetric or antisymmetric), b) global or local antisymmetric bifurcation, c) symmetric snap of a section other than #1, d) symmetric snap of section #1 only. If a) occurs, the load is increased until one of a) through c) occur. If b) occurs, the rings must be stiffened and/or closed up until no antisymmetric deformation takes place. If c) occurs a more rapid increase in ring-stiffness from section #1 up must be tried. Finally, by trial and error (preferably employing computer graphics), adjustments are made until section #1 buckles (snaps) first in an axisymmetric mode.

(3) Once section #1 snaps symmetrically, the resulting shell can be treated as a new shell. This new shell can be envisioned as a shell with a hole in place of section #1. The forces and moments at the edge of the hole then represent the action of section #1 (the snapped portion of the shell) upon the remaining part of the shell. These resultant forces and

moments must be calculated as a part of the problem.

(4) Single-fold strains due to axisymmetric snap-thru, and the corresponding resultant forces and moments are calculated.

(5) The prebuckled axisymmetric stresses and deformation of the new shell are now determined. This state is perturbed, and the stability of the perturbation equations are investigated. Again, the associated eigen-value problem will determine the buckling mode of the shell. The remaining ribs are adjusted until the #2 section snaps symmetrically at a load higher than that associated with the buckling of the #1 section, but lower than that required for either antisymmetric buckling or the axisymmetric snapping of any other section.

(6) The above process is repeated for the remaining sections of the shell.

(7) Single fold strains (due to axisymmetric snap-thru) are now determined and correlated with cycle life.

1.5.2 Numerical Details

Let us now discuss the details of constructing a numerical code to accomplish the objectives listed above. This task can be divided into the following basic areas: a) mathematical description of the bladder, b) numerical analysis of the axisymmetric state, c) stability analysis of the axisymmetric state, and d) detailed analysis of the strain due to single folds.

Item a) can be adequately accomplished in several ways. One method can be described as follows: Every axisymmetric bladder will consist of a shallow region near the apex, and a deep-shell region adjacent to this. That portion of the bladder in the vicinity of the apex can be represented by a nonlinear shallow-shell theory (e.g., Marguerer's equation). In the remaining part of the shell conical segments between ribs should serve as an adequate approximate model. The behavior of the shell in these two regions will, of course, be markedly different. In the shallow zone bending effects will be distributed throughout the entire domain; on the other hand, in the deep zone bending will be confined to edge or boundary layers adjacent to ribs. This suggests, therefore, a boundary layer analysis whereby that portion of the shell immediately adjacent to a rib is described by an appropriate single fold analysis, and that portion outside by a membrane theory, with proper matching of the two solutions.

Consider now items b) and c). Based upon the discussion under a) above, this task may be decomposed into an analysis of rib-reinforced shallow shell of revolution, an analysis of the boundary or single fold

region, and a determination of the membrane state in the deep-shell region with a matching to the edge layer. The first two items have been rather extensively investigated in the course of this study in order to determine whether or not they are within the current state-of-the-art.

Based upon a study of rib-reinforced shallow spherical caps, the details of which can be found in chapters II and IV, the response and stability of the shallow zone of a bladder can, it would appear, be adequately treated by the finite-difference method of N. C. Huang [4]. Here many meshpoints can be employed for accuracy, yet a relatively small computer core is necessary. A detailed program description covering the rib-reinforced shallow spherical cap can be found on page 46. Regarding the stability portion of this program, it would appear the technique could be extended to cover the entire bladder, once pre-buckled bladder deformation is known.

In contrast to the shallow-shell analysis, a finite-difference approach to the single-fold problem was found in Chapter III, to require a very large computer core. A description of this study and a recommended course of action will now be presented.

For a composite consisting of a thin layer of metal placed between two layers of elastomer, and undergoing folding, a good estimate of the state of stress is obtained if we use the following procedures: a) find the stress fields in the inner and outer layers of elastomer using large deformation theory of elasticity and treating the thin layer of metal as an

inextensible central sheet; b) under the bond stresses transmitted to the middle metal sheet by the elastomer, and using a plasticity theory, find the stress and strain fields in the metal layer. The assumption that the middle metal layer, in comparison with the elastomer, is inextensible can be justified on the grounds that the strains in the elastomer is by far larger than those in the metal, even when the metal undergoes plastic deformations. Moreover, such an assumption would yield a more conservative estimate of the stress-state in the elastomer as well as the bond stresses between the elastomer and metal, and hence is in the safe side. Since under a repeated loading of the type encountered in expulsion bladders, either the bond between metal and elastomer may be broken or the metal layer may fail under a cyclic plastic deformations, the analysis provides information for design against such failures.

In a single-fold, the state of deformation is plane with finite rotations as well as strains. Thus a plane-strain formulation for large rotations and strains is required. This is done in Chapter III. Because of the non-linear character of the field equations, however, their integration can be affected only numerically, using a step-by-step incremental loading. At a given step, on the other hand, one may employ: a) a finite difference scheme or b) a variational approach together with a finite-element scheme. In Chapter III, a) is fully developed, and b) is briefly discussed. Here we point out that while there exists a number of finite-element methods for solution of structural problems at large deflections (see Marcal [5] for a literature survey), these methods are not applicable to the bladder problem

which involves deformations with large strains of non-metalic materials.*

A complete formulation of plane-strain problems for general elastic materials which possess a strain-energy function, and which are isotropic in their undeformed (virgin) state is presented in Chapter III. For an incremental solution, the results are developed for small deformations superimposed on initially large deformations. A lagrangian formulation is used, and the field quantities are expressed in terms of the particle positions in the initial undeformed configuration. However, explicit expressions and transformation-equations are given for describing these field quantities in terms of the particle positions in the deformed state, i.e., Eulerian formulation. The resulting system of linear, partial differential equations and the corresponding boundary conditions are then expressed in a finite-difference form, using a central difference scheme and incorporating the corresponding difference-corrections. The correction terms are given explicitly, and may then be included by means of the matrix multiplications, yielding very accurate results.

While the finite-difference method developed in Chapter III may be used effectively to obtain the states of stress and strain in the elastomer part of the composite, the incorporation of various mixed boundary conditions may involve some difficulties. In this regard a correct and consistent finite-element approaching may prove more useful and more effective. Such a method must be based on a minimum principle, and

* For example, the latest and most advanced finite-element formulation by Felippa [6], that considers large deflections, ignores terms of the same order of magnitude as those included, and uses a constitutive law which, at best, can be applied to metals in the elastic range and at infinitesimal strains, see Chapter III for further discussion.

must include an assessment of stability and uniqueness of the solution at each increment of loading. These are briefly discussed in Section 5 of Chapter III where a complete and correct minimum principle is stated and the question of stability is discussed. This principle permits a correct formulation of a finite-element scheme for the incremental solution of folding which involves finite rotations and strains of elastomers with various constitutive relations. These formulations are not presented in this report, since it would have taken us far beyond the scope of the work. However, it is strongly recommended that such a study be further pursued.

To complete the study of single-folding of a metal-elastomer composite, an estimate of the plastic deformations of the metal sheet is also needed. While it is desirable to have a program which provides the stress and strain fields in both elastomer and metal layers simultaneously, in this study we have been contented with a conservative engineering estimate of plastic strains in the metal sheet. This is done by using the known state of stress in the elastomer, and assuming a linear variation of the stress-components across the thickness of the metal sheet. The corresponding plastic strain-increments are then given using Mises' yield condition.

1.6 Summary and Recommendations

1) It appears that bladder deformation can be classified as a) single folds, b) multi-legged folds without pointing, e) multi-legged folds with pointing, and d) double folds.

2) The analysis of single folds is within the present state-of-the-art and should be carried out in connection with the following deformation cycle: a) folding, b) unfolding, c) pure bi-axial extension and finally, d) re-folding.

3) The analysis of double folds and pointing appears not to be within the present state-of-the-art. Hence, experimental investigations of double folds should be undertaken. Early tests need not be conducted on complete bladders. In the interests of economy one may employ flat sheets of the proposed bladder material. These experiments should include the following deformation cycle: a) single folding, b) double folding, c) unfolding, and d) bi-axial extension.

4) The objective of the analyses and experiments mentioned above is a design which minimizes the undesirable effects of double folds and pointing.

5) The use of a homogeneous metallic bladder is not recommended because of the low fatigue life of metals under large strains.

6) The use of homogeneous non-metal bladders is not recommended because of their excessive permeability.

7) An optimum bladder material appears to be a layer of metal sandwiched between two layers of non-metal (polymer or elastomer).

8) The optimum bladder geometry appears to be a rib-reinforced shell of revolution.

9) The proper design of the bladder necessitates a numerical code which is capable of predicting: a) a shape of the meridianal midsurface of the shell, b) a spacing and stiffness distribution of the rings, c) a shell thickness distribution, and d) the material properties (structural) of the composite comprising the shell, such that the shell would deform symmetrically and sequentially from ring to ring. In addition, once a) through c) have been accomplished, the code must be capable of: d) predicting the strain history of the subsequent single folds with sufficient accuracy that an assessment of fatigue or cycle life could be made.

10) The construction of such a numerical code is within the present state-of-the-art.

11) It has been found that the conventional finite difference method for the solution of the single fold problem, while tractable, may not constitute the most efficient solution-technique. Further research (outside the present contract) has conclusively shown that the problem can be more advantageously approached by a finite-element scheme which utilizes the concept of small deformation superimposed upon large, and employs in each incremental loading an absolute minimum principle.

12) While a finite-difference scheme is both tractable and efficient for the stability portion of the foregoing code, it appears that a more uniform and flexible method would be to formulate the shell stability analysis in finite element form as well.

REFERENCES

1. Final Report, Improvement of Efficiency and Life of Expulsion Bladders," Prepared by Rocketdyne under Contract NAS7-506 for National Aeronautics and Space Administration. Feb. 1968.

2. Fung, Y. C. and Sechler, E. E., "Instability of Thin Elastic Shells," in Structural Mechanics edited by J. N. Goodier and N. J. Hoff, Pergamon Press, 1960, pp. 115-168.

3. Astro Research Corporation Preliminary Report No. 1, ARC-R-61, Mathematical Definition of Materials Strains During Folding of a Hemispherical Expulsion Bladder, 10 May 1962.

4. Huang, N. C., "Unsymmetrical Buckling of Thin Shallow Spherical Shells," J. Appl. Mech. 32 (1965) 323-330.

5. Marcal, P. V., "Finite-Element Analysis of Combined Problems of Nonlinear Material and Geometric Behavior," in Computational Approaches in Applied Mechanics, ASME Computer Conference (1969) 133-149.

6. Felippa, C. A., "Refined Finite Element Analysis of Linear and Nonlinear Two-Dimensional Structures," Ph.D. Thesis, University of California, Berkeley, Calif. (1966).

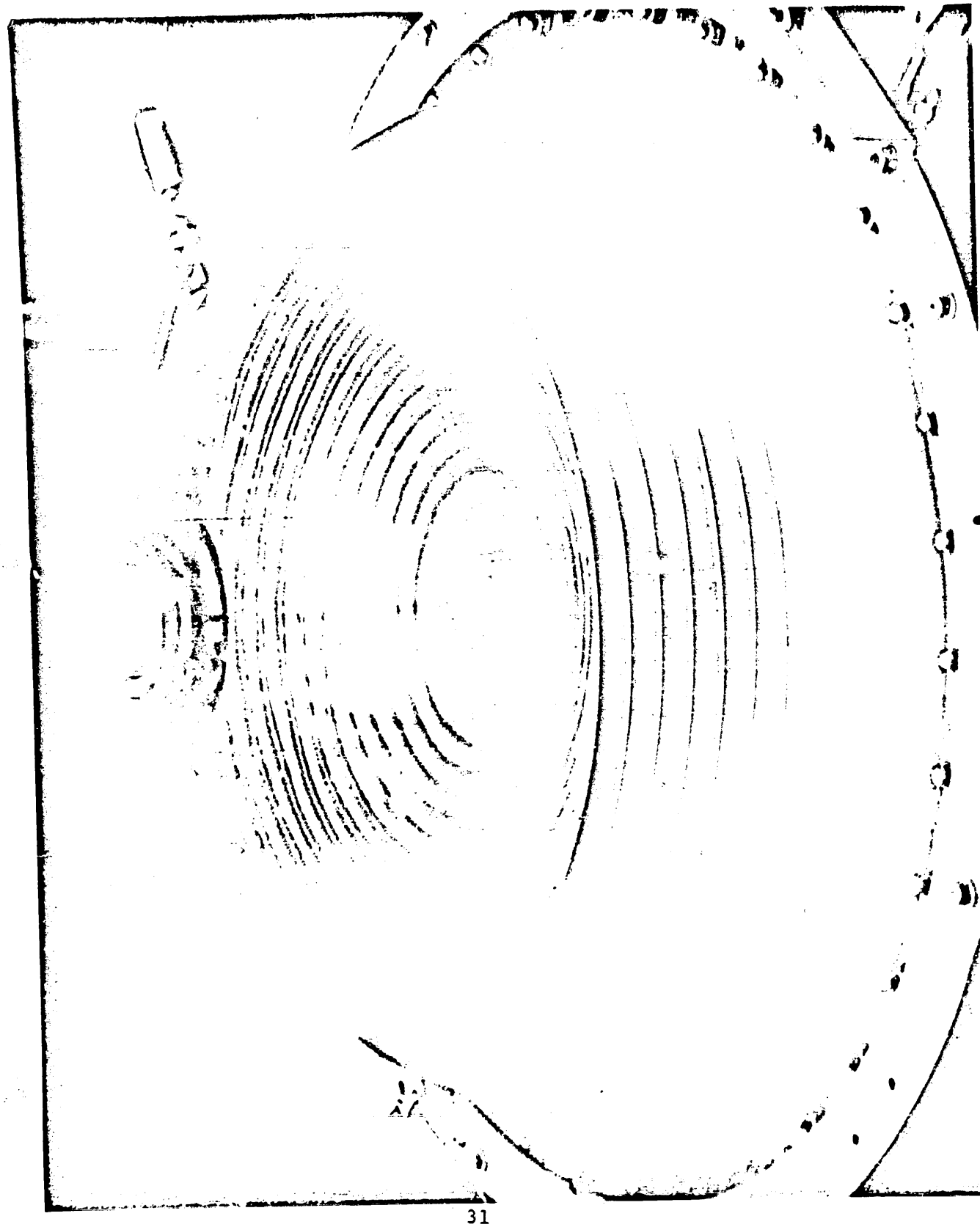

Figure 1.1a.

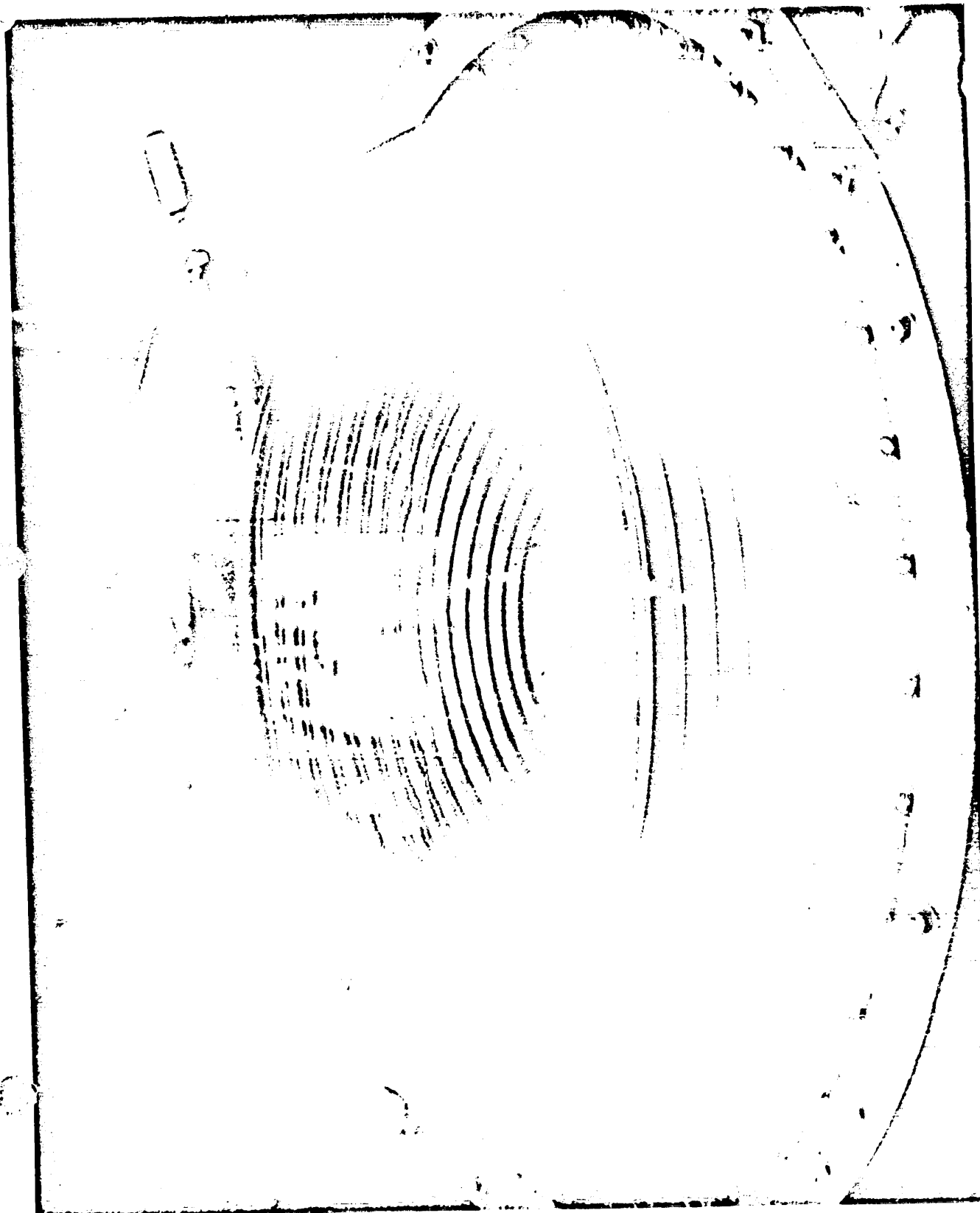

Figure 1.1b.

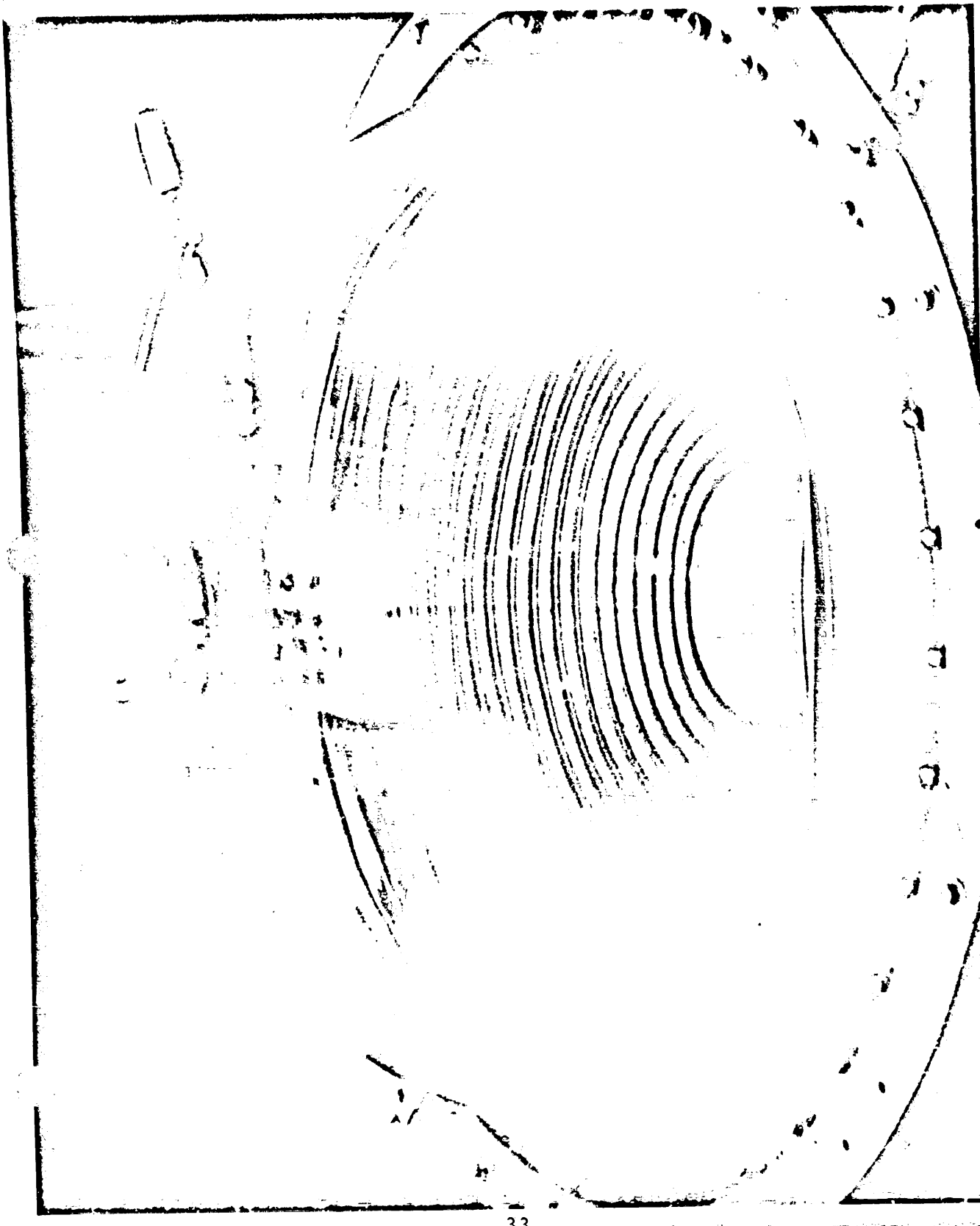

Figure 1.1c.

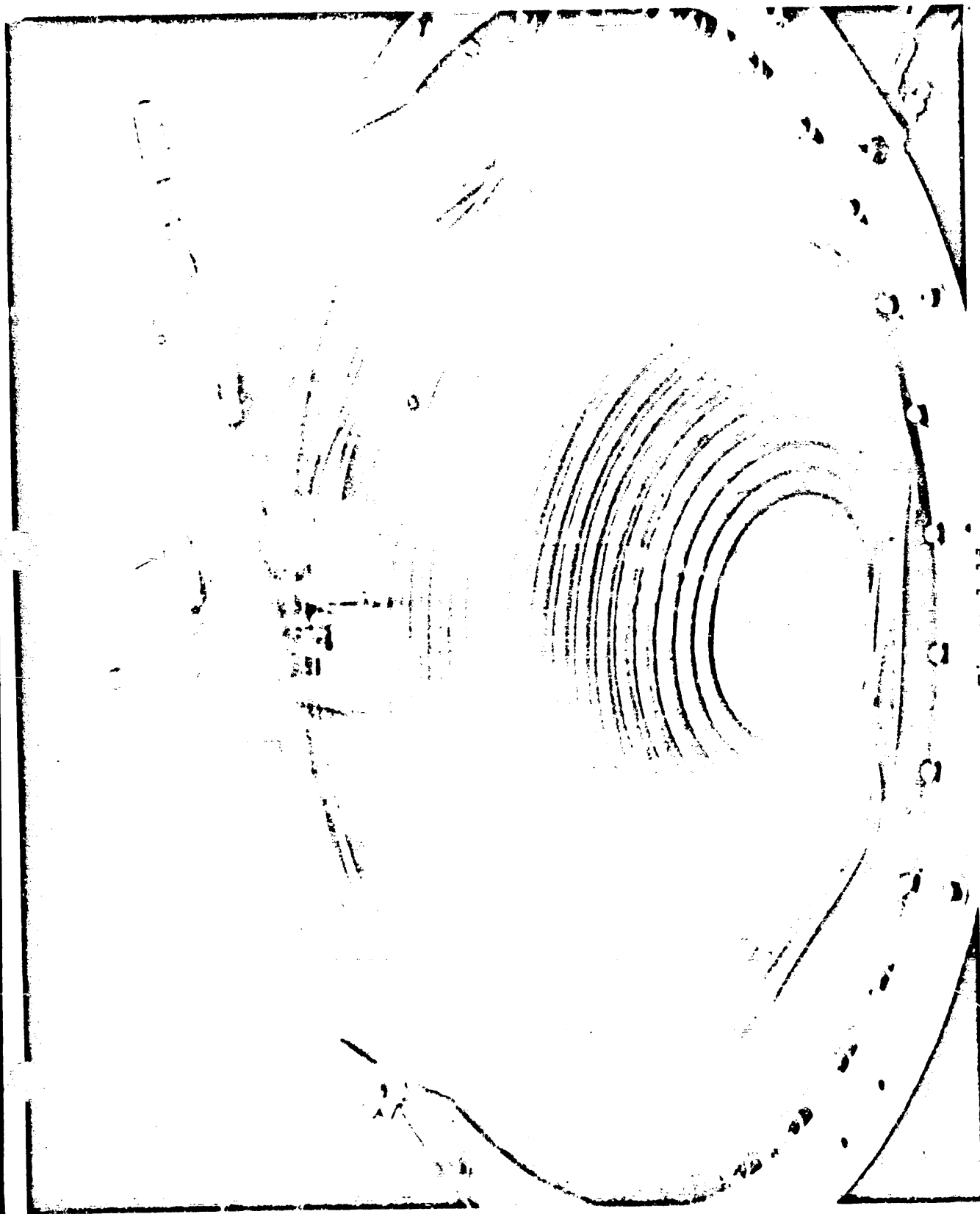

Figure 1.1d.

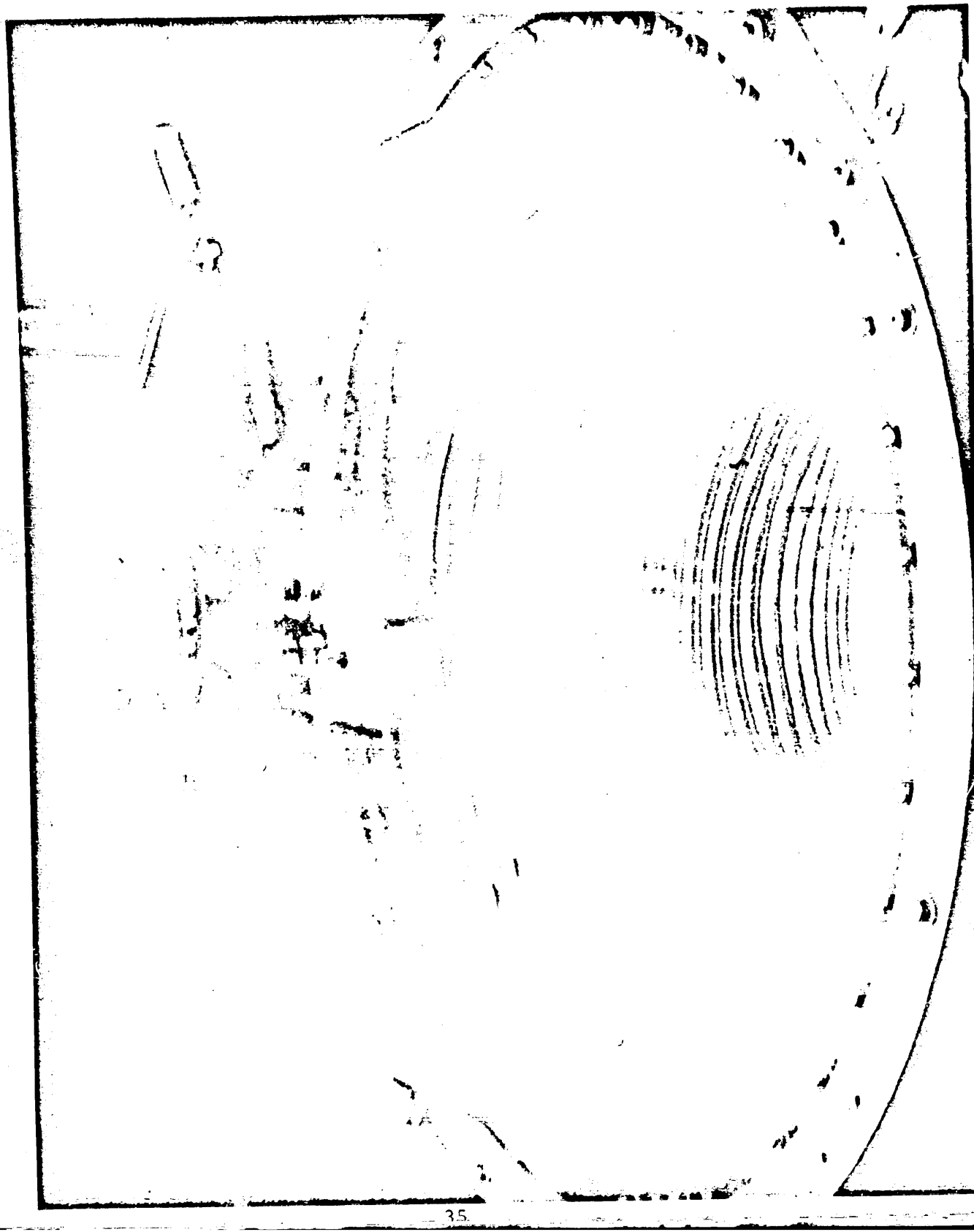

Figure 1.1e.

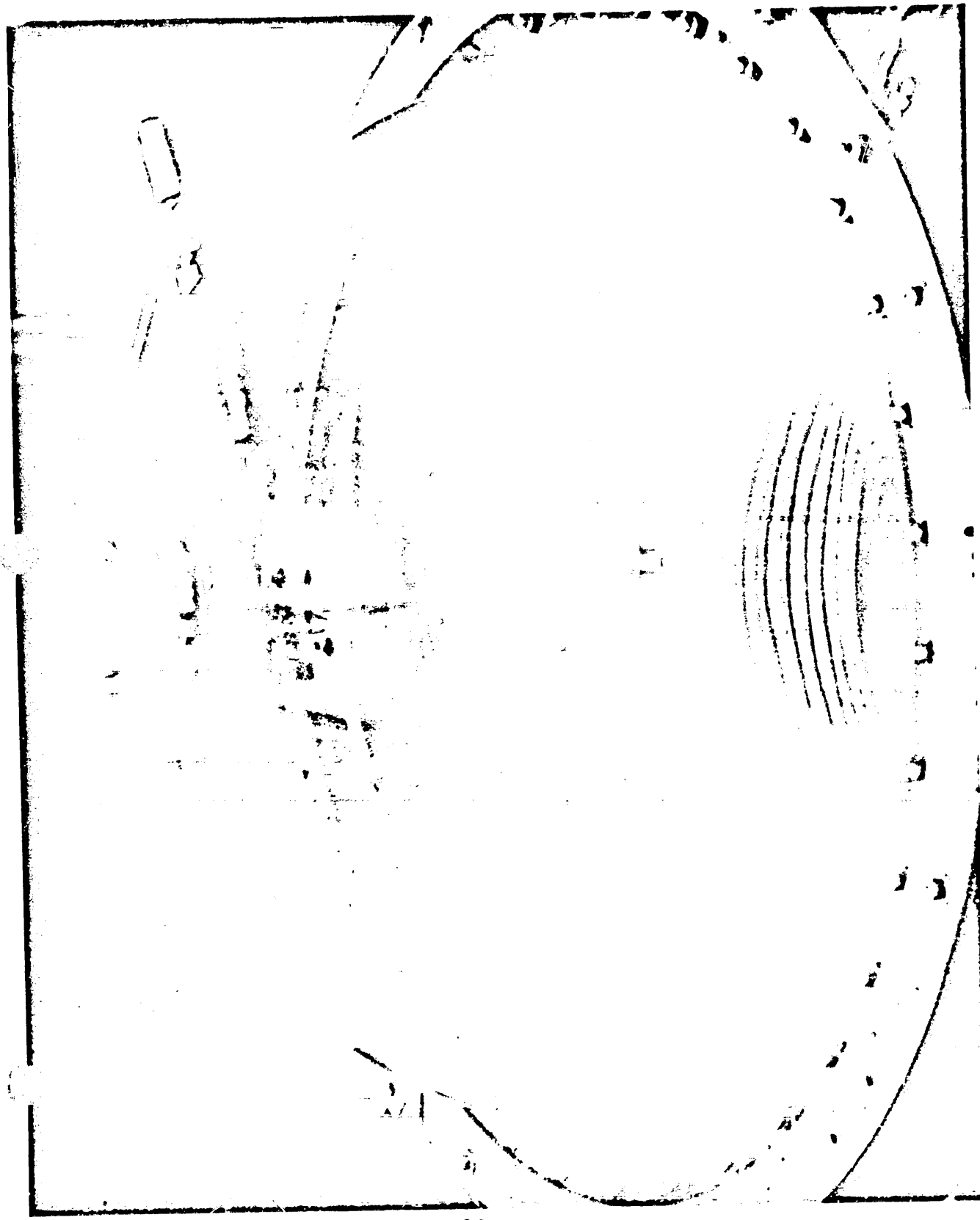

Figure 1.1f.

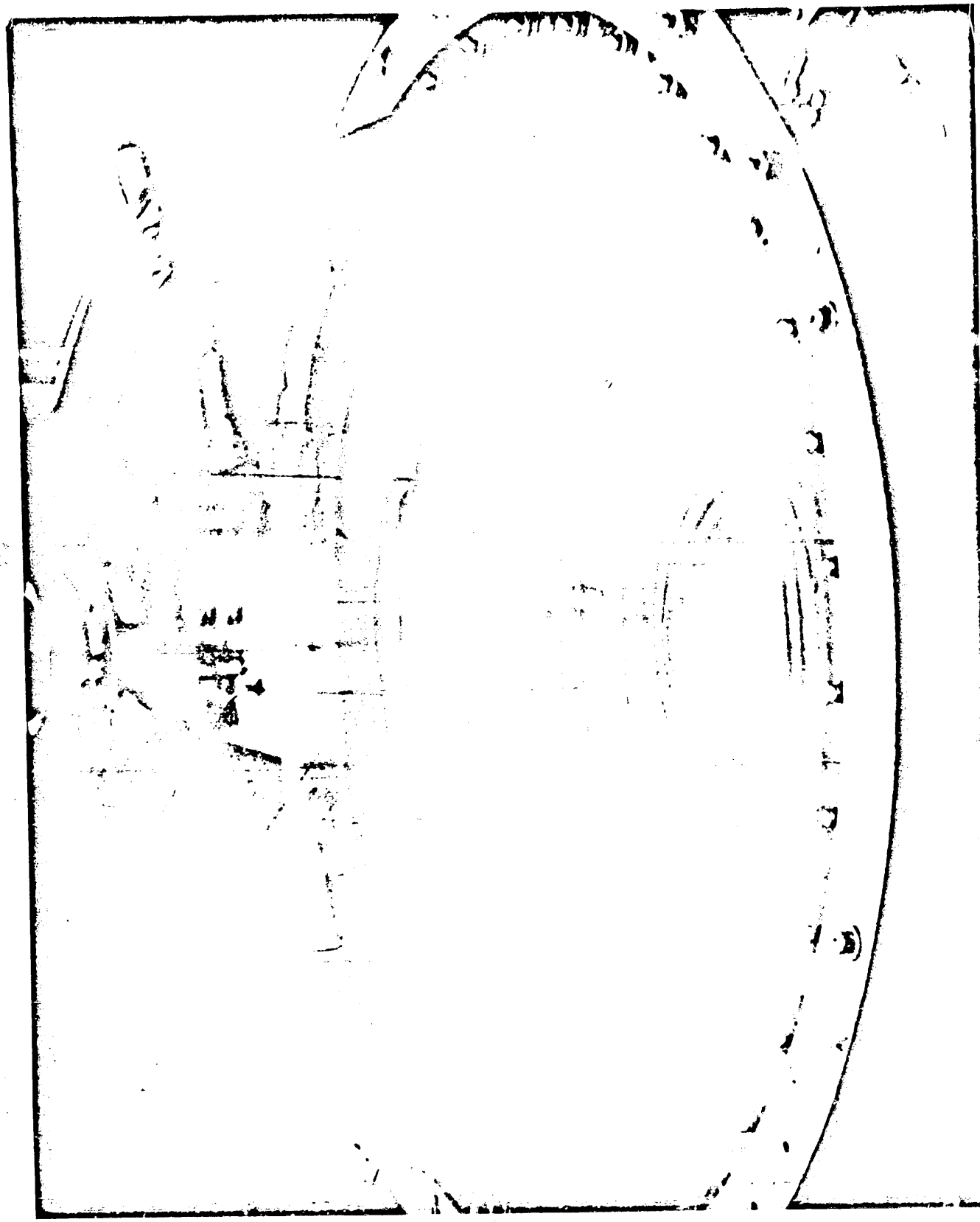

Figure 1.1g.

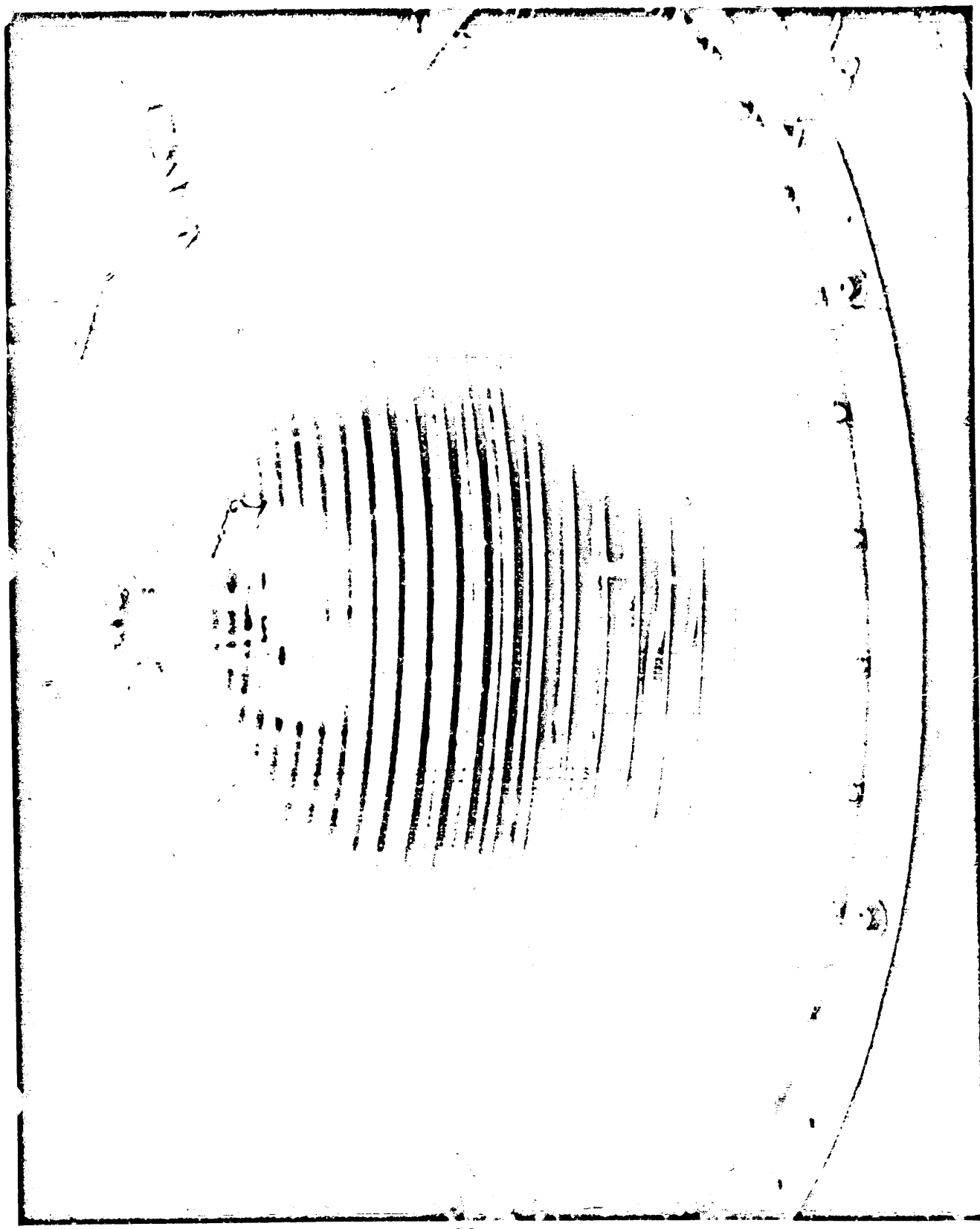

Figure 1.1h.

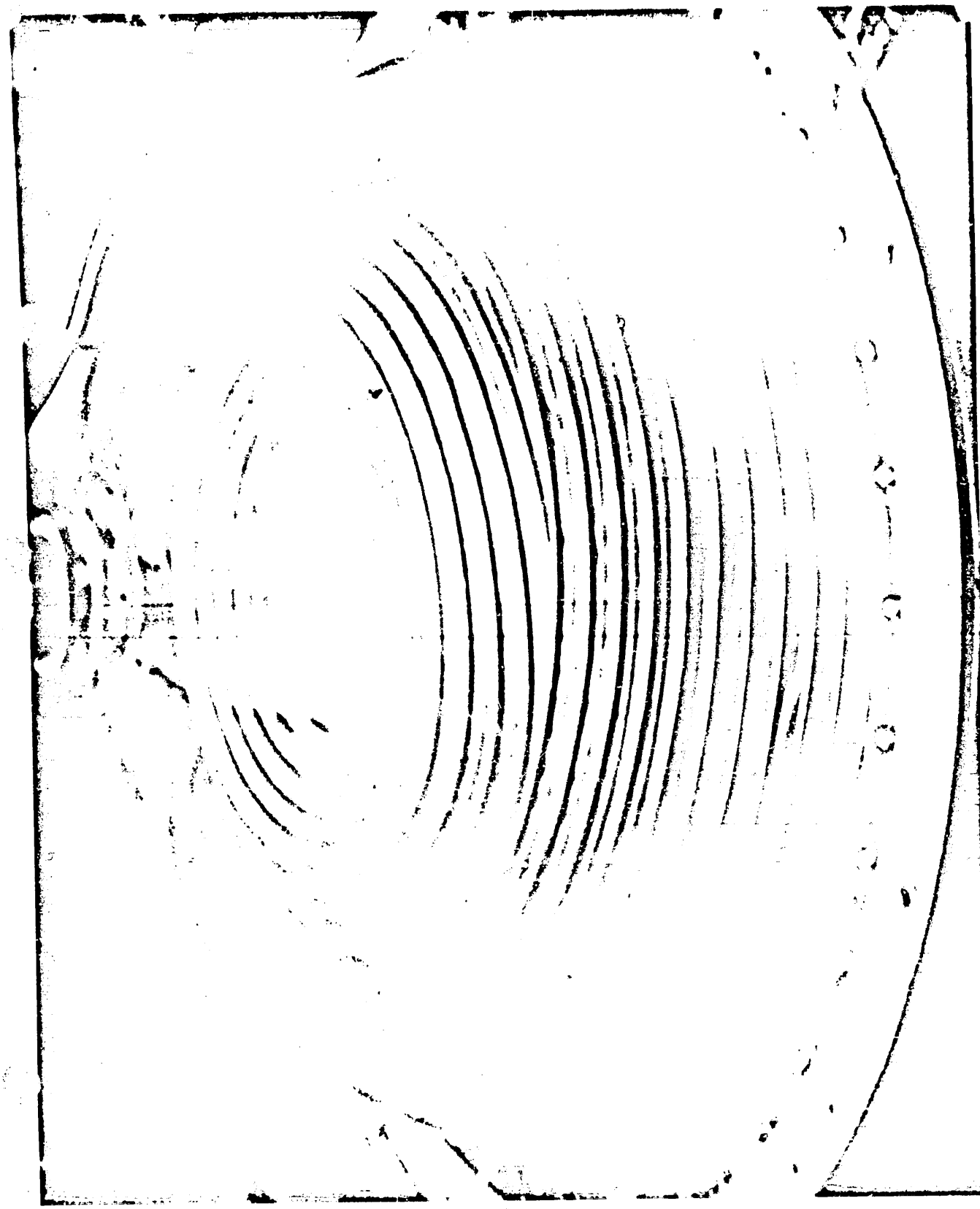

Figure 1.1i.

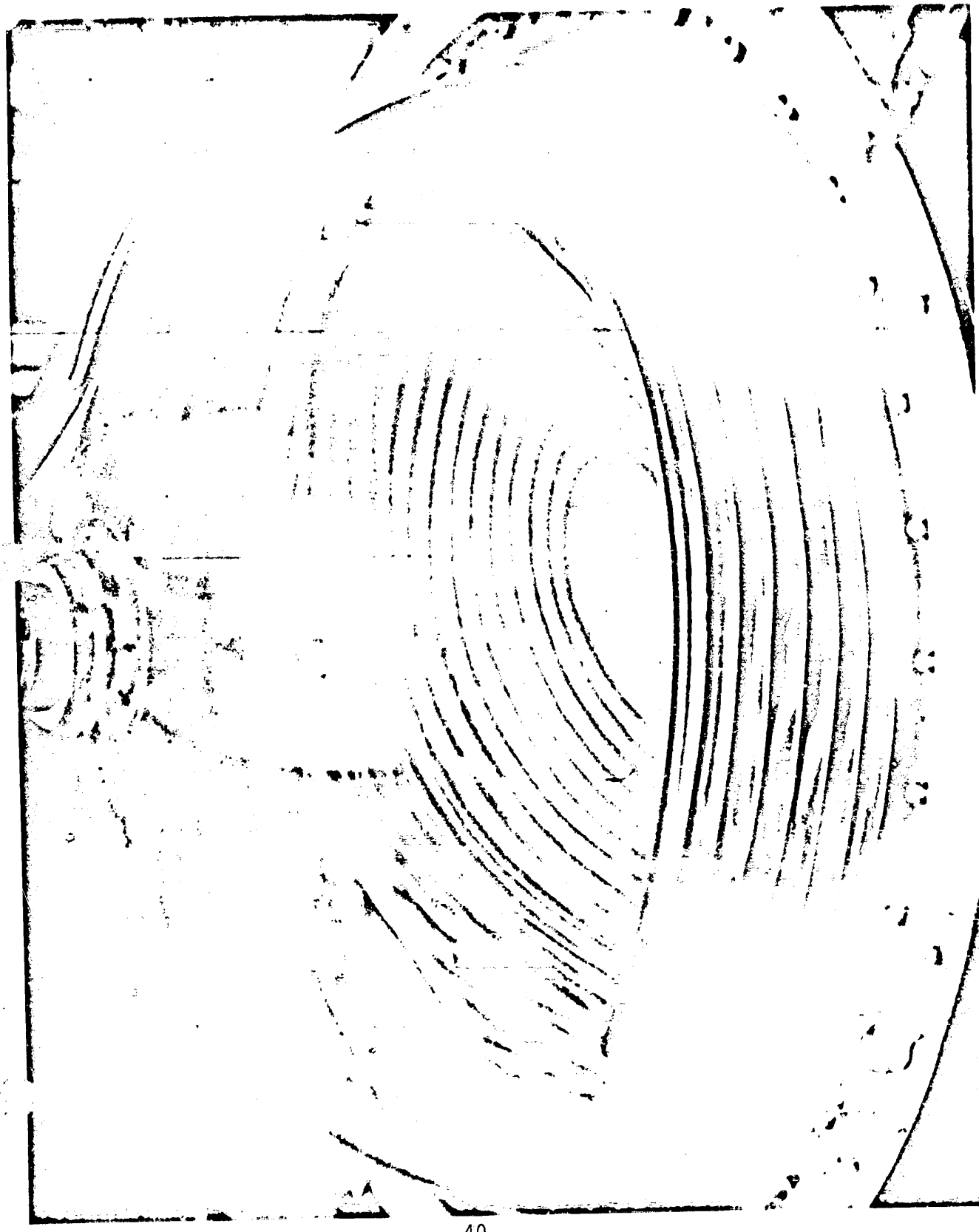

Figure 1.1j.

Figure 1.1k.

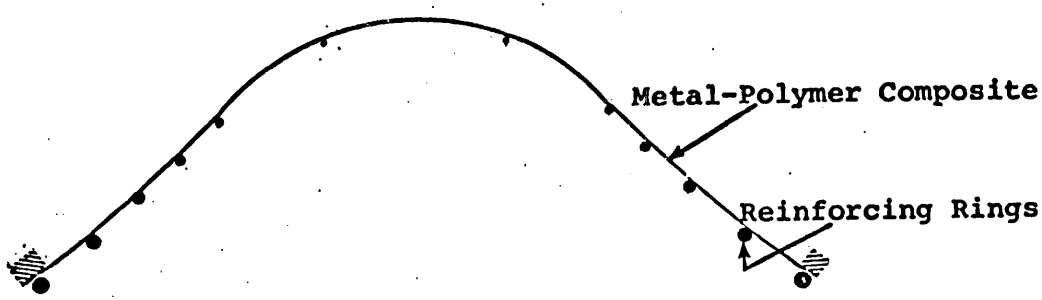

Figure 1.2 Modified Spherical Cap in Force-Controlled Explosion Mode

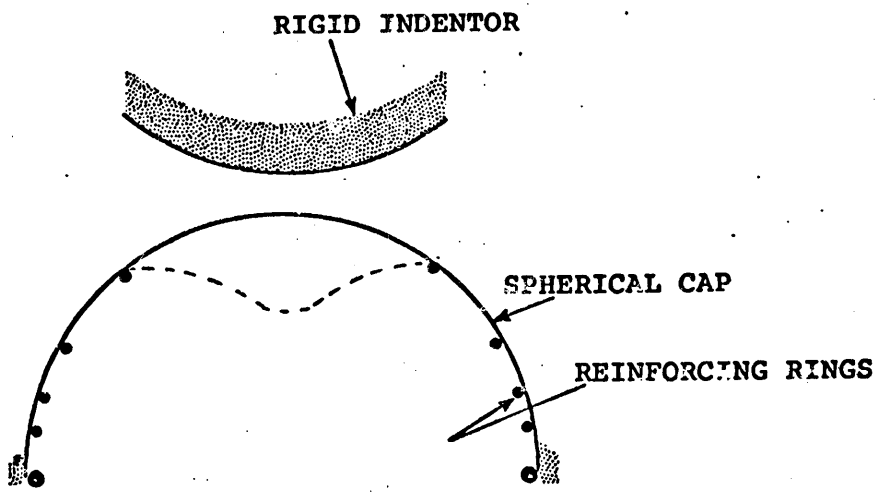

Figure 1.3 Rib-Reinforced Spherical Cap in Displacement-Controlled Explosion Mode

CHAPTER II

BLADDER DEFORMATION AND STABILITY

2.1 Introduction

As was noted in Chapter I, our basic design philosophy is to eliminate (or at least minimize) double folding and pointing through deformation control. For bladders that are shells of revolution, one promising method of obtaining deformation control is by a judicious choice of ring reinforcements (ribs). The most elementary problem of this type can be posed as follows: given a bladder (geometry and material properties), find a distribution of ring stiffness and spacing (along the shell meridian) that constrains the deformation field to be axisymmetric and sequential (ring to ring from vertex to bottom) under external pressure (expulsion), and similarly during re-cycle. A much more ambitious problem might be posed as follows: for a given fatigue (cycle) life, and external and expulsion volumes, find shell and ring geometries and material properties, and ring spacing, such that a) the deformation is axisymmetric and b) the weight of the structure is minimized.

A necessary first step in the solution of design problems of the above mentioned type is the construction of numerical programs to predict: a) nonlinear axisymmetric deformation of ring-reinforced shells of revolution under external pressure, and b) the stability of this displacement field with respect to

non-axisymmetric perturbations. For deep shells with arbitrary meridianal shape, this is indeed a difficult task.

As a beginning, and in the spirit of an exploratory investigation, let us restrict the following discussion to the more elementary case of an elastic shallow ring-reinforced spherical cap. The objective of the analysis shall be to construct a numerical scheme to predict the axisymmetric deformation of the shell, when subjected to external pressure, and the stability of this axisymmetric state with respect to non-axisymmetric perturbations.

2.2 Axisymmetric Deformation of Ring-Reinforced Spherical Caps

2.2.1 Basic Equations.

The axisymmetrical deformation of an unreinforced elastic shallow spherical shell is governed by the following two nonlinear differential equations [1]

$$(x\theta^{*\prime})' - \frac{\theta^*}{x} + x\Phi^* = -2px^2 + \theta^*\Phi^* , \qquad (2.1a)$$

$$(x\Phi^{*\prime})' - \frac{\Phi^*}{x} - x\theta^* = -\frac{1}{2}\theta^{*2} , \qquad (2.1b)$$

where x, θ^*, Φ^*, p are, respectively, the nondimensional radial coordinate, rotation, stress function and load parameter as given by N. C. Huang in [1], and $(\,)' \equiv d(\,)/dx$. For an unreinforced shell, Equations (2.1) hold for the entire shell. For reinforced shells, Equations (2.1) are valid in the region between rings, but certain continuity and jump conditions must now be imposed across each ring.

Consider, for example, a ring located at $x = x_o$. Let us assume the ring can be represented as an elastic space curve with bending and torsinal stiffnesses. Then, the requirement that the slope and the horizontal displacement of the deformed shell be continuous across $x = x_o$ yields

$$\theta^*(x_o^-) = \theta^*(x_o^+), \qquad (2.2a)$$

$$\Phi^{*\prime}(x_o^-) - \frac{\nu}{x_o}\Phi^*(x_o^-) = \Phi^{*\prime}(x_o^+) - \frac{\nu}{x_o}\Phi^*(x_o^+) . \qquad (2.2b)$$

In addition, a consideration of the relation between the radial displacement of the ring and the normal pressure reveals that

$$\tilde{N}_r\,(r_o^+) - \tilde{N}_r\,(r_o^-) = \frac{(AE)_r}{r_o^2}\,u(r_o)\,, \qquad (2.3)$$

where $\tilde{N}_r$ is the radial membrane stress in the shell, u is the radial displacement, and $(AE)_r$ is the extensional stiffness of the ring. Equation (2.3), which implies that a discontinuity in $\tilde{N}_r$ may exist across a ring, was obtained by use of the second of Equations (4.70), Chapter IV.

Similarly, if we consider the relation between the distributed twisting moment on the ring (due to ring-shell interaction) and ring twist, we obtain a further jump condition

$$\tilde{M}_r\,(r_o^+) - \tilde{M}_r\,(r_o^-) = -\frac{(EI)_r}{r_o^2}\,\frac{dw}{dr}\,(r_o)\,, \qquad (2.4)$$

where $\tilde{M}_r$ is the radial component of bending moment, w is the downward displacement of the shell, and $(EI)_r$ is the out-of-plane bending rigidity of the ring. Equation (2.4) was obtained by use of the fourth of Equations (4.70), Chapter IV.

As expressed in terms of the dimensionless quantities of [1], Equations (2.3), (2.4) become

$$\Phi^*(x_o^+) - \Phi^*(x_o^-) = c[\Phi^{*\prime}(x_o) - \frac{\nu}{x_o}\,\Phi^*(x_o)]\,, \qquad (2.5a)$$

$$\theta^{*\prime}(x_o^+) - \theta^{*\prime}(x_o^-) = \frac{b}{x_o^2}\,\theta^*(x_o)\,, \qquad (2.5b)$$

where

$$c = \frac{\lambda(AE)_r}{taE}\,, \quad b = \frac{\lambda(EI)_r}{aD}\,, \qquad (2.6)$$

$$\lambda = 2[3(1-\upsilon^2)]^{1/4} (H/t)^{1/2} ,$$

$$D = Et^3 /12(1-\upsilon^2) .$$

Here, H denotes the rise of the shell, and t, a, E, υ are the shell thickness, base radius, Young's modulus, and Poisson's ratio, respectively.

Finally, in addition to Equation (2.1) which govern the shell between rings, and the continuity and jump conditions (2.5) across any given ring, we must specify boundary conditions at the shell base. Let us assume that the bladder is fixed at the base; then the following boundary conditions must be satisfied at the boundary $x = \lambda$.

$$\theta^*(\lambda) = 0 ,$$

$$\Phi^{*\prime}(\lambda) - \frac{\nu}{\lambda} \Phi^*(\lambda) = 0 . \qquad (2.7)$$

2.2.2 Solution Method.

For a given p, the quantities θ^*, Φ^* can be determined numerically. To begin, let us define

$$f = -2px + \theta^*\Phi^* ,$$

$$g = (1/2)\theta^{*2} , \qquad (2.8)$$

and select a finite difference mesh along x with increment h. If we set

$$x = x_i = (i-1)h , \quad \theta_i^* = \theta^*(x_i) ,$$

$$\Phi_i^* = \Phi^*(x_i) , \quad f_i = f(x_i) ,$$

$$g_i = g(x_i) , \qquad (2.9)$$

where i is an arbitrary positive integer, and if we employ central difference formulae to approximate first and second

derivatives with respect to x, Equations (2.1) can be written in matrix form as

$$A_i\, y_{i+1} + B_i\, y_i + C_i y_{i+1} = D_i \quad , \qquad (2.10)$$

where

$$y_i = \begin{bmatrix} \theta_i^* \\ \Phi_i^* \end{bmatrix} \quad , \quad D_i = \begin{bmatrix} f_i \\ g_i \end{bmatrix} \quad ,$$

$$A_i = \begin{bmatrix} \frac{x_i}{h^2} + \frac{1}{2h} & 0 \\ 0 & \frac{x_i}{h^2} + \frac{1}{2h} \end{bmatrix} \quad , \quad B_i = \begin{bmatrix} -\left(\frac{2x_i}{h^2} + \frac{1}{x_i}\right) & x_i \\ -x_i & -\left(\frac{2x_i}{h^2} + \frac{1}{x_i}\right) \end{bmatrix} ,$$

$$C_i = \begin{bmatrix} \frac{x_i}{h^2} - \frac{1}{2h} & 0 \\ 0 & \frac{x_i}{h^2} - \frac{1}{2h} \end{bmatrix} \quad . \qquad (2.11)$$

Note that Equation (2.10) holds everywhere except in the neighborhood of a ring or the boundary. Specifically, if rings are placed at spatial stations $x = x_{N_j}$ $(j = 1,2,\ldots)$, then (2.10) holds at all x_i except x_{N_j} $(j = 1,2,\ldots)$ and the boundary.

Equations (2.2) and (2.5) imply that θ^* is continuous at x_{N_j}, but Φ^* and $\theta^{*\prime}$ are discontinuous. We shall adopt the backward three-point difference formulae to approximate the first and second derivatives of θ^* and Φ^* at $x = x_{N_j}^-$, and the forward

three-point difference formulae to approximate the first and second derivatives of θ^*, Φ^* at $x = x_{N_j}^+$. Then, we obtain the following matrix equations from Equations (2.1) at $x = x_{N_j}^-$ and $x = x_{N_j}^+$:

$$E_j\, Y_{N_j}^- + F_j\, Y_{N_j-1} + G_j\, Y_{N_j-2} = H_j \ ,$$

$$I_j\, Y_{N_j+2} + J_j\, Y_{N_j+1} + K_j\, Y_{N_j}^+ = L_j \ . \qquad (2.11)$$

Here

$$H_j = \begin{bmatrix} f_{N_j}^- \\ g_{N_j}^- \end{bmatrix} \ , \qquad L_j = \begin{bmatrix} f_{N_j}^+ \\ g_{N_j}^+ \end{bmatrix} \ ,$$

$$E_j = \begin{bmatrix} \dfrac{x_{N_j}}{h^2} + \dfrac{3}{2h} - \dfrac{1}{x_{N_j}} & x_{N_j} \\ -x_{N_j} & \dfrac{x_{N_j}}{h^2} + \dfrac{3}{2h} - \dfrac{1}{x_{N_j}} \end{bmatrix} \ ,$$

$$F_j = -\left(\frac{2x_{N_j}}{h^2} + \frac{2}{h} \right) I \ , \quad G_j = \left(\frac{x_{N_j}}{h^2} + \frac{1}{2h} \right) I$$

where I is the unit matrix. The remaining matrices G_j, F_j, E_j are obtained from I_j, J_j, K_j, respectively, by replacing h by -h in the latter.

The continuity and jump conditions (2.2) and (2.5) can be similarly written at $x=x_{N_j}$ as follows:

$$M_j y_{N_j}^{+} + N_j y_{N_j}^{-} + P_j y_{N_j-1} + Q_j y_{N_j-2} = 0 \quad ,$$

$$R_j y_{N_j+2} + S_j y_{N_j+1} + T_j y_{N_j}^{+} + U_j y_{N_j}^{-} + V_j y_{N_j-1} + W_j y_{N_j-2} = 0 , \quad (2.13)$$

where

$$M_j = I, \; N_j = \begin{bmatrix} -1 & 0 \\ 0 & -1-c\left(\frac{3}{2h} - \frac{\nu}{x_{N_j}}\right) \end{bmatrix} ,$$

$$P_j = \begin{bmatrix} 0 & 0 \\ 0 & \frac{2c}{h} \end{bmatrix} , \qquad R_j = \begin{bmatrix} 0 & \frac{1}{2h} \\ \frac{1}{2h} & 0 \end{bmatrix} ,$$

$$S_j = \begin{bmatrix} 0 & -\frac{2}{h} \\ -\frac{2}{h} & 0 \end{bmatrix} , \qquad T_j = \begin{bmatrix} 0 & \frac{3}{2h} + \frac{\nu}{x_{N_j}} \\ \frac{3}{2h} & 0 \end{bmatrix} ,$$

$$U_j = \begin{bmatrix} 0 & \frac{3}{2h} - \frac{\nu}{x_{N_j}} \\ \frac{3}{2h} + \frac{b}{x^2_{N_j}} & 0 \end{bmatrix} .$$

The matrices Q_j, W_j, V_j are obtained from P_j, R_j, S_j, respectively, by replacing h by -h in the latter.

The boundary conditions (2.7) at the bladder edge $x = \lambda$ and $i = I+1$, say, can be written as

$$G\, y_{I+2} + K\, y_{I+1} - G\, y_I = 0 \qquad (2.15)$$

where

$$G = \begin{bmatrix} 0 & 0 \\ 0 & \frac{1}{2h} \end{bmatrix} , \qquad K = \begin{bmatrix} 1 & 0 \\ 0 & -\frac{\nu}{\lambda} \end{bmatrix} \tag{2.16}$$

(Note that an extra station at $x = \lambda+h$ has been added for convenience.)

The matrix Equations (2.10), (2.11), (2.13), (2.15) can be solved by iteration. In this process we assume the column matrices D_i, H_j, L_j are known, and let

$$y_i = \alpha_i y_{i+1} + \beta_i \tag{2.17}$$

where α_i is a 2 X 2 matrix and β_i is a column vector. Substitution of (2.17) into (2.10) yields the following recurrence relations for α_i, β_i:

$$\alpha_i = - (B_i + C_i\alpha_{i-1})^{-1} ,$$

$$\beta_i = (B_i + C_i\alpha_{i-1})^{-1} (D_i - C_i\beta_{i-1}) . \tag{2.18}$$

Since $y_1 = 0$ (i.e., slope and stress function vanish at the shell apex for axisymmetric motion), Equation (2.17) implies that

$$\alpha_1 = \beta_1 = 0 . \tag{2.19}$$

Therefore, by use of Equations (2.18), all other α_i, β_i can be evaluated. Modifications must be imposed in the neighborhood of a ring. For this purpose let

$$y_{N_j-1} = \alpha_{N_j-1}\, y^{-}_{N_j} + B_{N_j-1} \quad , \qquad (2.20)$$

$$y^{-}_{N_j} = \alpha_j^*\, y^{+}_{N_j} + \beta_j^* \quad ,$$

$$y^{+}_{N_j} = \alpha_{N_j}\, y_{N_j+1} + \beta_{N_j} \quad .$$

Equations (2.11) and (2.13) furnish

$$\alpha_{N_j-1} = -\,(F_j + G_j\,\alpha_{N_j-2})^{-1}\, E_j \quad ,$$

$$\beta_{N_j-1} = (F_j + G_j\,\alpha_{N_j-2})^{-1}\,(H_j - G_j\beta_{N_j-2}) \quad ,$$

$$\alpha_j^* = -[N_j + (P_j + Q_j\,\alpha_{N_j-2})\,\alpha_{N_j-1}]^{-1}\, M_j \quad ,$$

$$\beta_j^* = -\,[N_j + (P_j + Q_j\,\alpha_{N_j-2})\,\alpha_{N_j-1}]^{-1}$$

$$[\,(P_j + Q_j\,\alpha_{N_j-2})\beta_{N_j-1} + Q_j\beta_{N_j-2}] \quad , \qquad (2.21a)$$

$$\alpha_{N_j} = (I_j^{-1}K_j - R_j^{-1}X_j)^{-1}\,(R_j^{-1}S_j - I_j^{-1}J_j) \quad ,$$

$$\beta_{N_j} = (R_j^{-1}X_j - I_j^{-1}K_j)^{-1}\,(R_j^{-1}\,Y_j - I_j^{-1}L_j) \quad ,$$

$$\alpha_{N_j+1} = -(S_j + X_j\alpha_{N_j})^{-1}\, R_j \quad ,$$

$$\beta_{N_j+1} = (S_j + X_j\alpha_{N_j})^{-1}\,(Y_j - X_j\beta_{N_j}) \quad ,$$

where

$$X_j = T_j + [U_j + (V_j + W_j\alpha_{N_j-2})\alpha_{N_j-1}]\alpha_j^* \quad ,$$

$$Y_j = -[U_j + (V_j + W_j\alpha_{N_j-2})\alpha_{N_j-1}]\,\beta^*_j \quad , \qquad (2.21b)$$

$$-\,(V_j + W_j\alpha_{N_j-2})\beta_{N_j-1} - W_j\beta_{N_j-2} \quad .$$

Note that α_{N_j+1} and β_{N_j+1} can also be calculated from Equations (2.18). However, for consistent accuracy, we prefer to employ the last two of Equations (2.21a).

Now, by virtue of Equations (2.18) and (2.21a), all α_i and β_i can be evaluated. In addition, from the boundary condition, Equation (2.15), we obtain Y_{I+2} (a second mesh point at $x = \lambda+2h$ is added for convenience) as

$$Y_{I+2} = -[G+(K-G\alpha_I)\ \alpha_{I+1}]^{-1}\ [(K-G\alpha_I)\ \beta_{I+1} - G\beta_I] . \qquad (2.22)$$

Since all α_i, β_i are known, Y_{I+2} can be evaluated from (2.22), and all other y_i can be computed from Equations (2.17) or (2.20).

The iteration procedure can now be described as follows: 1) iteration begins with an initial guess for y_i ($i = 1,2,\ldots$), from which D_i ($i \neq N_j$), H_j, and L_j can be calculated for $j = 1,2,\ldots$ A new set of y_i can then be evaluated by the process described above; 2) the process is repeated until "convergence" is obtained. A criterion for the latter can be defined by comparing the relative error in a dimensionless average deflection, ρ, between two consecutive iterations. Here ρ is defined by

$$\rho = \frac{1}{\lambda^2} \int_0^{\lambda} x^2\theta^* dx. \qquad (2.23)$$

The value of p can be plotted as a function of ρ. The pressure(s) at which axisymmetric snap-through occurs can be deduced from the local maximums of the p vs. ρ curve.

2.3 Stability of Axisymmetric State

The axisymmetric deformation of the shell is associated with an increase in the membrane stresses N_θ, N_r. If the values of these quantities exceed certain bounds, asymmetric buckling or bifurcation will take place. In terms of the p-ρ curve, a branch on the p-ρ curve will appear at the point of bifurcation. If the initial slope of the branch at the point of bifurcation is negative, snap-through is introduced due to asymmetric bifurcation; on the other hand, if the initial slope is positive, double folding or pointing (wrinkling) will occur due to bifurcation. Thus, a sufficient condition for the absence of double folding and pointing is that no bifurcation points occur. A necessary and sufficient condition for the absence of double folding and pointing is that the initial slopes of all bifurcation branches be positive (stable*).

2.3.1 Basic Relations.

Let ω be the dimensionless asymmetrical buckling mode associated with bifurcation and ψ the corresponding stress function. According to [2], for a non-reinforced shell ω and ψ are eigenfunctions of the following eigenvalue problem:

$$\nabla^4\omega = \nabla^2\psi - \left(\frac{1}{x}\psi' + \frac{1}{x^2}\ddot{\psi}\right)\theta^{*\prime} + \frac{1}{x}\omega''\Phi^* - \frac{1}{x}\psi''\theta^{*\prime} + \left(\frac{1}{x}\omega' + \frac{1}{x^2}\ddot{\omega}\right)\Phi^{*\prime}, \tag{2.24}$$

$$\nabla^4\psi = -\nabla^2\omega + \left(\frac{1}{x}\omega' + \frac{1}{x^2}\ddot{\omega}\right)\theta^{*\prime} + \frac{1}{x}\omega''\theta^*.$$

* In general, the stability of the bifurcation branch can be determined from the sign of the second variation of the potential energy as expressed in terms of the pre-bifurcation deformation and the bifurcation mode.

Here θ^*, Φ^* are solutions corresponding to the axisymmetric pre-bifurcation deformation of the shell and $\dot{()} \equiv \partial()/\partial\theta$, where θ is the circumferential shell coordinate (Figure 2.1). If we expand ω and ψ as follows:

$$\omega(x,\theta) = \sum_{n=0}^{\infty} \omega_n(x) \cos n\theta,$$
$$\psi(x,\theta) = \sum_{n=0}^{\infty} \psi_n(x) \cos n\theta, \qquad (2.25)$$

Equations (2.24) reduce to

$$L_n^2\,\omega_n = L_n\psi_n - \left(\frac{1}{x}\psi_n' - \frac{n^2}{x^2}\psi_n\right)\theta^{*\cdot\cdot} + \frac{1}{x}\omega_n''\,\Phi^* - \frac{1}{x}\psi_n''\,\theta^* + \left(\frac{1}{x}\omega_n' - \frac{n^2}{x^2}\omega_n\right)\Phi^{*\cdot\cdot},$$
$$L_n^2\,\psi_n = -L_n\omega_n + \left(\frac{1}{x}\omega_n' - \frac{n^2}{x^2}\omega_n\right)\theta^{*\cdot\cdot} + \frac{1}{x}\omega_n''\,\theta^*, \qquad (2.26)$$

where

$$L_n() = \left(\frac{d^2}{dx^2} + \frac{1}{x}\frac{d}{dx} - \frac{n^2}{x^2}\right)(), \quad L_n^2() = L_nL_n(). \qquad (2.27)$$

For reinforced shells, Equations (2.26) hold for the shell segments between rings. Matching across rings is accomplished with the aid of continuity and jump conditions. The latter are obtained by a consideration of ring forces and moments due to an asymmetric displacement about the axisymmetric state. For this purpose, consider Equations (4.72) of Chapter IV. These equations govern the perturbations in ring forces and moments about the axisymmetric state. In terms of the abridged notation:

$$p_n = -f_1, \quad q = -f_2, \quad p_s = f_3, \quad m_x = -m_1,$$

$$t = m_2, \quad m_s = -m_3, \quad S = N_1, \quad v = N_2,$$

$$F = N_3, \quad N = -M_1, \quad M = M_2, \quad T = M_3, \quad u = -u_1,$$

$$w = -u_2, \quad v = v_3, \quad \phi = \beta_{21} = -\beta_{12} \qquad (2.28)$$

Equations (4.72) can be written

$$p_n = -S' - \frac{f}{r_o} + H_1^* \bar{F} \ ,$$

$$p_s = -F' + \frac{S}{r_o} \ ,$$

$$q = -v' + H_2^* \bar{F} \ ,$$

$$m_t = -N' + v + \frac{T}{r_o} \ ,$$

$$m_s = -T' - \frac{N}{r_o} + H_1^* \bar{N} \ ,$$

$$0 = m' - S - H_3^* \bar{N} \ . \qquad (2.29)$$

From Equations (4.67) and (4.54), the axisymmetric (prebuckled) quantities $\bar{F}$, $\bar{N}$, as well as the perturbations in the curvatures H_1, H_2, are given by

$$\bar{F} = -p_r r_o, \quad \bar{N} = m_o r_o$$

$$H_1^* = -\left(\frac{u}{r_o^2} + u''\right), \quad H_2^* = \frac{\phi}{r_o} - w'' \ ,$$

$$p_r = -\bar{f}_1 \ , \quad m_o = -\bar{m}_3 = \text{const.}$$

In addition, from Equations (4.73), we obtain the following relations:

$$
\begin{aligned}
-M &= (E_r I_r^{\,i}) \left(u'' - \frac{v'}{r_o} \right) , \\
F &= (A_r E_r) \left(v' - \frac{u}{r_o} \right) , \\
N &= (E_r I_r^{\,o}) \left(-w'' + \frac{\phi}{r_o} \right) , \\
T &= GJ \left(\phi' + \frac{w'}{r_o} \right) .
\end{aligned}
\tag{2.31}
$$

Combining Equations (2.29), (2.30), and (2.31) we find

$$
\begin{aligned}
p_n &= -\left(\frac{A_r E_r}{r_o} \right) \left(v' - \frac{u}{r_o} \right) + (E_r I_r^{\,i}) \left(u^{IV} + \frac{u''}{r_o} \right) \\
&\quad + p_r r_o \left(\frac{u}{r_o^2} + u'' \right) , \\
p_s &= -(A_r E_r) \left(v'' - \frac{u'}{r_o} \right) - (E_r I_r^{\,i}) \left(\frac{u'''}{r_o} + \frac{v''}{r_o^2} \right) , \\
q + m_t' &= -(E_r I_r^{\,o}) \left(-w^{IV} + \frac{\phi''}{r_o} \right) + GJ \left(\frac{\phi''}{r_o} + \frac{w''}{r_o^2} \right) \\
&\quad + p r_o \left(w'' - \frac{\phi}{r_o} \right) , \\
m_s &= -GJ \left(\phi'' + \frac{w''}{r_o} \right) - (E_r I_r^{\,o}) \left(-\frac{w''}{r_o} + \frac{\phi}{r_o^2} \right) - m_\theta r_o \left(u'' + \frac{u}{r_o^2} \right) \\
&\quad + p_r r_o (I_p/A) \phi'' ,
\end{aligned}
\tag{2.32}
$$

where

$$
I_p = I_r^{\,i} + I_r^{\,o} .
$$

Let us now return to the shell bifurcation problem. We introduce the notation N_r, N_θ, $N_{r\theta}$, ϕ_r, ϕ_θ, M_r, M_θ, $M_{r\theta}$ as illustrated in Figure 2.4. Before bifurcation, $N_r = \tilde{N}_r$, $M_r = \tilde{M}_r$, $\phi_r = \tilde{\phi}_r$ and $\tilde{N}_\theta = \tilde{N}_{r\theta} = \tilde{\phi}_\theta = \tilde{M}_\theta = \tilde{M}_{r\theta} = 0$. After bifurcation, these membrane stresses, transverse shears, and moments become $N_r = \tilde{N}_r + n_r$, $N_\theta = n_\theta$, $N_{r\theta} = n_{r\theta}$, $\phi_r = \tilde{\phi}_r + q_r$, $\phi_\theta = q_\theta$, $M_r = \tilde{M}_r + m_r$, $M_\theta = m_\theta$ and $M_{r\theta} = m_{r\theta}$. Note that, at any ring, the values of $\tilde{N}_r$, n_r, $n_{r\theta}$, q_r, $\tilde{M}_r$, m_r and $m_{r\theta}$ are discontinuous. From Figure 2.3 it is evident that the jumps in these quantities are related to p, t, m_t, m_r, p_r and m_θ by

$$
\begin{aligned}
n_r^+ - n_r^- &= -p_n \quad , \\
n_{r\theta}^+ - n_{r\theta}^- &= -p_s \quad , \\
m_{r\theta}^+ - m_{r\theta}^- &= -m_t \quad , \\
m_r^+ - m_r^- &= -m_s \quad , \\
q_r^+ - q_r^- &= -q \quad , \\
\tilde{N}_r^+ - \tilde{N}_r^- &= -p_r \quad , \\
\tilde{M}_r^+ - \tilde{M}_r^- &= -m_\theta \quad .
\end{aligned}
\tag{2.33}
$$

Let U, V, W denote the horizontal radial, horizontal tangential, and vertical components of displacement introduced by bifurcation.

We have

$$U = -u,\ V = -v,\ W = w \tag{2.34}$$

$$\frac{\partial W}{\partial r} = \phi.$$

In addition, let $(\,)' = \partial(\,)/\partial_r$ and $(\dot{}) = \partial(\,)/\partial\theta$ where θ is the polar angle of the shell. Note that $d(\,)/ds = -(1/r_o)\,(\dot{})$. Then, Equation (2.32) can be written as

$$n_r^+ - n_r^- = \frac{A_r E_r}{r_o^2}(\dot{V} + U) + \frac{E_r I_r^i}{r_o^4}(\dddot{U} - \dddot{V}) - \frac{1}{r_o}(\tilde{N}_r - \tilde{N}_r)(\ddot{U}+V),$$

$$n_{r\theta}^+ - n_{r\theta}^- = -\frac{A_r E_r}{r_o^2}(\ddot{V} + \dot{U}) + \frac{E_r I_r^i}{r_o^4}(\dddot{U} - \ddot{V}),$$

$$(m_r^{+\prime} + \frac{1}{r_o} m_r^+ - \frac{1}{r_o} m_\theta^+) - (m_r^{-\prime} + \frac{1}{r_o} m_r^- - \frac{1}{r_o} m_\theta^-) \tag{2.35}$$

$$= \frac{E_r I_r^o}{r_o^4}(\ddot{\ddot{W}} - r_o\ddot{W}') - \frac{G_r J_r}{r_o^4}(\ddot{W} + r_o\ddot{W}') + \frac{1}{r_o}(\tilde{N}_r^+ - \tilde{N}_r^-)\ddot{W},$$

$$m_r^+ - m_r^- = \frac{E_r I_r^o}{r_o^3}(\ddot{W} - r_o W') + \frac{GJ}{r_o^3}(\ddot{W} + r_o\ddot{W}')$$

$$+ \frac{I_p}{A_r r_o}(\tilde{N}_r^+ - \tilde{N}_r^-)\ddot{W}' + \frac{1}{r_o}(\tilde{M}_r^+ - \tilde{M}_r^-)(\ddot{V}+U).$$

Next, we express the derivatives of U,V in terms of the stress function By use of the strain displacement relations, the stress-strain relations, and the stress-stress function relations as shown in [2], we obtain the following jump conditions, as written in terms of the dimensionless quantities defined in [2]:

$$x_o\psi^{+\prime} + \ddot{\psi}^{+} - x_o\psi^{-\prime} - \ddot{\psi}^{-}$$

$$= k_1(x_o\psi^{-\prime\prime\prime} - \nu\psi^{-\prime} - \frac{\nu}{x_o}\ddot{\psi}^{-}) - k_2\left[-x_o\dot{\ddot{\psi}}^{-\prime\prime\prime} - \ddot{\psi}^{-\prime\prime\prime} + \frac{1}{x_o}\ddot{\psi}^{-\prime} - (2+\nu)\frac{1}{x_o}\ddot{\psi}^{\cdot\cdot-\prime}\right.$$

$$\left. + (3+\nu)\frac{1}{x_o^2}\ddot{\psi}^{\cdot\cdot-} - x_o\ddot{w}^{-\prime} - \ddot{w}^{\cdot\cdot-}\right] - c_1(x_o\phi^{*+} - x_o\phi^{*-})\left[-x_o\psi^{-\prime\prime\prime} + (1-\nu)\right.$$

$$\left.\frac{1}{x_o}\psi^{-\prime} - (2+\nu)\frac{1}{x_o}\ddot{\psi}^{-\prime} + \frac{3}{x_o^2}\ddot{\psi}^{-} - x_o w^{-\prime} - \ddot{w}^{-}\right],$$

$$\dot{\psi}^{+\prime} - x_o\dot{\psi}^{+\prime} - \dot{\psi}^{-} + x_o\dot{\psi}^{-\prime}$$

$$= -k_1(x_o\dot{\psi}^{-\prime\prime} - \nu\dot{\psi}^{-\prime} - \frac{\nu}{x_o}\dot{\psi}^{-}) + k_2\left[-x_o\dot{\psi}^{-\prime\prime\prime} - \dot{\psi}^{-\prime\prime} + \frac{1}{x_o}\dot{\psi}^{-\prime} - (2+\nu)\right.$$

$$\left.\frac{1}{x_o}\dot{\ddot{\psi}}^{-\prime} + (3+\nu)\frac{1}{x_o^2}\dot{\ddot{\psi}}^{-} - x_o\dot{w}^{-\prime} - \dot{w}^{-}\right], \qquad (2.36)$$

$$w^{+\prime\prime\prime} + \frac{1}{x_o}w^{+\prime\prime} - w^{-\prime\prime\prime} - \frac{1}{x_o}w^{-\prime\prime} = \frac{k_3}{x_o^4}(\ddot{w}^{-} - x_o\ddot{w}^{-\prime}) - \frac{k_4}{x_o^4}(\ddot{w}^{-} + x_o\ddot{w}^{-\prime})$$

$$-c_2\frac{1}{x_o^2}(\phi^{*+} - \phi^{*-})\ddot{w}^{-},$$

$$w^{+\prime\prime} - w^{-\prime\prime} = -\frac{k_3}{x_o^3}(\ddot{w}^{-} - x_o w^{-\prime}) - \frac{k_4}{x_o^3}(\ddot{w}^{-} + x_o\ddot{w}^{-\prime}) - \frac{c_3}{x_o^2}(\phi^{*+} - \phi^{*-})\ddot{w}^{-}$$

$$-\frac{c_1}{\lambda^2}(\theta^{*+\prime} - \theta^{*-\prime})\left[-x_o\psi^{-\prime\prime\prime} + (1-\nu)\frac{1}{x_o}\psi^{-\prime} - (2+\nu)\frac{1}{x_o}\ddot{\psi}^{-\prime} + \frac{3}{x_o^2}\ddot{\psi}^{-}\right.$$

$$\left. - x_o w^{-\prime} - \ddot{w}^{-}\right],$$

where w is the dimensionless W, which is different from the ω used previously. Here $(\,)' \equiv \frac{\partial}{\partial x}(\,)$ and

$$k_1 = \frac{\lambda A_r E_r}{Eat}, \quad k_2 = \frac{\lambda^3 E_r I_r{}^i}{Ea^3 t}, \quad k_3 = \frac{\lambda E_r I_r{}^o}{Da}, \quad k_4 = \frac{\lambda G_r J_r}{Da},$$

$$c_1 = \frac{4H^2}{a^2}, \quad c_2 = \frac{4EH^2 t}{D\lambda^4} \text{ and } c_3 = c_2\frac{\lambda^2 I_p}{A_r a^2} \qquad (2.37)$$

Note that $k_1 = c$ and $k_3 = b$.

At each ring, W and $\frac{\partial W}{\partial r}$ are continuous and so are $\dot{V} + U$ and $\dot{U} - \dot{V}$. Hence, we have the following continuity conditions for the perturbed quantities due to bifurcation

$$w^+ = w^- \quad ,$$

$$w^{+\prime} = w^{-\prime} \quad ,$$

$$\Psi^{+\prime\prime} - \frac{\nu}{x_o}\Psi^{+\prime} - \frac{\nu}{x_o^2}\ddot{\Psi}^+ = \Psi^{-\prime\prime} - \frac{\nu}{x_o}\Psi^{-\prime} - \frac{\nu}{x_o^2}\ddot{\Psi}^- \quad ,$$

$$x_o\Psi^{+\prime\prime\prime} + \Psi^{+\prime\prime} - \frac{1}{x_o}\Psi^{+\prime} + (2+\nu)\frac{1}{x_o}\ddot{\Psi}^{+\prime} - (3+\nu)\frac{1}{x_o^2}\ddot{\Psi}^+$$

$$= x_o\Psi^{-\prime\prime\prime} + \Psi^{-\prime\prime} - \frac{1}{x_o}\Psi^{-\prime} + (2+\nu)\frac{1}{x_o}\ddot{\Psi}^{-\prime} - (3+\nu)\frac{1}{x_o^2}\ddot{\Psi}^- \qquad (2.38)$$

at each ring.

The boundary conditions for the clamped edge are given in [2]; they are

$$w = 0 \quad ,$$

$$w^{\prime} = 0 \quad ,$$

$$\Psi^{\prime\prime} - \frac{\nu}{\lambda}\Psi^{\prime} - \frac{\nu}{\lambda^2}\ddot{\Psi} = 0 \quad ,$$

$$\lambda\left(\Psi^{\prime\prime} - \frac{\nu}{x}\Psi^{\prime} - \frac{\nu}{x^2}\ddot{\Psi}\right)^{\prime} - \frac{1}{\lambda}\Psi^{\prime} - \frac{1}{\lambda^2}\ddot{\Psi} + \nu\,\Psi^{\prime\prime} + 2(1+\nu)\left(\frac{1}{x}\ddot{\Psi}\right)^{\prime} = 0 \quad , \qquad (2.39)$$

at $x = \lambda$.

If we express

$$w(x,\theta) = \sum_{h=1}^{\infty} \omega_n(x)\cos n\theta \quad , \quad \psi(x,\theta) = \sum_{n=1}^{\infty} \Psi_n(x)\cos n\theta, \qquad (2.40)$$

then for each n we obtain the following jump and continuity conditions, and boundary conditions from Equations (2.36-2.39):

$$(1-n^2)\ (\psi_n^+ - \psi_n^-) = -k_2\ (1-n^2) \left\{x_o\psi_n^{-'''} + \psi_n^{-''} - \frac{1}{x_o}\left[1+(2+\nu)n^2\right]\psi_n^{-'}\right.$$

$$\left. + \frac{n^2}{x_o^2}\ (3+\nu)\ \psi_n^- + x_o w_n^{-'} - n^2 w_n^-\right\} - c_1 x_o\ (\Phi^{*+} - \Phi^{*-})\left\{-x_o\psi_n^{-'''}\right.$$

$$\left. + \frac{1}{x_o}\ [1-\nu+(2+\nu)n^2]\psi_n^{-'} - \frac{3n^2}{x_o^2}\ \psi_n^- - x_o w_n^{-'} + n^2\omega_n^-\right\}$$

$$(1-n^2)\ (\psi_n^{+'} - \psi_n^{-'}) = k_1(1-n^2)\ (\psi_n^{-''} - \frac{\nu}{x_o}\ \psi_n^{-'} - \frac{\nu n^2}{x_o^2}\ \psi_n^-)$$

$$-c_1 x_o\ (\Phi^{*+} - \Phi^{*-})\left\{-x_o\psi_n^{-'''} + \frac{1}{x_o}\ [1-\nu(2+\nu)n^2]\psi_n^{-'} - \frac{3n^2}{x_o^2}\psi_n^-\right.$$

$$\left. -x_o\omega_n^{-'} + n^2\omega_n^-\right\},$$

$$\omega_n^{+''} - \omega_n^{-''} = \frac{k_3}{x_o^3}\ (n^2\omega_n^- + x_o\omega_n^{-'}) + \frac{k_4 n^2}{x_o^3}\ (\omega_n^- + x_o\omega_n^{-'})$$

$$+ \frac{c_3}{x_o^2}\ n^2(\Phi^{*+} - \Phi^{*-})\ \omega_n^{-'} - \frac{c_1}{\lambda^2}\ (\theta^{*+'} - \theta^{*-'})\left\{-x_o\psi_n^{-'''} + \frac{1}{x_o}\right.$$

$$\left.[1-\nu+(2+\nu)n^2]\ \psi_n^{-'} - \frac{3n^2}{x_o^2}\ \psi_n^- - x_o\omega_n^{-'} + n^2\omega_n^-\right\},$$

$$\omega_n^{+'''} - \omega_n^{-'''} = \frac{k_3}{x_o^4}\ (n^2-1)\ (n^2\omega_n^- + x_o\omega_n^{-'}) + \frac{n^2}{x_o^2}\ (\Phi^{*+} - \Phi^{*-})$$

$$(c_2\omega_n^- - c_3\ \frac{\omega_n^{-'}}{x_o}) + \frac{c_1}{\lambda^2}\ (\theta^{*+'} - \theta^{*-'})\left\{-\psi_n^{-'''} + \frac{1}{x_o^2}\ [1-\nu+(2+\nu)n^2]\psi_n^{-'}\right.$$

$$\left. - \frac{3n^2}{x_o^3}\ \psi_n^- - \omega_n^{-'} + n^2\ \frac{\omega_n}{x_o}\right\}, \qquad (2.41)$$

$$\omega_n^+ = \omega_n^-,$$

$$\omega_n^{+'} = \omega_n^{-'},$$

$$\psi_n^{+''} - \frac{\nu}{x_o}\ \psi_n^{+'} + \frac{n^2\nu}{x_o^2}\ \psi_n^+ = \psi_n^{-''} - \frac{\nu}{x_o}\ \psi_n^{-'} + \frac{n^2\nu}{x_o^2}\ \psi_n^-,$$

$$x_o\psi_n^{+'''} - \frac{1}{x_o}[1-\nu+(2+\nu)n^2]\,\psi_n^{+'} + \frac{3n^2}{x_o^2}\psi_n^{+} = x_o\psi_n^{-'''} - \frac{1}{x_o}[1-\nu+(2+\nu)n^2]\psi_n^{-'} + \frac{3n^2}{x_o^2}\psi_n^{-} \quad , \tag{2.41}$$

$$\omega_n(\lambda) = 0 \quad ,$$

$$\omega_n'(\lambda) = 0 \quad ,$$

$$\psi_n''(\lambda) - \frac{\nu}{\lambda}\psi_n'(\lambda) + \frac{n^2\nu}{\lambda^2}\psi_n(\lambda) = 0 \quad ,$$

$$\lambda\psi_n'''(\lambda) - \frac{1}{\lambda}[1-\nu+(2+\nu)n^2]\,\psi_n'(\lambda) + \frac{3n^2}{\lambda^2}\psi_n(\lambda) = 0 \quad . \tag{2.42}$$

It is interesting to note that the continuity conditions and boundary conditions are of similar form.

2.3.2 Solution Method.

Next, we shall solve this eigenvalue problem by the finite difference method. Accordingly, we let $x = x_i = (i-1)h$, $\omega_i = \omega_n(x_i)$, $\psi_i = \psi_n(x_i)$, $\theta_i^* = \theta^*(x_i)$, $\Phi_i^* = \Phi^*(x_i)$, $u_i = \omega_i''$, $v_i = \psi_i''$ and

$$\tilde{Y}_i = \begin{bmatrix} \omega_i \\ \psi_i \\ u_i \\ v_i \end{bmatrix} .$$

Equations (2.26) can be written

$$\tilde{A}_i\tilde{Y}_{i+1} + \tilde{B}_i\tilde{Y}_i + \tilde{C}_i\tilde{Y}_{i-1} = 0 \tag{2.43a}$$

where

$$\tilde{A}_i = \begin{bmatrix} -1 & 0 & 0 & 0 \\ 0 & -1 & 0 & 0 \\ \frac{1+2n^2}{2(i-1)^2} - \frac{h^2}{2(i-1)}\Phi_i^{*\prime} & -\frac{h^2}{2(i-1)}(1-\theta_i^{*\prime}) & h^2(1+\frac{1}{i-1}) & 0 \\ \frac{h^2}{2(i-1)}(1-\theta_i^{*}) & \frac{1+2n^2}{2(i-1)^3} & 0 & h^2(1+\frac{1}{i-1}) \end{bmatrix}, \qquad (2.43b)$$

$$\tilde{B}_i = \begin{bmatrix} 2 & 0 & h^2 & 0 \\ 0 & 2 & 0 & h^2 \\ -\frac{4n^2-n^4}{(i-1)^4}+\frac{h^2n^2}{(i-1)^2}\Phi_i^{*\prime} & \frac{h^2n^2}{(i-1)^2}(1-\theta_i^{*\prime}) & -h^2\left[2+\frac{1+2n^2}{(i-1)^2}+\frac{1}{i-1}\Phi_i^{*}\right] & -h^3(h-\frac{1}{i-1}\theta_i^{*}) \\ -\frac{h^2n^2}{(i-1)^2}(1-\theta_i^{*\prime}) & -\frac{4n^2-n^4}{(i-1)^4} & h^3(h-\frac{1}{i-1}\theta_i^{*}) & -h^2\left[2+\frac{1+2n^2}{(i-1)^2}\right] \end{bmatrix}, \qquad (2.43c)$$

$$\tilde{C}_i = \begin{bmatrix} -1 & 0 & 0 & 0 \\ 0 & -1 & 0 & 0 \\ -\frac{1+2n^2}{2(i-1)^3} + \frac{h^2}{2(i-1)}\phi_i^{*\prime} & \frac{h^2}{2(i-1)}(1-\theta_i^{*\prime}) & h^2(1-\frac{1}{i-1}) & 0 \\ -\frac{h^2}{2(i-1)}(1-\theta_i^{*\prime}) & -\frac{1+2n^2}{2(i-1)^3} & 0 & h^2(1-\frac{1}{i-1}) \end{bmatrix}. \tag{2.43d}$$

Equation (2.43) holds everywhere except in the neighborhood of rings and the boundary. For the ring at $x = x_{N_j}$, Equation (2.43) is replaced by the following equations

$$\begin{aligned} \tilde{E}_j \tilde{y}_{N_j} + \tilde{F}_j \tilde{y}_{N_j-1} + \tilde{G}_j \tilde{y}_{N_j-2} &= 0 \quad , \\ \tilde{I}_j \tilde{y}_{N_j+2} + \tilde{J}_j \tilde{y}_{N_j+1} + \tilde{K}_j \tilde{y}_{N_j} &= 0 \quad , \end{aligned} \tag{2.44}$$

where

$$\tilde{E}_j = \begin{bmatrix} -1 & 0 & h^2 \\ 0 & -1 & 0 \\ \frac{3}{2}\frac{h}{x_{N_j}^3}(1+2n^2) - \frac{4n^2-n^4}{x_{N_j}^4}h^2 - \frac{3h}{2x_{N_j}}\phi^{*=}_{N_j} + \frac{n^2h^2}{x_{N_j}^2}\phi^{*=}_{N_j} & -\left(\frac{3}{2}\frac{h}{x_{N_j}} - \frac{n^2h^2}{x_{N_j}^2}\right)(1-\theta^{*=}_{N_j}) & 1+\frac{3h}{x_{N_j}} - \frac{(1+2n^2)h^2}{x_{N_j}^2} - \frac{h^2}{x_{N_j}}\phi^{*-}_{N_j} \\ \left(\frac{3}{2}\frac{h}{x_{N_j}} - \frac{n^2h^2}{x_{N_j}}\right)(1-\theta^{*=}_{N_j}) & \frac{3}{2}(1+2n^2)\frac{h}{x_{N_j}^3} - \frac{4n^2-n^4}{x_{N_j}^4}h^2 & h^2 - \frac{h^2}{x_{N_j}}\theta^{*-}_{N_j} \end{bmatrix}$$

$$\begin{bmatrix} 0 \\ h^2 \\ -h^2 + \frac{h^2}{x_{N_j}}\theta^{*}_{N_j} \\ 1+\frac{3h}{x_{N_j}} - \frac{(1+2n^2)h^2}{x_{N_j}^2} \end{bmatrix}, \qquad (2.45a)$$

$$\tilde{F}_j = \begin{bmatrix} 2 & 0 & 0 & 0 \\ 0 & 2 & 0 & 0 \\ -2(1+2n^2)\frac{h}{x_{N_j}^3} + 2\frac{h}{x_{N_j}}\,\Phi^{*\prime}_{N_j} & 2\,\frac{h}{x_{N_j}}(1-\theta^{*\prime}_{N_j}) & -2-4\frac{h}{x_{N_j}} & 0 \\ -2\frac{h}{x_{N_j}}\,(1-\theta^{*\prime}_{N_j}) & -2(1+2n^2)\frac{h}{x_{N_j}^3} & 0 & -2-4\frac{h}{x_{N_j}} \end{bmatrix} \tag{2.45b}$$

$$\tilde{G}_j = \begin{bmatrix} -1 & 0 & 0 & 0 \\ 0 & -1 & 0 & 0 \\ \frac{1}{2}\,(1+2n^2)\frac{h}{x_{N_j}^3} - \frac{1}{2}\,\frac{h}{x_{N_j}}\,\Phi^{*\prime}_{N_j} & -\frac{1}{2}\,\frac{h}{x_{N_j}}\,(1-\theta^{*\prime}_{N_j}) & 1+\frac{h}{x_{N_j}} & 0 \\ \frac{1}{2}\,\frac{h}{x_{N_j}}\,(1-\theta^{*\prime}_{N_j}) & \frac{1}{2}\,(1+2n^2)\frac{h}{x_{N_j}^3} & 0 & 1+\frac{h}{x_{N_j}} \end{bmatrix} \tag{2.45c}$$

$$\tilde{I}_j = \begin{bmatrix} -1 & 0 & 0 & 0 \\ 0 & -1 & 0 & 0 \\ -\frac{1}{2}\frac{h}{x_{N_j}^3}(1+2n^2) + \frac{1}{2}\frac{h}{x_{N_j}}\Phi^{*'}_{N_j+} & \frac{1}{2}\frac{h}{x_{N_j}}(1-\theta^{*'}_{N_j+}) & 1-\frac{h}{x_{N_j}} & 0 \\ -\frac{1}{2}\frac{h}{x_{N_j}}(1-\theta^{*'}_{N_j+}) & -\frac{1}{2}(1+2n^2)\frac{h}{x_{N_j}^3} & 0 & 1-\frac{h}{x_{N_j}} \end{bmatrix}, \tag{2.45d}$$

$$\tilde{J} = \begin{bmatrix} 2 & 0 & 0 & 0 \\ 0 & 2 & 0 & 0 \\ 2(1+2n^2)\frac{h}{x_{N_j}^3} - 2\frac{h}{x_{N_j}}\Phi^{*'}_{N_j+} & -2\frac{h}{x_{N_j}}(1-\theta^{*'}_{N_j+}) & -2+4\frac{h}{x_{N_j}} & 0 \\ 2\frac{h}{x_{N_j}}(1-\theta^{*'}_{N_j+}) & 2(1+2n^2)\frac{h}{x_{N_j}^3} & 0 & -2+4\frac{h}{x_{N_j}} \end{bmatrix}, \tag{2.45e}$$

$$\tilde{K}_j = \begin{bmatrix} -1 & 0 & h^2 & 0 \\ 0 & -1 & 0 & h^2 \\ -\frac{3}{2}\frac{h}{x_{N_j}^3}(1+2n^2) - \frac{4n^2-n^4}{x_{N_j}^4}h^2 + \frac{3h}{2x_{N_j}}\Phi^{*'}_{N_j+} + n^2\frac{h^2}{x_{N_j}^2}\Phi^{*'}_{N_j+} & \left(\frac{3}{2}\frac{h}{x_{N_j}} + \frac{n^2h^2}{x_{N_j}^2}\right)(1-\theta^{*'}_{N_j+}) & 1-\frac{3h}{x_{N_j}} - \frac{(1+2n^2)h^2}{x_{N_j}^2} - \frac{h^2}{x_{N_j}}\Phi^{*}_{N_j+} & h^2 - \frac{h^2}{x_{N_j}}\theta^{*}_{N_j-} \\ -\left(\frac{3}{2}\frac{h}{x_{N_j}} + \frac{n^2h^2}{x_{N_j}^2}\right)(1-\theta^{*'}_{N_j+}) & -\frac{3}{2}(1+2n^2)\frac{h}{x_{N_j}^3} - \frac{4n^2-n^4}{x_{N_j}^4}h^2 & & \end{bmatrix}$$

74

$$
\begin{bmatrix}
0 \\
h^2 \\
-h^2 + \frac{h^2}{x_{N_j}}\theta^*_{N_j^+} \\
1 + \frac{3h}{x_{N_j}} - \frac{(1+2n^2)h^2}{x_{N_j}^2}
\end{bmatrix}
\tag{2.45f}
$$

The discontinuity and continuity conditions, Equations (2.41), can be written as

$$
\begin{aligned}
&\tilde{L}_j \tilde{y}_{N_j+2} + \tilde{M}_j \tilde{y}_{N_j+1} + \tilde{N}_j \tilde{y}_{N_j^+} + \tilde{P}_j \tilde{y}_{N_j^-} + \tilde{Q}_j \tilde{y}_{N_j-1} + \tilde{R}_j \tilde{y}_{N_j-2} = 0 \quad , \\
&\tilde{S}_j \tilde{y}_{N_j+2} + \tilde{T}_j \tilde{y}_{N_j+1} + \tilde{U}_j \tilde{y}_{N_j^+} + \tilde{V}_j \tilde{y}_{N_j^-} + \tilde{W}_j \tilde{y}_{N_j-1} + \tilde{X}_j \tilde{y}_{N_j-2} = 0 \quad ,
\end{aligned}
\tag{2.46}
$$

where

$$
\tilde{L}_j = \begin{bmatrix}
0 & 0 & 0 & 0 \\
0 & -\frac{1-n^2}{2h^2} & 0 & 0 \\
0 & 0 & 0 & 0 \\
0 & 0 & -\frac{1}{2h} & 0
\end{bmatrix} \quad ,
\tag{2.47a}
$$

$$
\tilde{M}_j = 4\tilde{L}_j \quad ,
\tag{2.47b}
$$

$$
\tilde{N}_j = \begin{bmatrix}
0 & 1-h^2 & 0 & 0 \\
0 & -\frac{3(1-n^2)}{2h} & 0 & 0 \\
0 & 0 & 1 & 0 \\
0 & 0 & -\frac{3}{2h} & 0
\end{bmatrix}
\tag{2.47c}
$$

$$\tilde{P}_j\ (1,1) = k_2(1-n^2)\left(\frac{3x_{N_j}}{2h} - n^2\right) - C_1 x_{N_j}\Delta_{N_j}\left(\frac{3x_{N_j}}{2h} - n^2\right) \quad ,$$

$$\tilde{P}_j\ (1,2) = -(1-n^2) + k_2(1-n^2)\left\{-[1+(2+\nu)n^2]\ \frac{3}{2hx_{N_j}} + (3+\nu)n^2\ \frac{1}{x_{N_j}^3}\right\} - C_1 x_{N_j}\Delta_{N_j}$$

$$-[1-\nu+(2+\nu)n^2]\ \frac{3}{2hx_{N_j}} + \frac{3n^2}{x_{N_j}^2}\Bigg\} \quad ,$$

$$\tilde{P}_j\ (1,3) = 0 \quad ,$$

$$\tilde{P}_j(1,4) = k_2(1-n^2)\left(\frac{3x_{N_j}}{2h} + 1\right) - C_1 x_{N_j}\Delta_{N_j}\ \frac{3x_{N_j}}{2h} \quad ,$$

$$\tilde{P}_j(2,1) = -C_1 x_{N_j}\Delta_{N_j}\left(\frac{3x_{N_j}}{2h} - n^2\right) \quad ,$$

$$\tilde{P}_j\ (2,2) = -(1-n^2)\frac{3}{2h} - k_1(1-n^2)\ -\ \frac{3\nu}{2hx_{N_j}} + \frac{\nu n^2}{x_{N_j}^2} - C_1 x_{N_j}\Delta_{N_j}\Big\{-[1-\nu+(2+\nu)n^2]$$

$$\frac{3}{2hx_{N_j}} + \frac{3n^2}{x_{N_j}^2}\Bigg\} \quad ,$$

$$\tilde{P}_j\ (2,3) = 0 \quad , \qquad (2.47d)$$

$$\tilde{P}_j(2,4) = -k_1(1-n^2) - C_1 x_{N_j}\Delta_{N_j}\ \frac{3x_{N_j}}{2h} \quad ,$$

$$\tilde{P}_j(3,1) = \frac{1}{x_{N_j}^3}\left[(k_3+k_4)n^2 + (k_3+n^2k_4+Cn^2\Delta_{N_j})\frac{3x_{N_j}}{2h}\right] + \frac{C_1\delta}{\lambda^2}\left(-\frac{3x_{N_j}}{2h} + n^2\right) \quad ,$$

$$\tilde{P}_j(3,2) = \frac{C_1\Delta_{N_j}}{\lambda^2}\left\{[1- +(2+\ )n^2]\ \frac{3}{2hx_{N_j}} - \frac{3n^2}{x_{N_j}^2}\right\} \quad ,$$

$$\tilde{P}_j\ (3,3) = -1 \quad ,$$

$$\tilde{P}_j\,(3,4) = \frac{C_1\delta_{N_j}}{\lambda^2}\left(-\frac{3x_{N_j}}{2h}\right) ,$$

$$\tilde{P}_j(4,1) = -\frac{1}{x_{N_j}^4}\left\{n^2[h_3(n^2-1)+C_2x_{N_j}^2\,\Delta_{N_j}] + [h_3(n^2-1)-n^2C_3\Delta_{N_j}]\,\frac{3x_{N_j}}{2h}\right\}$$
$$-\frac{C_1\delta_{N_j}}{\lambda^2}\left(-\frac{3}{2h}+\frac{n^2}{x_{N_j}}\right) ,$$

$$\tilde{P}_j(4,2) = -\frac{C_1\delta_{N_j}}{\lambda^2}\left\{[1-\nu+(2+\nu)n^2]\,\frac{3}{2hx_{N_j}^2} - \frac{3n^2}{x_{N_j}^3}\right\} ,$$

$$\tilde{P}_j\,(4,3) = -\frac{3}{2h} ,$$

$$\tilde{P}_j\,(4,4) = \frac{C_1\delta_{N_j}}{\lambda^2}\,\frac{3}{2h} ,$$

$$\tilde{Q}_j(1,1) = k_2(1-n^2)\left(-\frac{2x_{N_j}}{h}\right) - C_1x_{N_j}\Delta_{N_j}\left(-\frac{2x_{N_j}}{h}\right) ,$$

$$\tilde{Q}_j(1,2) = k_2(1-n^2)[1+(2+\nu)n^2]\frac{2}{hx_{N_j}} - C_1x_{N_j}\Delta_{N_j}\,[1-\nu+(2+\nu)n^2]\frac{2}{hx_{N_j}} ,$$

$$\tilde{Q}_j\,(1,3) = 0 ,$$

$$\tilde{Q}_j(1,4) = k_2(1-n^2)\left(-\frac{2x_{N_j}}{h}\right) - C_1x_{N_j}\Delta_{N_j}\left(-\frac{2x_{N_j}}{h}\right) , \qquad (2.47e)$$

$$\tilde{Q}_j(2,1) = -C_1x_{N_j}\Delta_{N_j}\left(-\frac{2x_{N_j}}{h}\right) ,$$

$$\tilde{Q}_j(2,2) = (1-n^2)\,\frac{2}{h} - k_1(1-n^2)\frac{2\nu}{hx_{N_j}} - C_1x_{N_j}\Delta_{N_j}[1-\nu+(2+\nu)n^2]\frac{2}{hx_{N_j}} ,$$

$$\tilde{Q}_j\,(2,3) = 0 ,$$

$$\tilde{Q}_j(2,4) = -C_1x_{N_j}\Delta_{N_j}\left(-\frac{2x_{N_j}}{h}\right) ,$$

$$\tilde{Q}_j(3,1) = -\frac{1}{x_{N_j}^3}\,(k_3+n^2k_4+Cn^2\Delta_{N_j})\left(-\frac{2x_{N_j}}{h}\right) + \frac{C_1\delta_{N_j}}{\lambda^2}\left(\frac{2x_{N_j}}{h}\right)$$

$$\tilde{Q}_j\ (3,2) = \frac{C_1\delta_{N_j}}{\lambda^2}\ [1-\nu+(2+\nu)n^2]\ \left(-\frac{2}{hx_{N_j}}\right)\ ,$$

$$\tilde{Q}_j\ (3,3) = 0\ ,$$

$$\tilde{Q}_j\ (3,4) = \frac{C_1\delta_{N_j}}{\lambda^2}\ \left(\frac{2x_{N_j}}{h}\right)\ ,$$

$$\tilde{Q}_j(4,1) = -\frac{1}{x_{N_j}^4}\ [k_j(n^2-1)-n^2C_3\Delta_{N_j}]\left(-\frac{2x_{N_j}}{h}\right)-\frac{C_1\delta_{N_j}}{\lambda^2}\ \frac{2}{h}\ ,$$

$$\tilde{Q}_j(4,2) = -\frac{C_1\delta_{N_j}}{\lambda^2}\ [1-\nu+(2+\nu)n^2]\left(-\frac{2}{hx_{N_j}^2}\right)\ ,$$

$$\tilde{Q}_j\ (4,3) = \frac{2}{h}\ ,$$

$$\tilde{Q}_j\ (4,4) = -\frac{C_1\delta_{N_j}}{\lambda^2}\ \frac{2}{h}\ ,$$

$$\tilde{R}_j = -\frac{1}{4}\ \tilde{Q}_j\ , \qquad (2.47e)$$

$$\tilde{S}_j = \begin{bmatrix} 0 & 0 & 0 & 0 \\ -1 & 0 & 0 & 0 \\ 0 & \frac{\nu}{2hx_{N_j}} & 0 & 0 \\ 0 & [1-\nu+(2+\nu)n^2]\frac{1}{2hx_{N_j}} & 0 & -\frac{x_{N_j}}{2h} \end{bmatrix} \qquad (2.47f)$$

$$\tilde{T}_j = -4\tilde{S}_j \qquad (2.47g)$$

$$\tilde{U}_j = \begin{bmatrix} 1 & 0 & 0 & 0 \\ -3 & 0 & 0 & 0 \\ 0 & \frac{3\nu}{2x_{N_j}h} + \frac{\nu n^2}{x_{N_j}^2} & 0 & 1 \\ 0 & [1-\nu+(2+\nu)n^2]\frac{3}{2hx_{N_j}} + \frac{3n^2}{x_{N_j}^2} & 0 & -\frac{3x_{N_j}}{2h} \end{bmatrix}, \tag{2.47h}$$

$$\tilde{V}_j = \begin{bmatrix} -1 & 0 & 0 & 0 \\ -3 & 0 & 0 & 0 \\ 0 & \frac{3\nu}{2x_{N_j}h} - \frac{\nu n^2}{x_{N_j}^2} & 0 & -1 \\ 0 & [1-\nu+(2+\nu)n^2]\frac{3}{2hx_{N_j}} - \frac{3n^2}{x_{N_j}^2} & 0 & -\frac{3x_{N_j}}{2h} \end{bmatrix}, \tag{2.47i}$$

$$\tilde{W}_j = \tilde{T}_j \ ,$$

$$\tilde{X}_j = \tilde{S}_j \ , \tag{2.47j}$$

where $\Delta = \Phi^{*+} - \Phi^{*-}$ and $\delta = \theta^{*+} - \theta^{*-}$. Equations (2.46) can be combined as

$$Q_j^{**}\tilde{y}_{N_j-1} + P_j^{**}\tilde{y}_{N_j}^- + N_j^{**}\tilde{y}_{N_j}^+ = 0 \ ,$$

$$P_j^{*}\tilde{y}_{N_j}^- + N_j^{*}\tilde{y}_{N_j}^+ + M_j^{*}\tilde{y}_{N+1} = 0 \ , \tag{2.48}$$

where

$$P_j^* = \bar{P}_j - \bar{Q}_j \bar{T}_j^{-1} \bar{U}_j \quad ,$$

$$N_j^* = \bar{N}_j - \bar{Q}_j \bar{T}_j^{-1} \bar{V}_j \quad ,$$

$$M_j^* = \bar{M}_j - \bar{Q}_j \bar{T}_j^{-1} \bar{\bar{T}}_j \quad ,$$

$$Q_j^* = \bar{Q}_j - \bar{M}_j \bar{\bar{T}}_j^{-1} \bar{T}_j \quad ,$$

$$P_j^{**} = \bar{P}_j - \bar{M}_j \bar{\bar{T}}_j^{-1} \bar{U}_j \quad ,$$

$$N_j^{**} = \bar{N}_j - \bar{M}_j \bar{\bar{T}}_j^{-1} \bar{V}_j \quad ,$$

$$\bar{Q}_j = \tilde{Q}_j - \tilde{R}_j \tilde{G}_j^{-1} \tilde{F}_j \quad ,$$

$$\bar{P}_j = \tilde{P}_j - \tilde{R}_j \tilde{G}_j^{-1} \tilde{E}_j \quad ,$$

$$\bar{T}_j = \tilde{T}_j - \tilde{S}_j \tilde{G}_j^{-1} \tilde{F}_j \quad ,$$

$$\bar{U}_j = \tilde{U}_j - \tilde{S}_j \tilde{G}_j^{-1} \tilde{E}_j \quad , \qquad (2.49)$$

$$\bar{N}_j = \tilde{N}_j - \tilde{L}_j \tilde{I}_j^{-1} \tilde{K}_j \quad ,$$

$$\bar{M}_j = \tilde{M}_j - \tilde{L}_j \tilde{I}_j^{-1} \tilde{J}_j \quad ,$$

$$\bar{V}_j = \tilde{V}_j - \tilde{S}_j \tilde{I}_j^{-1} \tilde{K}_j \quad ,$$

$$\bar{\bar{T}}_j = \tilde{T}_j - \tilde{S}_j \tilde{I}_j^{-1} \tilde{J}_j \quad ,$$

The boundary conditions, Equations (2.42) can be written as

$$\tilde{\tilde{Y}} y_{I+1} + \tilde{\tilde{Z}} y_I - \tilde{\tilde{Y}} y_{I-1} = 0 \qquad (2.50)$$

where

$$\tilde{Y} = \begin{bmatrix} 0 & 0 & 0 & 0 \\ 1 & 0 & 0 & 0 \\ 0 & -\frac{\nu}{2h\lambda} & 0 & 0 \\ 0 & -\frac{1}{2h\lambda}\left[1-\nu+(2+\nu)n^2\right] & 0 & \frac{\lambda}{2h} \end{bmatrix}, \tag{2.51a}$$

$$\tilde{Z} \begin{bmatrix} 1 & 0 & 0 & 0 \\ 0 & 0 & 0 & 0 \\ 0 & \frac{n^2\nu}{\lambda^2} & 0 & 1 \\ 0 & \frac{3n^2}{\lambda^2} & 0 & 0 \end{bmatrix} \tag{2.51b}$$

The solution of the critical load for bifurcation can be formed by the following procedure: Let α_i be a 4X4 matrix and

$$\tilde{y}_i = \alpha_i \tilde{y}_{i+1} \tag{2.52}$$

From Equations (2.43) we obtain the following recurrence relation between α_i $(i = 1,2,\ldots)$.

$$\alpha_i = (\tilde{B}_i + \tilde{C}_i \alpha_{i-1})^{-1} \tilde{A}_i \tag{2.53}$$

Since $\tilde{y}_i = 0$, we have

$$\alpha_1 = 0 \tag{2.54}$$

Thus from Equations (2.53) and (2.54), we can find all α_i up to the neighborhood of the first ring $i = N_1 - 2$. Note that

$$\tilde{y}_{N_j-2} = \alpha_{N_j-2}\tilde{y}_{N_j-1} \quad , \quad \tilde{y}_{N_j+1} = \alpha_{N_j+1}\tilde{y}_{N_j+2} \quad . \tag{2.55}$$

Let

$$\tilde{y}_{N_j-1} = \beta_{N_j-1}\tilde{y}_{N_j^-} \quad , \tag{2.56}$$

$$\tilde{y}_{N_j^-} = \beta_{N_j^-}\tilde{y}_{N_j^+} \quad , \tag{2.57}$$

$$\tilde{y}_{N_j^+} = \beta_{N_j^+}\tilde{y}_{N_j+1} \tag{2.58}$$

where β_{N_j-1}, $\beta_{N_j^-}$ and $\beta_{N_j^+}$ are 4X4 matrices. From Equations (2.44), (2.48), we have

$$\beta_{N_j-1} = -(\tilde{F}_j+\tilde{G}_j\alpha_{N_j-2})^{-1}\tilde{E}_j \quad , \tag{2.59}$$

$$\beta_{N_j^-} = -(P_j^{**}+Q_j^*B_{N_j-1})^{-1}N_j^{**} \quad , \tag{2.60}$$

$$\beta_{N_j^+} = -(N_j^*+P_j^*\beta_{N_j^-})^{-1}M_j^* \quad , \tag{2.61}$$

$$\alpha_{N_j+1} = -(\tilde{J}_j+\tilde{K}_j\beta_{N_j^+})\tilde{I}_j \quad . \tag{2.62}$$

For $i \geq N_j+2$, we again use the recurrence formula (2.53). Therefore, we are able to calculate all coefficient matrices α and β up to the boundary of the shell. From Equations (2.50) and (2.52) we have

$$S^*\tilde{y}_{I+1} = 0 \quad , \tag{2.63}$$

where

$$S^* = \tilde{Y} + (\tilde{Z}-\tilde{Y}\alpha_{I-1})\alpha_I \quad . \tag{2.64}$$

For a nontrivial solution $\tilde{y}_{I+1}$, we must have

$$\det S^* = 0 \quad . \tag{2.65}$$

Equation (2.65) is the characteristic equation for determination of the critical pressure for asymmetrical bifurcation.

The case n = 1 is a special case in which the differential Equations (2.26), the discontinuity and continuity conditions, Equations (2.41), and the boundary conditions, Equations (2.42), can be satisfied for all p by an exact solution $w_1 = o$ and $\psi_1 = x$. Hence, for the same reason explained in [2], we have the following equation for the case n = 1

$$[\bar{S}^*] \begin{bmatrix} \omega_{I+1} \\ u_{I+1} \\ v_{I+1} \end{bmatrix} = 0 \tag{2.66}$$

where $\bar{S}^*$ is the resulting matrix obtained from S^* by striking out the second column and the fourth row. Thus, for a nontrivial solution, we have

$$\det \bar{S}^* = 0 \quad . \tag{2.67}$$

Equation (2.67) is the characteristic equation for determination of the critical pressure for asymmetrical bifurcation with n = 1.

2.3.3 Numerical Procedures.

For a given geometry of a reinforced shallow clamped shell, we wish to find the critical load for axisymmetrical snap-through. Also, we want to know whether there is asymmetrical bifurcation before the axisymmetrical snap-through load is reached.

First of all, we choose a sufficiently small mesh size h such that the error due to the finite difference method is insignificantly small. For convenience, we shall assume that the positions of rings are arranged such that they are at the grid-points of the mesh. Therefore, we have $I = 1+\lambda/h$. The position of M rings, designated by $i = N_1, N_2, \ldots, N_M$ can be determined. Set IND = 0 .

In the initial trial, we set θ_i^* and Φ_i^* equal to zero. We may evaluate A_i, B_i and C_i from Equations (2.11), G and K from Equations (2.16). For $j = 1,2,\ldots, M$, we can calculate $x_j^* = x_{N_j}$, E_j, F_j and G_j, I_j, J_j and K_j from Equations (2.12), M_j, N_j, P_j, Q_j, R_j, S_j, T_j, U_j, V_j and W_j from Equation (2.14). For $i = 1$ and 2 and $j = 1,2,\ldots, M$, we can set $\theta_{ij} = \Phi_{ij} = 0$, where i = 1 stands for (-) and i = 2 for (+). Also we set $\alpha_1 = \beta_1 = \rho = \rho_s = 0$.

(A) For $i = 1,2,\ldots,I+1$, we may calculate f_i and g_i from Equations (2.8a) and (2.8b) and D_i from Equations (2.11). For i = 1 and 2 and $j = 1,2,\ldots, M$, calculate f_{ij} and g_{ij} from Equations (2.8), H_j and L_j from Equation (2.12). Then for $i = 2,3,\ldots N_1-2$ calculate α_i and β_i from Equation (2.18) and set j = 0.

(B) Set j = j+1. Find α_{N_j-1}, β_{N_j-1}, α_j^*, β_j^*, X_j, Y_j, α_{N_j}, βN_j, α_{N_j+1}, β_{N_j+1} from Equations (2.21).

(i) If $j < M$, for $i = N_j+2, N_j+3, \ldots N_{j+1}-2$, evaluate α_i and β_i by Equations (2.18) and then go to (B).

(ii) If $j = M$, for $i = N_j+2, N_j+3, \ldots, I+1$, calculate α_i and β_i from Equations (2.18) and calculate y_{I+2} from Equations (2.22). For $i = I+1, I, \ldots N_j$, calculate y_i from Equation (2.17) and set $j = M-1$.

(C) Calculate y_{2,N_j}, y_{1,N_j}, and y_{N_j-1} from Equation (2.20).

(i) If $j > 1$, then for $i = N_j-2, N_j-3, \ldots N_{j-1}+1$ calculate y_i from Equation (2.17), set $j = j-1$ and go to (C).

(ii) If $j = 1$, for $i = N_1-2, N_1-3, \ldots, 1$, calculate y_i from Equation (2.17) and then calculate ρ from Equation (2.23) using Simpson's rule where θ_{N_j} is θ_{1,N_j}.

(1) If $(\rho-\rho_s)/\rho_s$ is greater than a prescribed limit of error, set $\rho_s = \rho$ and IND = IND+1. If IND < 0, go to (A). Otherwise, go to end.

(2) If $(\rho-\rho_s)/\rho_s$ is smaller than a prescribed limit of error, set $j = 0$ and go to (D).

(D) $j = j+1$.

(i) If $j < M$ for $i = 1,2\ldots,N_j-1$ evaluate $\tilde{A}_i$, $\tilde{B}_i$, and $\tilde{C}_i$ from Equations (2.43), $\tilde{E}_j$, $\tilde{F}_j$, $\tilde{G}_j$, $\tilde{I}_j$, $\tilde{J}_j$, $\tilde{K}_j$, $\tilde{L}_j$, $\tilde{M}_j$, $\tilde{N}_j$, $\tilde{P}_j$ $\tilde{Q}_j$, $\tilde{R}_j$, $\tilde{S}_j$, $\tilde{U}_j$, $\tilde{V}_j$, $\tilde{W}_j$, $\tilde{X}_j$ from Equations (2.45-47), P_j^*, N_j^*, M_j^*, Q_j^*, P_j^{**}, N_j^{**}, $\bar{Q}_j$, $\bar{P}_j$, $\bar{T}_j$, $\bar{U}_j$, $\bar{N}_j$, $\bar{M}_j$, $\bar{V}_j$, $\bar{\bar{T}}_j$ from Equations (2.49). Go to (D).

(ii) If $j = M$, for $i = N_M+1, N_M+2, \ldots I-2$, evaluate $\tilde{A}_i$, $\tilde{B}_i$ and $\tilde{C}_i$ from Equations (2.43), $\tilde{Y}$ and $\tilde{Z}$ from Equations (2.51). Set $\alpha_1 = 0$, for $i = 2,3,\ldots, N_1-2$, calculate α_i from Equation (2.53) and set $j = 0$.

(E) Set $j = j+1$. Find β_{N_j-1} from Equations (2.59), $\beta_{N_j^-}$ from Equations (2.60), $\beta_{N_j^+}$ from Equations (2.61) and α_{N_j+1} from Equations (2.62).

(i) If $j < M$ for $i = N_j+2, N_j+3, \ldots, N_{j+1}-2$ calculate α_i from Equation (2.53) and go to (E).

(ii) If $j = M$ for $i = N_j+2, N_j+3, \ldots, I+1$, calculate α_i from Equation (2.53), S^* from Equation (2.64).

(1) If $n = 1$, evaluate $\overline{S}^*$ and $\det \overline{S}^*$. Print p, n, $\det \overline{S}^*$. Set $p = p+\Delta p$. If $p \leq p_f$ (p_f is an assigned value), then go to (A), otherwise go to end.

(2) If $n > 1$, evaluate S^* from Equation (2.64) and $\det S^*$. Print p, n, $\det S^*$. Set $p = p+\Delta p$. If $p \leq p_f$, go to (A). Otherwise, go to end.

2.4 Discussion

As was noted previously, a sufficient condition for the elimination of double folding and pointing in bladders consisting of rib-reinforced shells of revolution, is that no asymmetric bifurcation points exist. A necessary and sufficient condition (but less conservative) for the elimination of double folding and pointing is that all existing bifurcation branches be unstable. It is evident, therefore, that numerical programs are necessary to predict asymmetrical bifurcation if a rib-reinforced bladder is to be successfully designed.

In this chapter, a finite-difference method was developed to predict the nonlinear axisymmetrical deformation, and asymmetrical bifurcation of shallow, ring-reinforced spherical caps. The method employed appears to be quite tractable, in spite of the complexity of the problem. Only minor modifications would be necessary to include the case of a shallow, ring-reinforced shell of revolution with arbitrary meridianal shape. Extension of the method to deep ring-reinforced shells of revolution should also be possible, but would certainly constitute a major analytical effort.

For deep shells the foregoing program constitutes a first step in the solution procedure. A segment of a deep shell of revolution sufficiently near the apex can always be approximated by shallow shell theory. It would appear, therefore, that one

sensible solution procedure for bladders that are deep rib-reinforced shells of revolution would be to couple a shallow shell (representation near vertex) to conical shell segments, the latter approximating the deep portion of the shell between rings. It should, of course, be noted that the treatment of the shallow and deep portions of the shell would be quite different. For example, in the deep portion (under large axisymmetric deformation) the central portions of the shell would act primarily as a membrane, bending moments being important only in edge zones near a ring or boundary. This is in contrast to the prebuckling (axisymmetric) deformation of shallow shells for which the bending moments are significant over the entire shell. In order to properly calculate the edge moments in the deep sections, an asymptotic analysis, together with the results of Chapter I, would be necessary.

REFERENCES

1. Marguerre, K., "Zur Theorie der gekrümmnten Platte grosser Formänderung," Jahrbuch der 1939 der deutschen Luft hakrtforschung, p.413.

2. Huang, N. C., "Unsymmetrical Buckling of Thin Shallow Spherical Shells", J. Appl. Mech. 32, (1965) 323-330.

3. Fitch, J. R. and B. Budiansky, "The Buckling and Post-buckling Behavior of Spherical Caps Under Axisymmetric Load". Paper Presented at the 10th ASME/AIAA Structures, Structural Dynamics and Materials Conference, New Orleans, La., April, 1969.

4. Krenzke, M. A. and J. J. Kiernan, "Elastic Stability of Near Perfect Shallow Spherical Shells", AIAA Journal Vol. 1, p. 3855.

5. Parmeoter, R. R., "The Buckling of Clamped Shallow Spherical Shells Under Uniform Pressure, Aeroelasticity and Structural Dynamics SM 63-53, AFOSR5362. Graduate Aeronautical Laboratories, California Institute of Technology, Pasadena, California, November 1963.

6. Korter, W. T., "Over de stabiliteit van bet elastisch evenwicht" (in Dutch with English summary). Thesis Delft. H. J. Paris, Amsterdam, 1945.

7. Timoshenko, S., "Strength of Materials" Part II, D. Van Nostrand Company, Inc., New York, pp. 273-277.

8. Federhofer, K., "Nicht-lineare Biegungschwingungen des Kreisings", Ingenieur Archiv, Vol. 28, 1959, pp. 53-58.

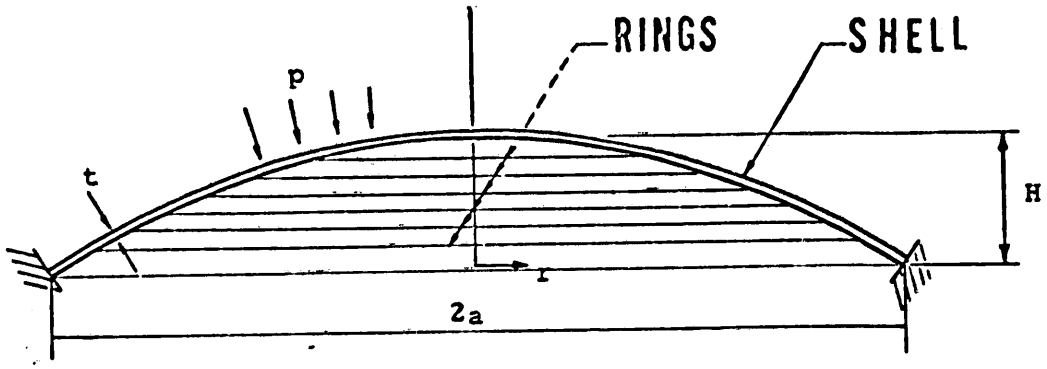

Figure 2.1 Geometry of Reinforced Clamped Shallow Spherical Shells.

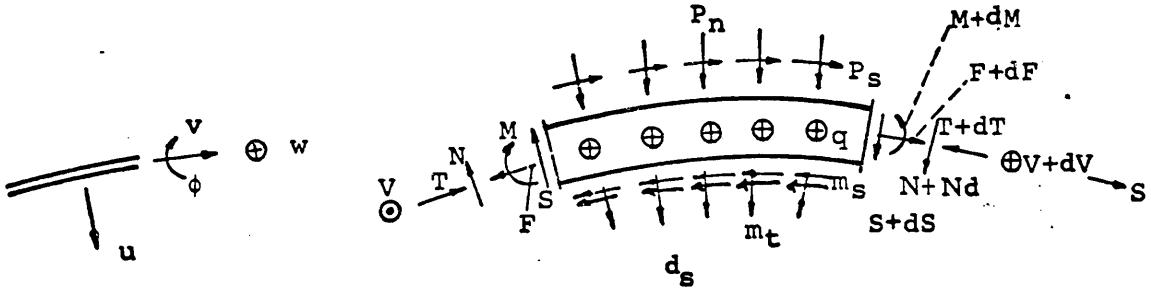

Figure 2.2 Forces, Moments, and Displacements of An Element of the Ring.

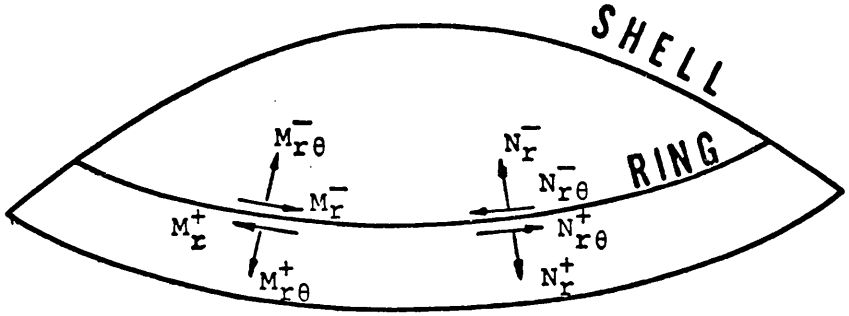

Figure 2.3 Discontinuity in Membrane Stresses and Bending Moments.

CHAPTER III

ANALYSIS OF A SINGLE FOLD IN AN ELASTOMER-METAL COMPOSITE

3.1. Introduction

For a composite that consists of a thin layer of metal placed between two layers of elastomer, and that undergoes folding, a good estimate of the state of stress is obtained if we use the following procedures: a) find the stress fields in the inner and outer layers of elastomer, using large deformation theory of elasticity, and treating the thin layer of metal as an inextensible central sheet (one may also regard the metal sheet as an elastic layer with an equivalent elastic constant, but we shall not do this here); b) under the bond stresses transmitted to the middle metal sheet by the elastomer, and using a plasticity theory, find the stress and strain fields in the metal layer. The assumption that the inner metal layer is inextensible can be justified on the grounds that the strains in the elastomer is by far larger than that in the metal, even when the metal undergoes plastic deformations. (On the other hand, the fact that the central metal sheet in fact is not inextensible can be accounted for by using some equivalent elastic constants, which may be taken to depend on the state of deformation in the metal or may be regarded constant throughout the metal layer at each state of loading.)

In the following, we shall formulate a plane-strain problem for the analysis of a single fold, using large deformation theory. In this formul-

ation, we employ the Lagrangian (or the initial particle position) variables as our independent variables, and integrate the basic field equations using an incremental loading and a finite-difference scheme.

Although the idea of accounting for both geometrical and material non-linearities in finite deformations by means of a step-by-step integration is not new [1-4], the use of the Lagrangian coordinates in conjunction with small deformations superimposed on finite initial deformations is new. In fact, it appears that a consistent and exact formulation of this kind has not, as yet, been developed. For example, in such a formulation one must be careful if Cauchy's stress tensor is used, since after each loading step the stress increment cannot be directly added to the initial stress field if they are not both referred to the same configuration of the body. Moreover, even if the body may consist of a material which is homogeneous and isotropic in its natural (virgin) state, at a given state of stress the same material, in general, is nonhomogeneous and anisotropic in its response to an incremental deformation superimposed on the initial stress-state. These and similar facts are unfortunately not fully appreciated by most numerical analysts in the field of structural mechanics.

A complete and correct numerical formulation of finite deformation, including thermal and material memory effects, has been given by Oden in a series of papers [5, 6]. Oden, however, casts his field equations directly into a system of non-linear algebraic equations which may not readily lend themselves to a numerical evaluation; the required iterative numerical process may become divergent. We note that a method of this kind has been first used by Becker [7].

An incremental formulation of large deformation problems is presented by Felippa [8] , using an Eulerian formulation in which all the field quantities are referred to the current deformed state of the body. The fact that the geometry of the body in finite deformation is continually changing makes such a formulation cumbersome. In addition to this, Felippa's results are based on a stress-increment which is incorrect in the sense that it lacks a term linear in the displacement gradient and proportional to the stress tensor at the given state. For metallic materials with elastic moduli of the order of 30×10^6 psi , this term can be neglected without inducing substantial errors. For non-metallic materials, and also for metals in the plastic range, on the other hand, this term is of the same order of magnitude or larger than those included, and hence may not be neglected. In addition,to this, Felippa uses the isotropic version of Hooke's Law to relate his stress-increments to the corresponding strain-increments at a finitely deformed state. Such a relation, in general, is incorrect.

In Section 5 of this chapter, we shall formulate a general variational approach for an incremental loading at large deformations. We shall employ consistently a Lagrangian formulation, leading to results which are exact in the framework of the considered incremental loading. Moreover, no assumption will be made regarding the elasticity coefficients in the stress-strain incremental relations so that our result would be applicable to elastic materials of all kinds which may even be anisotropic in their initial undeformed state. The numerical formulation of this variational approach is not presented here. The method however, lends itself to a consistent finite element approximation, see Nemat-Nasser and Shatoff [9].

3.2 Kinematics, Dynamics, and Constitutive Relations

We choose a fixed rectangular Cartesian coordinate system with the unit base vectors $\underset{\sim}{e}_1$, $\underset{\sim}{e}_2$, and $\underset{\sim}{e}_3$, and let $\underset{\sim}{X} = X_1 \underset{\sim}{e}_1 + X_2 \underset{\sim}{e}_2 + X_3 \underset{\sim}{e}_3$, denote the positions of the particles X in their initial unstrained state. We refer to $\underset{\sim}{X} = X_\alpha \underset{\sim}{e}_\alpha$ as the Lagrangian coordinates, and let

$$\begin{aligned} x_1 &= x_1(X_1, X_2) \quad , \\ x_2 &= x_2(X_1, X_2) \quad , \\ x_3 &= X_3 \quad , \end{aligned} \tag{2.1}$$

denote the positions of the particles in a deformed state; $\underset{\sim}{x} = x_i \underset{\sim}{e}_i$ will be referred to as the Eulerian coordinates. Here, the repeated subscripts, α and i, are to be summed for $\alpha, i = 1, 2, 3$. We assume that (2.1) is a smooth and invertable mapping, having the following inverse:

$$\begin{aligned} X_1 &= X_1(x_1, x_2) \quad , \\ X_2 &= X_2(x_1, x_2) \quad , \\ X_3 &= x_3 \quad . \end{aligned} \tag{2.2}$$

Hence, we assume that the Jacobian

$$J = \begin{vmatrix} \dfrac{\partial x_1}{\partial X_1} & \dfrac{\partial x_1}{\partial X_2} \\ \dfrac{\partial x_2}{\partial X_1} & \dfrac{\partial x_2}{\partial X_2} \end{vmatrix} = \frac{\partial x_1}{\partial X_1}\frac{\partial x_2}{\partial X_2} - \frac{\partial x_1}{\partial X_2}\frac{\partial x_2}{\partial X_1} \tag{2.3}$$

is neither zero nor infinity.

For the sake of conciseness in the presentation, we shall use Greek subscript letters to refer to the Lagrangian, and the Italic subscript letters to the Eulerian variables, respectively. Since plane-strain problems are considered, these subscript letters will have the range 1, 2. A comma followed by a subscript letter will denote partial differentiation with respect to the corresponding coordinate.

The so-called Green's and Finger's deformation tensors are

$$\underset{\sim}{C} = C_{\alpha\beta}\,\underset{\sim}{e}_\alpha \underset{\sim}{e}_\beta = x_{i,\alpha} x_{i,\beta}\,\underset{\sim}{e}_\alpha \underset{\sim}{e}_\beta \quad , \tag{2.4a}$$

$$\underset{\sim}{b} = b_{ij}\,\underset{\sim}{e}_i \underset{\sim}{e}_j = x_{i,\alpha} x_{j,\alpha}\,\underset{\sim}{e}_i \underset{\sim}{e}_j \quad , \tag{2.4b}$$

and the Lagrangian strain tensor is given by

$$\underset{\sim}{\varepsilon} = \tfrac{1}{2}\,(\underset{\sim}{C} - \underset{\sim}{\delta}) \quad , \tag{2.4c}$$

where $\underset{\sim}{\delta}$ denotes the identity tensor. We note that the normal component* of $\underset{\sim}{C}$ in a direction defined by the unit vector $\underset{\sim}{M}$ gives the squared stretch, $(ds/dS)^2$, of an element initially in that direction, where dS is the initial and ds the current length of the element. In particular, the principal values of the symmetric tensor $\underset{\sim}{C}$ (or those of $\underset{\sim}{b}$) are the squared stretches Λ_K^2, $K = I, II, III$. We note that, since a state of plane-strain is assumed, the $\underset{\sim}{e}_3$-direction is one of the principal directions. If we let this direction be that of the third principal axis, we then have $\Lambda_{III} = 1$. The squared stretches, Λ_K^2, are the roots of the equation

---

* If M_α and $C_{\alpha\beta}$, $\alpha, \beta = 1, 2$, are components of $\underset{\sim}{M}$ and $\underset{\sim}{C}$, respectively, then the normal component of $\underset{\sim}{C}$ in the direction $\underset{\sim}{M}$ is given by $C_{\alpha\beta} M_\alpha M_\beta$.

$$z^3 - \bar{I}\, z^2 + \bar{II}\, z - \bar{III} = 0 \quad , \tag{2.5a}$$

where, for the considered plane-strain problem, the basic invariants of $\underset{\sim}{C}$ (or those of $\underset{\sim}{b}$) are

$$\begin{aligned} \bar{I} &= \mathrm{tr}\, \underset{\sim}{C} = \Lambda_I^2 + \Lambda_{II}^2 + 1 \\ \bar{II} &= \Lambda_I^2 \Lambda_{II}^2 + \Lambda_I^2 + \Lambda_{II}^2 \\ &= \bar{III} + \bar{I} - 1 \\ \bar{III} &= \Lambda_I^2 \Lambda_{II}^2 \end{aligned} \tag{2.5b}$$

Substitution from (2.5b) into (2.5a) now yields

$$z^3 - \bar{I}\, z^2 + (\bar{III} + \bar{I} - 1)\, z - \bar{III} = 0 \tag{2.5c}$$

which has one root equal to 1. Since in (2.5b) there are only two independent invariants, we shall denote them by

$$\begin{aligned} I &= \Lambda_I^2 + \Lambda_{II}^2 \\ II &= \Lambda_I^2 \Lambda_{II}^2 \end{aligned} \tag{2.5d}$$

For incompressible materials, we have

$$J = \sqrt{\bar{II}} = \frac{\partial x_1}{\partial X_1} \frac{\partial x_2}{\partial X_2} - \frac{\partial x_1}{\partial X_2} \frac{\partial x_2}{\partial X_1} = 1 \tag{2.6a}$$

Now setting $\Lambda_I^2 = \Lambda^2$, we reduce (2.5d) to

$$I = \Lambda^2 + \frac{1}{\Lambda^2} \quad , \qquad II = 1 \tag{2.6b}$$

Let us now consider conditions for the equilibrium of an element. To this end, we denote by $\underset{\sim}{\mathcal{T}} = T_{ij}\, \underset{\sim}{e}_i\, \underset{\sim}{e}_j$ the Cauchy* (or true) stress tensor, and note that the traction vector on an element having a unit normal $\underset{\sim}{\nu} = \nu_j\, \underset{\sim}{e}_j$ in its deformed state is given by

$$t_i = T_{ji}\, \nu_j \quad , \tag{2.7}$$

where $\underset{\sim}{t} = t_i\, \underset{\sim}{e}_i$ is traction per unit current area of the considered element. Now, in the absence of body forces, the equilibrium equations are

$$\frac{\partial T_{ji}}{\partial x_j} = 0 \quad . \tag{2.8}$$

For our formulation, it is more convenient to work with the so-called first Pialo-Kirchhoff stress tensor, $\underset{\sim}{\mathcal{T}}^R = T^R_{\alpha i}\, \underset{\sim}{e}_\alpha\, \underset{\sim}{e}_i$, defined by

$$T^R_{\alpha i} = J\, \frac{\partial X_\alpha}{\partial x_j}\, T_{ji} \quad . \tag{2.9}$$

We note that $T^R_{\alpha i}$ is the component in the $\underset{\sim}{e}_i$-direction of the traction vector, measured per unit initial area, acting on an element that initially was perpendicular to the $\underset{\sim}{e}_\alpha$-direction. $T^R_{\alpha i}$ is not a symmetric tensor.

In terms of the stress tensor $\underset{\sim}{\mathcal{T}}^R$ the equilibrium equations (2.8) become

$$\frac{\partial T^R_{\alpha i}}{\partial X_\alpha} = 0 \tag{2.10}$$

which are expressed in terms of the Lagrangian variables.

---

* Since no couple stresses will be considered, $\underset{\sim}{\mathcal{T}}$ is a symmetric tensor.

To formulate the constitutive equations for elastomers, we shall ignore all thermal effects,* and assume that the elastic solid is homogeneous and isotropic, possessing a strain-energy function given by

$$\Sigma = \Sigma(\bar{I}, \bar{II}, \bar{III}) \quad , \tag{2.11}$$

where $\bar{I}$, $\bar{II}$, and $\bar{III}$ are the basic invariants of the Green deformation tensor $\underset{\sim}{C}$. In this case, it can readily be shown that the stress tensor $T^R_{\alpha i}$ is given by

$$T^R_{\alpha i} = \frac{\partial \Sigma}{\partial x_{i,\alpha}} \quad . \tag{2.12}$$

Using a straight forward but lengthy calculation, one can show that Cauchy's stress tensor may now be expressed as

$$T_{ij} = \frac{2}{J}\left\{\bar{III}\,\frac{\partial \Sigma}{\partial \bar{III}}\,\delta_{ij} + \left(\frac{\partial \Sigma}{\partial \bar{I}} + \bar{I}\,\frac{\partial \Sigma}{\partial \bar{II}}\right) b_{ij} - \frac{\partial \Sigma}{\partial \bar{II}}\, b_{ik}\, b_{kj}\right\} \quad , \tag{2.13}$$

where b_{ij} are the components of Finger's strain tensor defined by (2.4b).

For incompressible materials, (2.13) becomes

$$T_{ij} = -\,p\,\delta_{ij} + 2\left[\frac{\partial \Sigma}{\partial \bar{I}} + \bar{I}\,\frac{\partial \Sigma}{\partial \bar{II}}\right] b_{ij} - 2\,\frac{\partial \Sigma}{\partial \bar{II}}\, b_{ik}\, b_{kj} \quad , \tag{2.14}$$

where p is the hydrostatic pressure to be determined as part of solution. From (2.14) it can be seen that the principal stresses T_K, $K = I, II, III$, are related to the principal stretches Λ_K, $K = I, II, III$, by

$$T_K = -\,p + 2\,\frac{\partial \Sigma}{\partial \bar{I}}\,\Lambda_K^2 - 2\,\frac{\partial \Sigma}{\partial \bar{II}}\,\Lambda_K^{-2} \quad , \tag{2.15}$$

---

* These effects can be included, but we shall not do this here, since it will take us beyond the scope of the present work.

where we also have

$$\Lambda_I \, \Lambda_{II} \, \Lambda_{III} = 1$$

because of incompressibility.

Ideal materials for which the strain-energy function, Σ, takes on the form

$$\Sigma = \tfrac{1}{2} \alpha (I-3) - \tfrac{1}{2} \beta (II - 3) \tag{2.16}$$

were considered by Mooney [10] for representing the elastic behavior of rubber-like materials. Here $\alpha = 2 \dfrac{\partial \Sigma}{\partial \bar{I}}$, and $\beta = -2 \dfrac{\partial \Sigma}{\partial \bar{II}}$ are assumed to be constants characterizing the material. For $\beta = 0$, we have the strain-energy function of the so-called neo-Hookean materials considered by Rivlin [11]. This type of strain-energy functions can also be developed using a statistical approach and a molecular theory for highly elastic materials, as is shown by Treloar [12].

For incompressible plane-strain problems, (2.16) may be written as

$$\Sigma = \tfrac{1}{2} \mu (\bar{I} - 3) \quad , \tag{2.17}$$

where, for small deformations, μ can be interpreted as the classical shear modulus. In the following, we shall illustrate our results using the strain-energy function (2.17). However, these results can readily be modified to account for more complicated constitutive relations that may correspond to a given elastomer.

3.3 Formulation of Basic Problem

3.3.1 Field Equations: Using the expression (2.17), we express $T^R_{\alpha i}$ as

$$\frac{1}{\mu} T^R_{\alpha i} = \frac{\partial x_i}{\partial X_\alpha} - \bar{p} \frac{\partial X_\alpha}{\partial x_i} \quad , \tag{3.1}$$

where $\bar{p} = \frac{p}{\mu}$. Equilibrium equations now are

$$\left[\frac{1}{\mu} T^R_{\alpha i}\right]_{,\alpha} = \frac{\partial^2 x_i}{\partial X_\alpha \partial X_\alpha} - \frac{\partial \bar{p}}{\partial X_\alpha} \frac{\partial X_\alpha}{\partial x_i} - \bar{p} \frac{\partial^2 X_\alpha}{\partial x_i \partial X_\alpha}$$

Since $\partial^2 X_\alpha / \partial x_i \partial X_\alpha = 0$, we obtain

$$\left[\frac{1}{\mu} T^R_{\alpha i}\right]_{,\alpha} = \frac{\partial^2 x_i}{\partial X_\alpha \partial X_\alpha} - \frac{\partial \bar{p}}{\partial X_\beta} \frac{\partial X_\beta}{\partial x_i} = 0 \quad . \tag{3.2}$$

Consider now a deformed (equilibrium) state of the body, and let $u_i = u_i(X_1, X_2)$ and $q = q(X_1, X_2)$ denote, respectively, variations in x_i and $\bar{p}$ that are induced by increasing the applied loads or the imposed surface displacements by small amounts. We assume that the new state of the body, defined by $x_i + u_i$ and $\bar{p} + q$, constitutes an equilibrium state. Writing the equations of equlibrium for the new state, and using (3.2), we obtain

$$\left(\frac{\partial x_i}{\partial X_\beta}\right) \frac{\partial^2 u_i}{\partial X_\alpha \partial X_\alpha} + \left(\frac{\partial^2 x_i}{\partial X_\alpha \partial X_\alpha}\right) \frac{\partial u_i}{\partial X_\beta} = \frac{\partial q}{\partial X_\beta} \quad , \quad i, \alpha, \beta = 1, 2 \quad . \tag{3.3}$$

Since the material is assumed to be incompressible, we have $J = \det |x_{i,\alpha}|$ $= \det \left| \frac{\partial x_i}{\partial X_\alpha} + \frac{\partial u_i}{\partial X_\alpha} \right| = 1$ which yields

$$\frac{\partial u_1}{\partial X_1}\frac{\partial x_2}{\partial X_2} + \frac{\partial u_2}{\partial X_2}\frac{\partial x_1}{\partial X_1} - \frac{\partial u_1}{\partial X_2}\frac{\partial x_2}{\partial X_1} + \frac{\partial u_2}{\partial X_1}\frac{\partial x_1}{\partial X_2} = 0 \quad . \tag{3.4}$$

To simplify notation, let us set

$$X_1 = X \quad , \quad X_2 = Y \quad , \quad x_1 = x \quad , \quad x_2 = y$$

$$u_1 = u \quad , \quad u_2 = v \quad , \quad \nabla^2 \equiv \frac{\partial^2}{\partial X^2} + \frac{\partial^2}{\partial Y^2} \quad , \tag{3.5}$$

and obtain, from (3.3) and (3.4),

$$\left(\frac{\partial x}{\partial X}\right)\nabla^2 u + \left(\frac{\partial y}{\partial X}\right)\nabla^2 v + (\nabla^2 x)\frac{\partial u}{\partial X} + (\nabla^2 y)\frac{\partial v}{\partial X} = \frac{\partial q}{\partial X} \tag{3.6a}$$

$$\left(\frac{\partial x}{\partial Y}\right)\nabla^2 u + \left(\frac{\partial y}{\partial Y}\right)\nabla^2 v + (\nabla^2 x)\frac{\partial u}{\partial Y} + (\nabla^2 y)\frac{\partial v}{\partial Y} = \frac{\partial q}{\partial Y} \tag{3.6b}$$

$$\left(\frac{\partial y}{\partial Y}\right)\frac{\partial u}{\partial X} + \left(\frac{\partial x}{\partial X}\right)\frac{\partial v}{\partial Y} - \left(\frac{\partial y}{\partial X}\right)\frac{\partial u}{\partial Y} - \left(\frac{\partial x}{\partial Y}\right)\frac{\partial v}{\partial X} = 0 \quad . \tag{3.6c}$$

For a given state, x and y are known functions of X and Y. Hence all the coefficients in equations (3.6) are known functions of X and Y. These equations, therefore, are coupled linear partial differential equations defining small changes in the particle positions and the pressure caused by a small change in the boundary conditions.

Beginning with the undeformed state, we apply the first increment of loading (or displacement) on the boundary. Corresponding to this boundary condition, we solve the following equations:

$$\nabla^2 u = \frac{\partial q}{\partial X} \quad , \tag{3.7a}$$

$$\nabla^2 v = \frac{\partial q}{\partial Y} \quad , \tag{3.7b}$$

$$\frac{\partial u}{\partial X} + \frac{\partial v}{\partial Y} = 0 \quad . \tag{3.7c}$$

Denoting the solution to these equations by a superposed zero, we write

$$x^{(1)} = X + u^{(0)} \quad ,$$

$$y^{(1)} = Y + v^{(0)} \quad ,$$

$$q^{(1)} = 0 + p^{(0)} \quad .$$

Using $x^{(1)}$, and $y^{(1)}$, we calculate $\partial x^{(1)}/\partial X$, $\partial x^{(1)}/\partial Y$, etc., and substituting into (3.6), we solve for $u^{(1)}$, $v^{(1)}$, and $q^{(1)}$ that correspond to a new incremental loading. In this manner, the field equations are integrated step-by-step.

3.3.2 Stress Boundary Conditions: Let S_1 denote that part of the boundary S of the body on which the surface tractions T_i are applied. We then have

$$T^R_{\alpha i} N_\alpha = T_i \quad \text{on} \quad S_1 \quad , \tag{3.8a}$$

where $\underset{\sim}{N} = N_\alpha \underset{\sim}{e}_\alpha$ is the unit normal on S_1 in its undeformed state. Substitution from (3.1) into (3.8a) now yields

$$T_i = N_\alpha \left(\mu \frac{\partial x_i}{\partial X_\alpha} - p \frac{\partial X_\alpha}{\partial x_i} \right) \quad . \tag{3.8b}$$

To express this equation in terms of the Lagrangian variables only, we write

$$[X_{\alpha,i}] = [x_{i,\alpha}]^{-1}$$

or

$$\begin{bmatrix} \frac{\partial X}{\partial x} & \frac{\partial X}{\partial y} & 0 \\ \frac{\partial Y}{\partial x} & \frac{\partial Y}{\partial y} & 0 \\ 0 & 0 & 1 \end{bmatrix} = \begin{bmatrix} \frac{\partial y}{\partial Y} & -\frac{\partial y}{\partial X} & 0 \\ -\frac{\partial x}{\partial Y} & \frac{\partial x}{\partial X} & 0 \\ 0 & 0 & 1 \end{bmatrix} . \qquad (3.9)$$

With the aid of (3.9), (3.8b) becomes

$$\frac{1}{\mu} T_1 = N_1 \left(\frac{\partial x}{\partial X} - \bar{p} \frac{\partial y}{\partial Y} \right) + N_2 (1+\bar{p}) \frac{\partial x}{\partial Y} , \qquad (3.10a)$$

$$\frac{1}{\mu} T_2 = N_1 (1+\bar{p}) \frac{\partial y}{\partial X} + N_2 \left(\frac{\partial y}{\partial Y} - \bar{p} \frac{\partial x}{\partial X} \right) . \qquad (3.10b)$$

If ΔT_i denotes the increment in surface tractions on S_1, we obtain

$$\frac{1}{\mu} \Delta T_1 = N_1 \left(\frac{\partial u}{\partial X} - \bar{p} \frac{\partial v}{\partial Y} \right) + N_2 (1+\bar{p}) \frac{\partial u}{\partial Y} + \left(- N_1 \frac{\partial y}{\partial Y} + N_2 \frac{\partial x}{\partial Y} \right) q , \qquad (3.11a)$$

$$\frac{1}{\mu} \Delta T_2 = N_1 (1+\bar{p}) \frac{\partial v}{\partial X} + N_2 \left(\frac{\partial v}{\partial Y} - \bar{p} \frac{\partial u}{\partial X} \right) + \left(N_1 \frac{\partial y}{\partial X} - N_2 \frac{\partial x}{\partial X} \right) q . \qquad (3.11b)$$

Since the final stress field must be expressed in terms of the true (or Cauchy) stress tensor, we shall note here the following relations:

$$T^R_{11} = \frac{\partial y}{\partial Y} T_{11} - \frac{\partial y}{\partial X} T_{12} ,$$

$$T^R_{12} = \frac{\partial y}{\partial Y} T_{21} - \frac{\partial y}{\partial X} T_{22} ,$$

$$T^R_{21} = - \frac{\partial x}{\partial Y} T_{11} + \frac{\partial x}{\partial X} T_{12} ,$$

$$T^R_{22} = - \frac{\partial x}{\partial Y} T_{21} + \frac{\partial x}{\partial X} T_{22} . \qquad (3.12)$$

Solving (3.12) for T_{ij}, we obtain

$$T_{11} = \frac{\partial x}{\partial X} T^R_{11} + \frac{\partial x}{\partial Y} T^R_{21} \quad ,$$

$$T_{12} = T_{21} = \frac{\partial y}{\partial X} T^R_{11} + \frac{\partial y}{\partial Y} T^R_{21} \quad ,$$

$$T_{21} = T_{12} = \frac{\partial x}{\partial X} T^R_{12} + \frac{\partial x}{\partial Y} T^R_{22} \quad ,$$

$$T_{22} = \frac{\partial y}{\partial X} T^R_{12} + \frac{\partial y}{\partial Y} T^R_{22} \quad . \tag{3.13}$$

3.3.3 Boundary Conditions at Elastomer-Metal Interface: As was pointed out in Section 3.1, when calculating the stress field in the elastomer, the thin middle layer of metal may be regarded inextensible. The condition of inextensibility is that the normal component of the Lagrangian strain tensor, taken in the direction of a unit vector tangent to the initial elastomer-metal interface, is zero, that is

$$2E_{\alpha\beta} M_\alpha M_\beta = x_{i,\alpha} x_{i,\beta} M_\alpha M_\beta - 1 = 0$$

or

$$x_{i,\alpha} x_{i,\beta} M_\alpha M_\beta = 1 \quad , \tag{3.14a}$$

where $\underset{\sim}{M} = M_\alpha \underset{\sim}{e}_\alpha$ is a unit vector tangent to the elastomer-metal interface in its initial undeformed state. For the incremental loading, (3.14a) must hold in each step, leading to

$$u_{i,\alpha} x_{i,\beta} M_\alpha M_\beta = 0 \quad . \tag{3.14b}$$

In particular, if $\underset{\sim}{M}$ is taken to be parallel to the X-axis, we have $M_1 = 1$, $M_2 = 0$, reducing (3.14b) to

$$\frac{\partial u}{\partial X}\frac{\partial x}{\partial X} + \frac{\partial v}{\partial X}\frac{\partial y}{\partial X} = 0 \quad . \tag{3.14c}$$

In addition to the kinematical condition (3.14) at the interface, the normal tractions exerted on one face of the metal sheet by the elastomer must be balanced by that applied on the other face of the metal. Assuming that the metal sheet is very thin relative to the elastomer, and using the inextensibility condition, we get

$$\left[T^R_{\alpha i}\, X_{\beta,i}\, N_\alpha N_\beta\right]^{(+)} - \left[T^R_{\alpha i}\, X_{\beta,i}\, N_\alpha N_\beta\right]^{(-)} = 0 \quad , \tag{3.15a}$$

where the superscript (+) refers to one face of the metal sheet and the superscript (-) refers to the other face. Note that the usual sign convention in elasticity is used, namely that normal stresses are positive in tension and negative in compression, and that the positive shear stress points towards the positive direction of the corresponding axis when it acts on a plane whose unit normal points toward the positive direction of a perpendicular axis. Here $\underset{\sim}{N} = N_\alpha \underset{\sim}{e}_\alpha$ is a unit vector normal to the interface. In particular, if we take $\underset{\sim}{N}$ parallel to the Y-axis, we have $N_1 = 0$, $N_2 = 1$, which yields

$$\left[T^R_{22}\frac{\partial x}{\partial X} - T^R_{21}\frac{\partial x}{\partial Y}\right]^{(+)} = \left[T^R_{22}\frac{\partial x}{\partial X} - T^R_{21}\frac{\partial x}{\partial Y}\right]^{(-)} \quad , \tag{3.15b}$$

where (3.9) is also used. For an incremental loading, (3.15b) becomes

$$\left[\Delta T^R_{22}\frac{\partial x}{\partial X} + T^R_{22}\frac{\partial u}{\partial X} - \Delta T^R_{21}\frac{\partial x}{\partial Y} - T^R_{21}\frac{\partial u}{\partial Y}\right]^{(+)}$$

$$= \left[\Delta T^R_{22}\frac{\partial x}{\partial X} + T^R_{22}\frac{\partial u}{\partial X} - \Delta T^R_{21}\frac{\partial x}{\partial Y} - T^R_{21}\frac{\partial u}{\partial Y}\right]^{(-)} \quad . \tag{3.15c}$$

3.4 Numerical Scheme of Finite-Differencing

The system of partial differential equations (3.6) will now be written in the following form:

$$\underset{\sim}{A}\,\underset{\sim}{u} = \underset{\sim}{d} - \underset{\sim}{C}\,\underset{\sim}{u} \qquad (4.1)$$

where $\underset{\sim}{A}$ is a square matrix with known elements, $\underset{\sim}{u}$ is a vector of unknowns, $\underset{\sim}{d}$ is a known vector, and $\underset{\sim}{C}$ is an operator matrix representing the difference correction. When the appropriate boundary conditions are incorporated in (4.1), the solution at each step of incremental loading may be obtained as follows: 1) neglect the second term in the right-hand side of (4.1) and write

$$\underset{\sim}{u}^{(1)} = \underset{\sim}{A}^{-1}\,\underset{\sim}{d} \quad ; \qquad (4.2a)$$

2) obtain a first correction $\underset{\sim}{\eta}^{(1)}$ as

$$\underset{\sim}{\eta}^{(1)} = -\,\underset{\sim}{A}^{-1}\,\underset{\sim}{C}\,\underset{\sim}{u}^{(1)} \quad ; \qquad (4.2b)$$

3) with $\underset{\sim}{u}^{(2)} = \underset{\sim}{u}^{(1)} + \underset{\sim}{\eta}^{(1)}$, obtain a second correction as

$$\underset{\sim}{\eta}^{(2)} = -\,\underset{\sim}{A}^{-1}\,\underset{\sim}{C}\,\underset{\sim}{u}^{(2)} \quad ; \qquad (4.2c)$$

4) continue this process until a sufficiently accurate result is obtained. We note that the above method requires only one matrix inversion. All corrections are then obtained by means of the matrix multiplication. We shall now outline a way for obtaining equation (4.1) for the considered problem.

3.4.1 The δ-Operators: For a given function f, we define the so-called δ-operators as shown in Table 3.4-1. With the mesh sizes h in

TABLE 3.4-1

Definition of δ-Operator

	δ^1	δ^2	δ^3	δ^4	
f_{-4}					
	$f_{-3}-f_{-4}$				
f_{-3}		$f_{-2}-2f_{-3}+f_{-4}$			
	$f_{-2}-f_{-3}$		$f_{-1}-3f_{-2}+f_{-3}-f_{-4}$		
f_{-2}		$f_{-1}-2f_{-2}+f_{-3}$		$f_0-4f_{-1}+6f_{-2}-4f_{-3}+f_{-4}$	backward
	$f_{-1}-f_{-2}$		$f_0-3f_{-1}+3f_{-2}-f_{-3}$		
f_{-1}		$f_0-2f_{-1}+f_{-2}$		$f_1-4f_0+6f_{-1}-4f_{-2}+f_{-3}$	
	f_0-f_{-1}		$f_1-3f_0+3f_{-1}-f_{-2}$		
f_0 →	$\frac{1}{2}(f_1-f_{-1})$ →	$f_1-2f_0+f_{-1}$ →	$\frac{1}{2}(f_2-2f_1+2f_{-1}-f_{-2})$	$f_2-4f_1+6f_0-4f_{-1}+f_{-2}$	→ central
	f_1-f_0		$f_2-3f_1+3f_0-f_{-1}$		
f_1		$f_2-2f_1+f_0$		$f_3-4f_2+6f_1-4f_0+f_{-1}$	
	f_2-f_1		$f_3-3f_2+3f_1-f_0$		
f_2		$f_3-2f_2+f_1$		$f_4-4f_3+6f_2-4f_1+f_0$	forward
	f_3-f_2		$f_4-3f_3+3f_2-f_1$		
f_3		$f_4-2f_3+f_2$			
	f_4-f_3				
f_4					

the X-direction, and k in the Y-direction (Fig. 3.4-1), we have

$$h = X(j+1) - X(j) \quad , \quad k = Y(i+1) - Y(i) \quad ,$$

where a node (j, i) has coordinates (X(j) , Y(i)) in the reference state. Introducing the notation

$$D_X \equiv \frac{\partial}{\partial X} \quad , \quad D_X^2 \equiv \frac{\partial^2}{\partial X^2} \quad , \quad D_Y \equiv \frac{\partial}{\partial Y} \quad , \quad D_Y^2 \equiv \frac{\partial^2}{\partial Y^2} \quad ,$$

we write

$$h\, D_X = \delta_X^1 + C_X^1 \quad , \quad h^2 D_X^2 = \delta_X^2 + C_X^2 \quad , \tag{4.3a}$$

$$k\, D_Y = \delta_Y^1 + C_Y^1 \quad , \quad k^2 D_Y^2 = \delta_Y^2 + C_Y^2 \quad , \tag{4.3b}$$

where the correction operators are

$$C_K^1 = -\frac{1}{6}\,\delta_K^3 + \frac{1}{30}\,\delta_K^5 - \cdots \approx -\frac{1}{6}\,\delta_K^3 \quad , \tag{4.3c}$$

$$C_K^2 = -\frac{1}{12}\,\delta_K^4 + \frac{1}{90}\,\delta_K^6 - \cdots \approx -\frac{1}{12}\,\delta_K^4 \quad , \quad K = X, Y \quad . \tag{4.3d}$$

Now, with $[X(j) , Y(i)] \equiv [(j-1)h , (i-1)k]$ defining the node (j, i) , see Fig. 3.1, we have

$$h\frac{\partial f}{\partial X} = \tfrac{1}{2}[f(j+1, i) - f(j-1, i)] + C_X^1 f(j, i) \quad , \tag{4.4a}$$

where

$$C_X^1 f(j, i) = -\frac{1}{12}[f(j+2, i) - 2f(j+1, i) + 2f(j-1, i) - f(j-2, i)] \quad , \tag{4.4b}$$

$$k\frac{\partial f}{\partial Y} = \tfrac{1}{2}[f(j, i+1) - f(j, i-1)] + C_Y^1 f(j, i) \quad , \tag{4.5a}$$

$$C_Y^1 f(j, i) = -\frac{1}{12}[f(j, i+2) - 2f(j, i+1) + 2f(j, i-1) - f(j, i-2)] \quad . \tag{4.5b}$$

In this manner $\nabla^2 f = \partial^2 f/\partial X^2 + \partial^2 f/\partial Y^2$ can be expressed as

$$h^2 \nabla^2 f = f(j-1, i) + f(j+1, i) + r^2[f(j, i-1) + f(j, i+1)]$$

$$- 2(1+r^2) f(j, i) + C_\nabla f(j, i) \quad , \tag{4.6a}$$

where

$$C_\nabla f_{ij} = -\frac{1}{12}\{f(j-2, i) + f(j+2, i) - 4[f(j-1, i) + f(j+1, i)] + r^2 f(j, i-2)$$

$$+ r^2 f(j, i+2) - 4r^2[f(j, i-1) + 4f(j, i+1) + 6(1+r^2) f(j, i)\} \quad , \quad r = \frac{h}{k} \quad . \tag{4.6b}$$

3.4.2 Finite-Difference Equations: The system of partial differential equations to be written in a finite-difference form is given by (3.6), where the coefficients $\frac{\partial x}{\partial X}$, $\frac{\partial x}{\partial Y}$, etc., are known functions. We define

$$g_{11} = \frac{\partial x}{\partial X} \quad , \quad g_{12} = \frac{\partial x}{\partial Y} \quad , \quad g_{21} = \frac{\partial y}{\partial X} \quad , \quad g_{22} = \frac{\partial y}{\partial Y} \quad , \tag{4.7a}$$

$$G_1 = \nabla^2 x \quad , \quad G_2 = \nabla^2 y \quad , \tag{4.7b}$$

where all operators are defined explicitly in Eqs. (4.4) to (4.6). We then obtain

$$g_{11} \nabla^2 u + g_{21} \nabla^2 v + G_1 \frac{\partial u}{\partial X} + G_2 \frac{\partial v}{\partial X} - \frac{\partial q}{\partial X} = 0 \quad , \tag{4.8a}$$

$$g_{12} \nabla^2 u + g_{22} \nabla^2 v + G_1 \frac{\partial u}{\partial Y} + G_2 \frac{\partial v}{\partial Y} - \frac{\partial q}{\partial Y} = 0 \quad , \tag{4.8b}$$

$$g_{22} \frac{\partial u}{\partial X} + g_{11} \frac{\partial v}{\partial Y} - g_{21} \frac{\partial u}{\partial Y} - g_{12} \frac{\partial v}{\partial X} = 0 \quad , \tag{4.8c}$$

where g_{AB} and G_A, A, B = 1, 2, are known functions of X and Y, the unknowns being u, v, and q. For an interior nodal point (j, i), $2 \le j \le N$, $2 \le i \le M$, Eqs. (4.8) reduce to

$$[G_1 \mid G_2 \mid G_3]\{u, v, q\}^T = \{C\} \quad , \tag{4.9a}$$

where

$$G_1 = \begin{bmatrix} r^2 g_{11} & g_{11} - \frac{h}{2} G_1 & -2(1+r^2) g_{11} & g_{11} + \frac{h}{2} G_1 & r^2 g_{11} \\ r^2 g_{12} - \frac{hr}{2} G_1 & g_{12} & -2(1+r^2) g_{12} & g_{12} & r^2 g_{12} + \frac{hr}{2} G_1 \\ r g_{21} & -g_{22} & 0 & g_{22} & -r g_{21} - r g_{11} \end{bmatrix} \tag{4.9b}$$

$$G_2 = \begin{bmatrix} r^2 g_{21} & g_{21} - \frac{h}{2} G_2 & -2(1+r^2) g_{21} & g_{21} + \frac{h}{2} G_2 & r^2 g_{21} \\ r^2 g_{22} - \frac{hr}{2} G_2 & g_{22} & -2(1+r^2) g_{22} & g_{22} & r^2 g_{22} + \frac{hr}{2} G_2 \\ -r g_{11} & g_{12} & 0 & -g_{12} & r g_{11} \end{bmatrix} \tag{4.9c}$$

$$G_3 = \begin{bmatrix} 0 & \frac{h}{2} & -\frac{h}{2} & 0 \\ \frac{hr}{2} & 0 & 0 & -\frac{hr}{2} \\ 0 & 0 & 0 & 0 \end{bmatrix} \quad , \tag{4.9d}$$

$$u = \{u(j, i-1) \ , \ u(j-1, i) \ , \ u(j, i) \ , \ u(j+1, i) \ , \ u(j, i+1)\} \quad , \tag{4.9e}$$

$$v = \{v(j, i-1) \ , \ v(j-1, i) \ , \ v(j, i) \ , \ v(j+1, i) \ , \ v(j, i+1)\} \quad , \tag{4.9f}$$

$$q = \{q(j, i-1) \ , \ q(j-1, i) \ , \ q(j+1, i) \ , \ q(j, i+1)\} \quad , \tag{4.9g}$$

$$\{C\} = \begin{Bmatrix} [-g_{11} C_\nabla - G_1 C_X^1] u(j, i) + [-g_{21} C_\nabla - G_2 C_X^1] v(j, i) + C_X^1 q(j, i) \\ [-g_{12} C_\nabla - G_1 C_Y^1] u(j, i) + [-g_{22} C_\nabla - G_2 C_Y^1] v(j, i) + C_Y^1 q(j, i) \\ [-g_{22} C_X^1 + g_{21} C_Y^1] u(j, i) + [g_{12} C_X^1 - g_{11} C_Y^1] v(j, i) \end{Bmatrix} \quad , \tag{4.9h}$$

where the right-hand side of (4.9a) denotes the correction term at the interior points. From (4.9h), (4.4), (4.5) and (4.6) this correction can be written as

$$\{C\} = \underset{\sim}{C}(j,i)\{u(j,i-2)\ ,\ u(j,i-1)\ ,\ u(j-2,i)\ ,\ u(j-1,i)\ ,$$
$$u(i,j)\ ,\ u(j+1,i)\ ,\ u(j+2,i)\ ,\ u(j,i+1)\ ,$$
$$u(j,i+2)\ ,\ v(j,i-2)\ ,\ v(j,i-1)\ ,\ v(j-2,i)\ ,$$
$$v(j-1,i)\ ,\ v(i,j)\ ,\ v(j+1,i)\ ,\ v(j+2,i)\ ,$$
$$v(j,i+1)\ ,\ v(j,i+2)\ ,\ q(j,i-2)\ ,\ q(j,i-1)\ ,$$
$$q(j-2,i)\ ,\ q(j-1,i)\ ,\ q(j+1,i)\ ,\ q(j+1,i)\ ,$$
$$q(j,i+1)\ ,\ q(j,i+2)\}^T \quad , \qquad (4.10a)$$

where $\underset{\sim}{C}(j,i)$ is a 3 x 26 correction matrix associated with an interior point (j,i). This matrix is defined in Eq. (4.10b). Note that in (4.10b) there are three rows and twenty-six columns.

$\underset{\sim}{C}(j,i) =$

$\frac{1}{12} g_{21}$	$\frac{r^2}{12} g_{12} - \frac{G_1}{12}$	$\frac{r^2}{12} g_{11}$
$-\frac{1}{6} g_{21}$	$-\frac{r^2}{3} g_{12} + \frac{G_1}{6}$	$-\frac{r^2}{3} g_{11}$
$-\frac{1}{12} g_{22}$	$\frac{1}{12} g_{12}$	$\frac{1}{12} g_{11} - \frac{G_1}{12}$
$\frac{1}{6} g_{22}$	$-\frac{1}{3} g_{12}$	$-\frac{1}{3} g_{11} + \frac{G_1}{6}$
0	$\frac{1}{2}(1+r^2) g_{12}$	$\frac{1}{2}(1+r^2) g_{11}$

$-\frac{1}{6} g_{22}$	$-\frac{1}{3} g_{12}$	$-\frac{1}{3} g_{11} - \frac{G_1}{6}$
$\frac{1}{12} g_{22}$	$\frac{1}{12} g_{12}$	$\frac{1}{12} g_{11} + \frac{G_1}{12}$
$\frac{1}{6} g_{21}$	$-\frac{r^2}{3} g_{12} - \frac{G_1}{6}$	$-\frac{r^2}{3} g_{11}$
$-\frac{1}{12} g_{21}$	$\frac{r^2}{12} g_{12} + \frac{G_1}{12}$	$\frac{r^2}{12} g_{11}$
$-\frac{1}{12} g_{11}$	$\frac{r^2}{12} g_{22} - \frac{G_2}{12}$	$\frac{r^2}{12} g_{21}$
$\frac{1}{6} g_{11}$	$-\frac{r^2}{3} g_{22} + \frac{G_2}{6}$	$-\frac{r^2}{3} g_{21}$
$\frac{1}{12} g_{12}$	$\frac{1}{12} g_{22}$	$\frac{1}{12} g_{21} - \frac{G_2}{12}$
$-\frac{1}{6} g_{12}$	$-\frac{1}{3} g_{22}$	$-\frac{1}{3} g_{21} + \frac{G_2}{6}$
0	$\frac{1}{2}(1+r^2) g_{22}$	$\frac{1}{2}(1+r^2) g_{21}$
$\frac{1}{6} g_{12}$	$-\frac{1}{3} g_{22}$	$-\frac{1}{3} g_{21} - \frac{G_2}{6}$
$-\frac{1}{12} g_{12}$	$\frac{1}{12} g_{22}$	$\frac{1}{12} g_{21} + \frac{G_2}{12}$
$-\frac{1}{6} g_{11}$	$-\frac{r^2}{3} g_{22} - \frac{G_2}{6}$	$-\frac{r^2}{3} g_{21}$
$\frac{1}{12} g_{11}$	$\frac{r^2}{12} g_{22} + \frac{G_2}{12}$	$\frac{r^2}{12} g_{21}$
0	$\frac{1}{12}$	0

$$
\begin{array}{ccc}
0 & -\frac{1}{6} & 0 \\
0 & 0 & \frac{1}{12} \\
0 & 0 & -\frac{1}{6} \\
0 & 0 & \frac{1}{6} \\
0 & 0 & -\frac{1}{12} \\
0 & \frac{1}{6} & 0 \\
0 & -\frac{1}{12} & 0
\end{array}
\qquad (4.10b)
$$

Note that for $3 \le j \le N-2$ and $3 \le i \le M-2$, the expression for $\underset{\sim}{C}(j, i)$ does not involve out-boundary points, which are points added outside of the considered domain so as to improve the finite-difference representation of derivatives at the boundaries. For $2 > i$ and $2 > j$, and for $i > M-2$ and $j > N-2$, on the other hand, the correction matrix involves out-boundary points. We must therefore express the quantities associated with the out-boundary points in terms of their values inside of the boundary. This can be done as follows:

a) Out-boundary points at the vicinity of the axis of symmetry: Let $j = 1$ denote an axis of symmetry. Along $j = 0$, we have, see Fig. 3.2,

$$
\begin{aligned}
u(0, i) &= -\, u(2, i) \quad , \\
v(0, i) &= v(2, i) \quad , \\
q(0, i) &= q(2, i) \quad .
\end{aligned}
\qquad (4.11)
$$

b) Out-boundary points along other sides: Equations (4.9a) may be written for points on the boundary. The additional unknowns at points outside of the boundary are then expressed in terms of the corresponding interior quantities using the finite-difference form of the given boundary conditions.

3.4.3 Boundary Conditions: With the apparatus developed in this section, all boundary conditions that may be of interest can easily be expressed in a finite difference form. For example, on a stress-free side $(N+1, i)$, which is initially normal to the Y-direction, we have

$$\frac{\partial v}{\partial Y} - \bar{p}\,\frac{\partial u}{\partial X} - q\,\frac{\partial x}{\partial X} = 0 \quad ,$$

$$\frac{\partial u}{\partial Y} = 0 \quad .$$

These equations now become

$$\begin{bmatrix} 0 & \frac{\bar{p}(N+1,i)}{2} & -\frac{\bar{p}(N+1,i)}{2} & 0 & \frac{r}{2} & \frac{r}{2} & 0 & 0 & -g_{11}(N+1,i) \\ 0 & 0 & 0 & -1 & 0 & 0 & 0 & 0 & 0 \end{bmatrix} \begin{bmatrix} u(N+1,i-1) \\ u(N,i) \\ u(N+2,i) \\ u(N+1,i+1) \\ v(N+1,i-1) \\ v(N,i) \\ v(N+2,i) \\ v(N+1,i+1) \\ q(N+1,i) \end{bmatrix}$$

$$i = 1, 2, \ldots, M, M+1 \quad .$$

For each i , there are two such boundary conditions which can be used to obtain u(N+2, i) and v(N+2, i) in terms of the other quantities* that are evaluated at the node (N+1, i). Note that, if the components of the surface tractions are prescribed to be non-zero on the considered boundary, the right-hand side of the above equation must then be set equal to

$$\frac{1}{\mu}\begin{Bmatrix} \nabla T_1(N+1, i) \\ \nabla T_2(N+1, i) \end{Bmatrix} ,$$

where $\nabla T_1(N+1, i)$ and $\nabla T_2(N+1, i)$ are the corresponding <u>equivalent concentrated incremental</u> forces acting at the node (N+1, i).

* Note that we have not incorporated the required correction terms here, but they must be included after the first estimate of the unknowns at out-boundary points is established.

3.5 A Variational Approach

A variational method is being now developed by the present investigators, which method can be used effectively to formulate a finite element approximation for solution of large elastic deformation problems. We shall give an outline of this method in what follows.

Since for each incremental loading, we are actually dealing with a nonhomogeneous, anisotropic, linearly elastic problem, it is possible to formulate this problem in the framework of a variational technique. To retain the effectiveness of the basic approach, however, one must retain the original Lagrangian formulation.

Consider an equilibrium (deformed) state C of the elastic solid under surface loads T_i. Let the surface loads be increased by the amount ΔT_i, measured per unit area in C_0, resulting in an incremental deformation u_i. The change in the strain energy is

$$\Delta\Sigma = \frac{\partial \Sigma}{\partial x_{i,\alpha}} u_{i,\alpha} + \tfrac{1}{2} \frac{\partial^2 \Sigma}{\partial x_{i,\alpha} \partial x_{j,\beta}} u_{i,\alpha} u_{j,\beta} + \cdots$$

$$= T^R_{\alpha i} u_{i,\alpha} + \tfrac{1}{2} C_{\alpha i \beta j} u_{i,\alpha} u_{j,\beta} + \cdots \quad , \tag{5.1}$$

where

$$C_{\alpha i \beta j} = \frac{\partial^2 \Sigma}{\partial x_{i,\alpha} \partial x_{j,\beta}} \quad , \tag{5.2}$$

and where $T^R_{\alpha i}$ is the Piola-Kirchhoff stress tensor in C. The potential energy associated with this incremental loading then is

$$\pi = \int_V \Delta\Sigma \, dV - \int_S (T_i + \Delta T_i)\, u_i \, dS = \int_V [T^R_{\alpha i}\, u_{i,\alpha} + \tfrac{1}{2} C_{\alpha i \beta j}\, u_{i,\alpha}\, u_{j,\beta}$$

$$+ \ldots \,] dV - \int_S (T^R_{\alpha i} N_\alpha)\, u_i \, dS - \int_S \Delta T_i \, u_i \, dS \quad . \tag{5.3}$$

Using Gauss' theorem, and the fact the C is in equilibrium, we reduce (5.3) to

$$\pi = \tfrac{1}{2} \int_V C_{\alpha i \beta j}\, u_{i,\alpha}\, u_{j,\beta} \, dV - \int_S \Delta T_i \, u_i \, dS \quad . \tag{5.4}$$

It can be shown that if the state C is a stable equilibrium state [13] that is, if $\int_V C_{\alpha i \beta j}\, u_{i,\alpha}\, u_{j,\beta} \, dV$ is positive-definite for all displacement fields which comply with all the geometrical boundary conditions of the problem and are sufficiently smooth, then π has an absolute minimum for the actual displacement field. To develop a finite element approach for solving plane-strain problems, one may, for example, consider a set of piecewise linear displacement fields, and substituting into (5.4), minimize π to obtain a system of linear equations for the amplitudes of the displacement-components at the nodal points [9]. Note that, in this formulation, all quantities may be referred to the original undeformed state. Moreover, Eq. (5.2) shows that (5.4) is valid for elastic materials of all kind. Note also that $C_{\alpha i \beta j}$ <u>cannot</u> be identified with the usual elastic constants; they are not constants.

For incompressible materials, (5.4) must be modified to read

$$\pi = \int_V \{\tfrac{1}{2}[C_{\alpha i \beta j} - p X_{\alpha,j} X_{\beta,i}]\, u_{i,\alpha}\, u_{j,\beta} - \bar{q}\, X_{\alpha,i}\, u_{i,\alpha}\} dV - \int_S \Delta T_i \, u_i \, dS \quad , \tag{5.5}$$

where $\bar{q}$ is the Lagrangian multiplier, and $u_{i,i} = 0$ because of incompressibility. With straightforward calculations, it can readily be verified

that the first variation of (5.5) would yield the equations of equilibrium (3.3) and the appropriate boundary conditions provided that Σ is identified with (2.17), and q is taken equal to $\bar{q}/\mu$.

3.6 Estimate of Plastic Strains in Metal Layer

The analysis presented in the preceding sections can be employed to obtain the stress and strain fields in the elastomer-metal composite. In particular, this analysis yields a conservative estimate of the shear stresses between the metal and elastomer that must be carried by the bond between them. Since under a repeated loading of the type encountered in expulsion bladders, the bond between metal and elastomer may be broken, the analysis provides information for design against such a failure.

In addition to the possible bond-failure, the metal layer may fail during a cyclic plastic deformation. It is therefore desirable to have a complete formulation and an analytical technique which would yield directly not only the stress and strain fields in the elastomer layers, but also the stress and strain fields in the inner metal sheet. Although attempt is being made to develop such a program, at the present time we shall be content with a conservative engineering estimate of plastic strains in the metal sheet that can be obtained directly using the known stress fields in the elastomer.

Consider the free-body diagram of the elastic sheet in its undeformed initial configuration, Fig. 3.3. In a continued incremental loading, this metal layer deforms incrementally under the action of surface tractions transmitted to it across its interface with the elastomer. At a given state of loading, the deformed metal sheet is in an equilibrium state under a given set of surface loads $T^{R}_{\alpha i} N_{\alpha} = T_i$ applied on its boundary, where these tractions are conveniently referred to the initial undeformed configuration

of the metal layer, Fig. 3.3. We note that, because of the assumption that the normal tractions are continuous across the metal layer, from Eq. (3.15b), we have

$$[T_{22}^{R(+)} + T_{22}^{R(-)}] \frac{\partial x_1}{\partial X_1} - [T_{21}^{R(+)} - T_{21}^{R(-)}] \frac{\partial x_1}{\partial X_1} = 0 \quad , \qquad (6.1)$$

where the stresses are viewed positive when they are in the positive direction of the coordinates. The individual components T_{22}^R and T_{21}^R, however, may not be continuous across the metal sheet, that is we may have $T_{22}^{R(+)} \neq - T_{22}^{R(-)}$ and $T_{21}^{R(+)} \neq - T_{21}^{R(-)}$, where these tractions are viewed positive if they are in the positive direction of the corresponding coordinate axis.

Since the metal layer is thin, a linear stress distribution across its thickness appears to be a good approximation, and, therefore, from the values of T_{22}^R and T_{21}^R we can calculate their values at the interior of the metal sheet. We must, however, obtain an estimate of the values of T_{11}^R and T_{12}^R which are not known on the boundary. (Note that although $T_{12} = T_{21}$, $T_{12}^R \neq T_{21}^R$ because the first Piola-Kirchhoff stress tensor is not symmetric.) To obtain an estimate for T_{11}^R, we proceed as follows.

On a section C-C located at a distant X from X = 0, there act a resultant force P and a resultant moment M given, respectively, by

$$P = \int_X^L (T_{21}^{R(+)} - T_{21}^{R(-)}) \, d\eta + F \quad , \qquad (6.2)$$

and

$$M = \int_X^L [T_{21}^{R(+)} + T_{21}^{R(-)}] \frac{t}{2} \, d\eta$$

$$+ \int_X^L (- T_{22}^{R(+)} - T_{22}^{R(-)})(\eta - X) \, d\eta - T(L-X) \quad , \qquad (6.3)$$

where T and F are the tangential and normal loads applied at section A-A. Now, if we use a linear stress distribution across the metal thickness, we obtain

$$T_{11}^{R} = \frac{P}{t} \pm \frac{12MZ}{t^2} \quad , \tag{6.3}$$

where a new coordinate system $0X, Z$ is used here. Hence, T_{11}^{R}, T_{21}^{R}, and T_{22}^{R} are known throughout the metal sheet at each state of loading. These results can then be used to obtain an estimate for the corresponding plastic strains as follows.

From Eqs. (3.13), we first calculate the Cauchy stress tensor T_{ij} throughout the metal layer. This then defines the state of stress at a given state of loading. Using an identical procedure, we calculate the incremental stress-field ΔT_{ij} that corresponds to an incremental loading. Then, using the Mises yield condition

$$f \equiv \frac{3\sqrt{2}}{2} \{T'_{ij}\, T'_{ij}\} - \sigma = 0 \quad , \tag{6.4}$$

where $T'_{ij} = T_{ij} - \frac{1}{3} T_{kk}\, \delta_{ij}$, and σ is the yield stress in tension, we write

$$\Delta\epsilon_{ij}^{P} = \left[\frac{3}{2} \frac{T'_{ij}}{\bar{\sigma}\, E'}\right] \Delta\bar{\sigma} \quad , \tag{6.5}$$

where

$$\bar{\sigma} = \sqrt{3/2}\, \{T'_{ij}\, T'_{ij}\}^{\frac{1}{2}} \quad , \qquad \Delta\bar{\sigma} = \sqrt{3/2}\, \{\Delta T'_{ij}\, \Delta T'_{ij}\}^{\frac{1}{2}} \quad , \tag{6.6}$$

and

$$E' = \frac{d\bar{\sigma}}{d\bar{\epsilon}^{P}} \tag{6.7}$$

which can be measured as the slope of the stress-plastic strain curve in simple tension.

REFERENCES

1. Turner, M. J., Dill, E. H., Martin, H. C., and Melosh, R. J., "Large Deflection Analysis of Complex Structures Subjected to Heating and External Loads," J. Aero. Science 27 (1960) 97-106.

2. Martin, H. C., "Derivation of Stiffness Matrices for the Analysis of Large Deflection and Stability Problems," Proc. 1st. Conf. on Matrix Methods in Struct. Mech., AFFDL-TR-66-80 (1966) 697-715.

3. Mallet, R. H., and Marcal, P. V., "Finite Element Analysis of Nonlinear Structures," J. Struct. Div., ASCE 94 (1968) 2801-2106.

4. Marcal, P. V., "Finite-Element Analysis of Combined Problems of Nonlinear Material and Geometric Behavior," in Computational Approaches in Applied Mechanics, ASME Computer Conference (1969) 133-149.

5. Oden, J. T., "Numerical Formulation of Nonlinear Elasticity Problems," J. Struct. Div. ASCE 93 (1967) 235-255.

6. Oden, J. T., and Kubitza, W. K., "Numerical Analysis of Nonlinear Pneumatic Structures," Proc. 1st. Int. Clloq. on Pneumatic Structures, Stuttgat, May 1967.

7. Becker, E. B., "A Numerical Solution of a Class of Problems of Finite Elastic Deformations," Ph.D. Thesis, University of California, Berkeley, Calif., (1966).

8. Felippa, C. A., "Refined Finite Element Analysis of Linear and Nonlinear Two-Dimensional Structures," Ph.D. Thesis, University of California, Berkeley, Calif., (1966).

9. Nemat-Nasser, S., and Shatoff, H. D., "A Consistent Numerical Method for the Solution of Nonlinear Elasticity Problems at Finite Strains," ONR Rept. # 2, University of California, San Diego, January 1970.

10. Mooney, M., "A Theory of Large Elastic Deformation," J. Appl. Phys. 11 (1940), 582.

11. Rivlin, R.S., "Large Elastic Deformations of Isotropic Materials, I. Fundamental Concepts," Phil. Trans. Roy. Soc. (London) (A) 240 (1948) 459-490.

12. Treloar, L. R. G., The Physics of Rubber Elasticity, Oxford University Press, 1958.

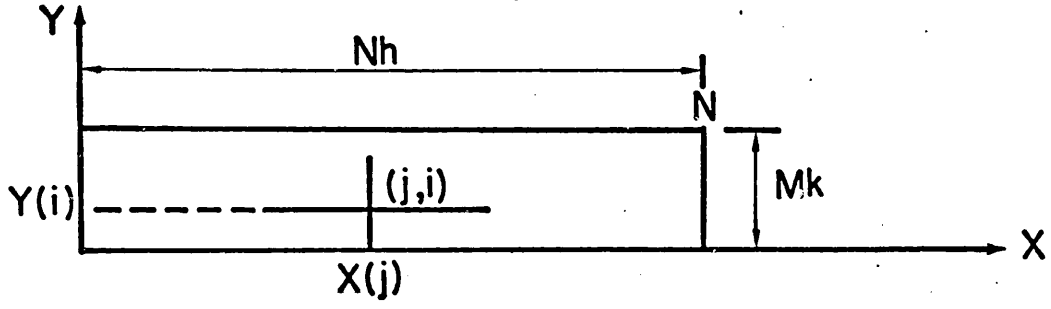

Fig. 3.1

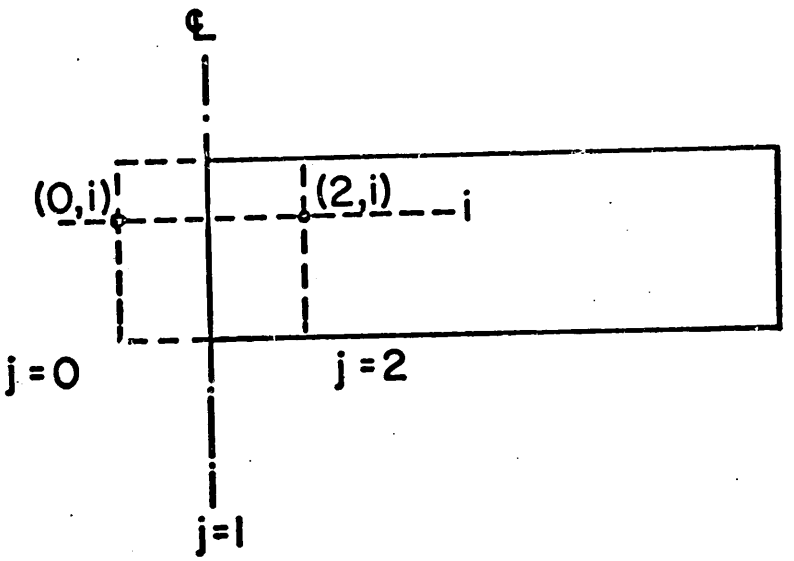

Fig. 3.2

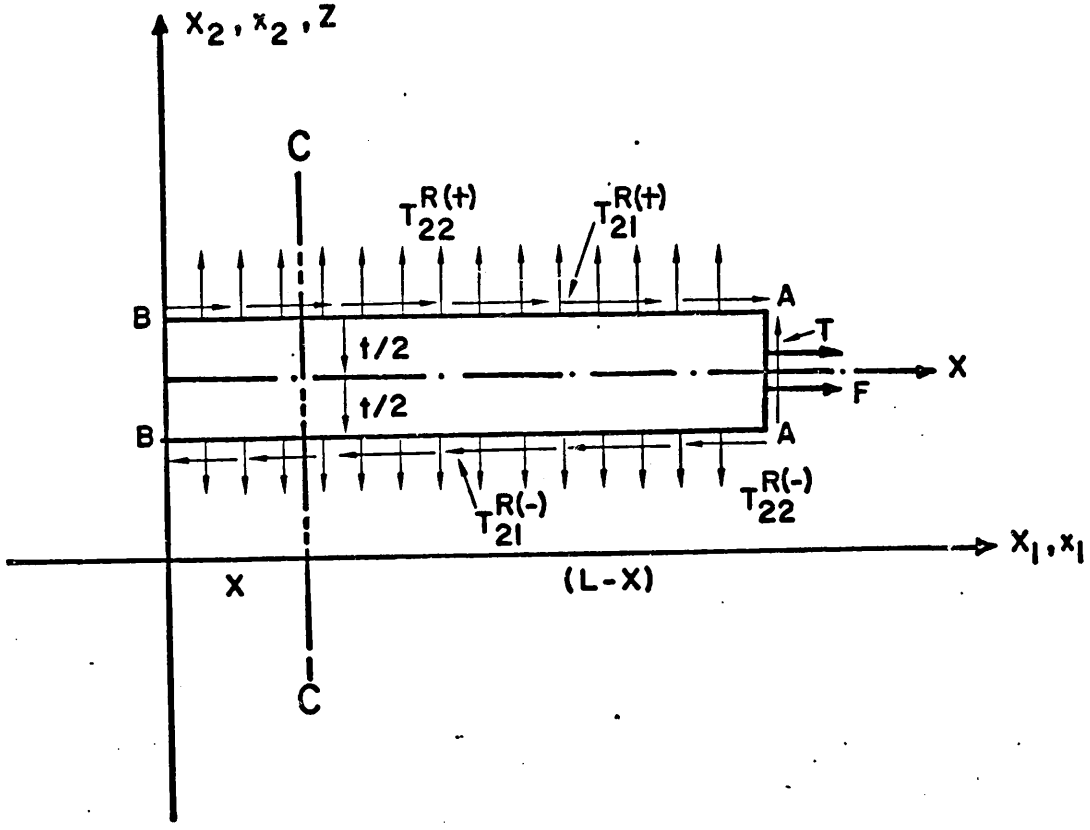

Fig. 3.3

CHAPTER IV

ANALYSIS OF RIB-REINFORCEMENTS

4.1 Introduction

In Chapter II, the expulsion bladder was assumed to be reinforced with circumferential rings. A more general analysis might include helical or other types of reinforcements, i.e., reinforcing rods whose centerlines are tangent to a given curve on the surface of the bladder. In any event, the differential equations governing the deformation of these structural elements must be known in order to formulate a bladder stability analysis. For this purpose, a geometrically nonlinear rod theory is developed in this section, a special case of which includes circular rings. It will suffice to base this theory upon the assumptions of 1) small strain, 2) symmetric cross sections, uniform along the rod length, 3) linearly elastic, homogeneous, isotropic material, and 4) Bernoulli-Euler bending and St. Venant free torsion.

4.2 Geometrical Preliminaries

Notation

In portions of the subsequent analysis indicial notation [1] will be employed. Latin indicies range over 1, 2, 3; Greek indices range over 1, 2. The summation convention holds in each case.

Reference Curve and Directors

As a reference, let us select the locus of material points on the cross sectional centroids of the reinforcing rod, which we assume to be a smooth curve C in space. We define C by

$$\underset{\sim}{r} = \underset{\sim}{r}(s) \tag{4.1}$$

where $\underset{\sim}{r}$ is the position vector, relative to a fixed origin, of a material point on C, and s denotes distance along C. In the stress free undeformed state, we shall denote this curve by c and the corresponding position vector by

$$\underset{\sim}{r}_0 = \underset{\sim}{r}_0(s_0) \tag{4.2}$$

where s_0 represents distance along c. If the strain ϵ of c is defined by

$$2\epsilon = \frac{ds^2 - ds_0^2}{ds^2} = \left| d\underset{\sim}{r}/ds_0 \right|^2 - 1 \quad , \tag{4.3a}$$

then the quantities s_0 and s are related through

$$ds = (1+2\epsilon)^{\frac{1}{2}}\, ds_0 \quad . \tag{4.3b}$$

To each point of C we now assign three mutually orthogonal unit vectors (directors) $\underset{\sim}{A}_i(s)$, $i = 1, 2, 3$, as follows: The vector $\underset{\sim}{A}_3(s)$ is the unit tangent vector to C, defined by

$$\underset{\sim}{A}_3(s) = d\underset{\sim}{r}/ds \quad , \tag{4.4}$$

and the vectors $\underset{\sim}{A}_\alpha(s)$, $\alpha = 1, 2$, are orthogonal to $\underset{\sim}{A}_3$, orthogonal to each other, and are coincident with the principal axis of the rod cross section. In a similar manner, a set of directors $\underset{\sim}{a}_i$ are assigned to the curve c. The latter are defined by

$$\begin{aligned} &\underset{\sim}{a}_3(s_0) = d\underset{\sim}{r}_0/ds_0 \quad , \\ &\underset{\sim}{a}_\alpha(s_0) = \underset{\sim}{A}_\alpha(s) \quad \text{in initial state} \end{aligned} \tag{4.5}$$

In view of the definitions of $\underset{\sim}{A}_i$, $\underset{\sim}{a}_i$, note that

$$\underset{\sim}{A}_i \cdot \underset{\sim}{A}_j = \underset{\sim}{a}_i \cdot \underset{\sim}{a}_j = \delta_{ij} \tag{4.6}$$

where δ_{ij} is the Kronecker delta.

Differentiation of the Directors

It will be necessary to differentiate the directors $\underset{\sim}{A}_i$ with respect to s. For this purpose it will be instructive to review a little elementary differential geometry.

The curvature vector $\mathcal{K}\underset{\sim}{\mu}$ at a point of C is defined by

$$d\underset{\sim}{A}_3/ds = \mathcal{K}\underset{\sim}{\mu} \tag{4.7}$$

where $\mathcal{K}$ is the curvature of C and $\underset{\sim}{\mu}$ is a unit vector. Since $\underset{\sim}{\mu}$ is orthogonal to $\underset{\sim}{A}_3$, we can write

$$\mathcal{K}\,\underset{\sim}{\mu} = \mathcal{K}_\alpha\,\underset{\sim}{A}_\alpha \tag{4.8}$$

where $\mathcal{K}_\alpha = \mathcal{K}\,\underset{\sim}{\mu}\cdot\underset{\sim}{A}_\alpha$. Now, since $\underset{\sim}{A}_3\cdot\underset{\sim}{A}_\alpha = 0$, we have

$$\underset{\sim}{A}_3\cdot d\underset{\sim}{A}_\alpha/ds = -\,\underset{\sim}{A}_\alpha\cdot d\underset{\sim}{A}_3/ds = -\,\underset{\sim}{A}_\alpha\cdot(\mathcal{K}\underset{\sim}{\mu}) = -\,\mathcal{K}_\alpha \tag{4.9}$$

and therefore

$$\underset{\sim}{A}_3\cdot(d\underset{\sim}{A}_\alpha/ds + \mathcal{K}_\alpha\,\underset{\sim}{A}_3) = 0 \tag{4.10}$$

Also, it is evident that

$$\underset{\sim}{A}_\alpha\cdot(d\underset{\sim}{A}_\alpha/ds + \mathcal{K}_\alpha\,\underset{\sim}{A}_3) = 0 \tag{4.11}$$

Equations (4.10) and (4.11) imply that

$$\begin{aligned} d\underset{\sim}{A}_1/ds + \mathcal{K}_1\,\underset{\sim}{A}_3 &= f_1\,\underset{\sim}{A}_2 \\ d\underset{\sim}{A}_2/ds + \mathcal{K}_2\,\underset{\sim}{A}_3 &= f_2\,\underset{\sim}{A}_1 \end{aligned} \tag{4.12}$$

In addition, since $\underset{\sim}{A}_1\cdot\underset{\sim}{A}_2 = 0$, we have

$$\underset{\sim}{A}_1\cdot d\underset{\sim}{A}_2/ds = -\,\underset{\sim}{A}_2\cdot d\underset{\sim}{A}_1/ds \tag{4.13}$$

Define

$$\mathcal{K}_3 = \underset{\sim}{A}_2\cdot d\underset{\sim}{A}_1/ds = -\,\underset{\sim}{A}_1\cdot d\underset{\sim}{A}_2/ds \tag{4.14}$$

Then, Eqs. (4.12) and (4.14) furnish

$$f_1 = -\,\mathcal{K}_3\ , \quad f_2 = \mathcal{K}_3 \tag{4.15}$$

In summary, therefore, it has been shown that

$$d\underset{\sim}{A}_1/ds = \mathcal{K}_3\,\underset{\sim}{A}_2 - \mathcal{K}_1\,\underset{\sim}{A}_3\ ,$$

$$d\underset{\sim}{A}_2/ds = -\mathcal{K}_3\,\underset{\sim}{A}_1 - \mathcal{K}_2\,\underset{\sim}{A}_3 \quad ,$$

$$d\underset{\sim}{A}_3/ds = \mathcal{K}_1\,\underset{\sim}{A}_1 + \mathcal{K}_2\,\underset{\sim}{A}_2 \quad . \tag{4.16}$$

Equations (4.16) are similar to the well known Frenet-Seret formulae [2 , p. 159] relating the tangent vector $\underset{\sim}{A}_3$, the normal or curvature vector $\mathcal{K}\underset{\sim}{\mu}$, and the binomial vector $\underset{\sim}{\nu}$ of C as follows:

$$d\underset{\sim}{A}_3/ds = \mathcal{K}\underset{\sim}{\mu} \quad , \qquad d\underset{\sim}{\mu}/ds = \tau\underset{\sim}{\nu} - \mathcal{K}\underset{\sim}{A}_3 \quad ,$$

$$d\underset{\sim}{\nu}/ds = -\tau\underset{\sim}{\mu} \quad , \tag{4.17}$$

where τ is the "torsion" of C . If the angle Θ is introduced through $\underset{\sim}{A}_2 \cdot \underset{\sim}{\mu} = \cos\Theta$, then $\underset{\sim}{A}_1 \cdot \underset{\sim}{\mu} = \sin\Theta$ and the Frenet-Seret formulae are related to the curvatures $\mathcal{K}_i$ by

$$\mathcal{K}_1 = \mathcal{K}\sin\Theta \quad , \quad \mathcal{K}_2 = \mathcal{K}\cos\Theta \quad , \quad \mathcal{K}_3 = \tau + d\Theta/ds \quad . \tag{4.18}$$

Finally, the physical meaning of the quantities $\mathcal{K}_i$ can be illustrated as follows: employing the right hand screw rule, let $d\beta_i$ denote differential angles of rotation of the directors about the $\underset{\sim}{A}_i$ axes respectively. Then, an elementary calculation reveals that

$$\mathcal{K}_1 = d\beta_2/ds \quad , \quad \mathcal{K}_2 = -d\beta_1/ds \quad , \quad \mathcal{K}_3 = d\beta_3/ds \quad . \tag{4.19}$$

4.3 Displacement and Strain

Metric Tensor of Undeformed State

We represent the position vector $\underset{\sim}{R}_0$ of a material point of the undeformed rod by

$$\underset{\sim}{R}_0(\theta_1, \theta_2, \theta_3) = \underset{\sim}{r}_0(\theta_3) + \theta_\alpha \underset{\sim}{a}_\alpha(\theta_3) \tag{4.20}$$

where $\theta_3 = s_0$, and θ_α denote distance along the $\underset{\sim}{a}_\alpha$ axes respectively. Employing $(\theta_1, \theta_2, \theta_3)$ as reference coordinates, the base vectors $\underset{\sim}{g}_i$ and the metric tensor $g_{ij} = \underset{\sim}{g}_i \cdot \underset{\sim}{g}_j$ of the undeformed state are

$$\underset{\sim}{g}_\alpha = \partial \underset{\sim}{R}_0 / \partial \theta_\alpha = \underset{\sim}{a}_\alpha \quad ,$$

$$\underset{\sim}{g}_3 = \partial \underset{\sim}{R}_0 / \partial \theta_3 = \sqrt{g}\ \underset{\sim}{a}_3 + \theta_1 \mathcal{K}_3^{(0)} \underset{\sim}{a}_2 - \theta_2 \mathcal{K}_3^{(0)} \underset{\sim}{a}_1 \quad , \tag{4.21}$$

$$g_{11} = g_{22} = 1 \quad , \quad g_{12} = g_{21} = 0 \quad ,$$

$$g_{13} = g_{31} = -\theta_2 \mathcal{K}_3^{(0)} , \quad g_{23} = g_{32} = \theta_1 \mathcal{K}_3^{(0)} \quad , \tag{4.22}$$

$$g_{33} = g + (\theta_1 \mathcal{K}_3^{(0)})^2 + (\theta_2 \mathcal{K}_3^{(0)})^2 \quad ,$$

$$g = | g_{ij} | = (1 - \theta_1 \mathcal{K}_1^{(0)} - \theta_2 \mathcal{K}_2^{(0)})^2 \quad .$$

The relations (4.16) were used to derive (4.21). Here the superscript "0" denotes values of the curvatures in the undeformed state, i.e., they refer to the curve c .

Displacement Field

A basic assumption regarding the deformation of the rod

is now introduced: the position vector $\underset{\sim}{R}$ of a material point of the deformed rod, originally at $\underset{\sim}{R}_0$ in the undeformed state, is assumed in the form*

$$\underset{\sim}{R}(\theta_1, \theta_2, \theta_3) = \underset{\sim}{r}(\theta_3) + \theta_\alpha \underset{\sim}{A}_\alpha(\theta_3) + \alpha(\theta_3)\, \varphi(\theta_1, \theta_2)\, \underset{\sim}{A}_3(\theta_3) \tag{4.23a}$$

where φ denotes St. Venant's warping function and $\alpha(\theta_3)$ is given by

$$\alpha(\theta_3) = (1+2\epsilon)^{-\frac{1}{2}} \mathfrak{K}_3 - \mathfrak{K}_3^{(0)} \tag{4.23b}$$

The quantity $\alpha(\theta_3)$ represents twist per unit undeformed length. The function φ satisfies

$$\frac{\partial^2 \varphi}{\partial \theta_1^2} + \frac{\partial^2 \varphi}{\partial \theta_2^2} = 0 \tag{4.24a}$$

throughout the cross section $\mathcal{C}$ of the rod, and

$$\frac{\partial \varphi}{\partial n} = \theta_2 n_1 - \theta_1 n_2 \tag{4.24b}$$

on the lateral surface (boundary of $\mathcal{C}$). The quantities n_α in (4.24b) are direction cosines of the external normal $\underset{\sim}{n}$ to the lateral surface ($n_3 = 0$), i.e., $n_\alpha = (\underset{\sim}{n} \cdot \underset{\sim}{A}_\alpha)$.

Under (4.23), the displacement vector $\underset{\sim}{U}$ is

$$\underset{\sim}{U} = \underset{\sim}{R} - \underset{\sim}{R}_0 = \underset{\sim}{u} + \theta_\alpha (\underset{\sim}{A}_\alpha - \underset{\sim}{a}_\alpha) + \alpha \varphi \underset{\sim}{A}_3 \tag{4.25a}$$

where

$$\underset{\sim}{u} = \underset{\sim}{r} - \underset{\sim}{r}_0 \tag{4.25b}$$

---

* θ_α are undeformed (Lagrangian) coordinates in (4.23), they are <u>not</u> convected.

is the displacement of the point of intersection of the directors $\underset{\sim}{A}_\alpha$ with the curve C, $\theta_\alpha(\underset{\sim}{A}_\alpha - \underset{\sim}{a}_\alpha)$ represents a displacement due to rotation of cross sections, and $\alpha\omega\underset{\sim}{A}_3$ denotes cross sectional warping due to the twist α.

Equations (4.23), (4.25) represent a combination of Bernoulli-Euler bending and St. Venant torsion. The character of this displacement field is illustrated in Fig. 4.1.

Metric Tensor of Deformed State

With reference to the undeformed coordinates $(\theta_1, \theta_2, \theta_3)$, the base vectors $\underset{\sim}{G}_i = \partial \underset{\sim}{R}/\partial\theta^i$ of the deformed state are, from Eqs. (4.23), (4.4), (4.16), (4.3b),

$$\underset{\sim}{G}_\alpha = \underset{\sim}{A}_\alpha + \alpha\frac{\partial\varphi}{\partial\theta_\alpha}\underset{\sim}{A}_3 \quad ,$$

$$(1+2\epsilon)^{-\frac{1}{2}}\underset{\sim}{G}_3 = (\alpha\varphi\mathcal{K}_1 - \mathcal{K}_3\theta_2)\underset{\sim}{A}_1 + (\alpha\varphi\mathcal{K}_2 + \mathcal{K}_3\theta_1)\underset{\sim}{A}_2$$

$$+ [1 - \theta_1\mathcal{K}_1 - \theta_2\mathcal{K}_2 + (1+2\epsilon)^{-\frac{1}{2}}\varphi\alpha']\underset{\sim}{A}_3 \quad , \qquad (4.26)$$

where $(\,)' = d(\,)/d\theta_3 = d(\,)/ds_0$.

The metric tensor G_{ij} of the deformed state can be computed from (4.26) through

$$G_{ij} = \underset{\sim}{G}_i \cdot \underset{\sim}{G}_j \quad . \qquad (4.27)$$

Strain

If Green's strain tensor, γ_{ij}, is employed as a measure of deformation, we have

$$2\gamma_{ij} = G_{ij} - g_{ij} \tag{4.28}$$

where the components of γ_{ij} are referred to the coordinates $(\theta_1, \theta_2, \theta_3)$. In portions of the subsequent discussion, however, the analysis can be facilitated by referring the components of the strain tensor to local rectangular cartesian coordinates Y_1, Y_2, Y_3 along $\underset{\sim}{A}_1, \underset{\sim}{A}_2, \underset{\sim}{A}_3$ respectively (note $Y_\alpha = \theta_\alpha$). Denoting these new components by e_{ij}, we have

$$e_{ij} = \gamma_{rs} \frac{\partial \theta^r}{\partial Y^i} \frac{\partial \theta^s}{\partial Y^j} \tag{4.29}$$

Now, from the geometrical relation

$$d\underset{\sim}{R} = \underset{\sim}{G}_i \, d\theta^i = \underset{\sim}{A}_i \, dY^i \tag{4.30}$$

we obtain

$$\frac{\partial \theta^i}{\partial Y^j} = \underset{\sim}{G}^i \cdot \underset{\sim}{A}_j \tag{4.31}$$

where the contravariant base vectors $\underset{\sim}{G}^i$ are defined in terms of the covariant base vectors $\underset{\sim}{G}_i$ by

$$\sqrt{G}\, e_{rst}\, \underset{\sim}{G}^t = \underset{\sim}{G}_r \times \underset{\sim}{G}_s \tag{4.32}$$

The quantity e_{rst} in (4.32) is the permutation symbol, and G denotes the determinant of the metric tensor, i.e., $G = |G_{ij}|$. The transformation (4.31) was obtained from (4.30) by an inner product of both sides of (4.30) with $\underset{\sim}{G}^j$, and noting that $\underset{\sim}{G}^i \cdot \underset{\sim}{G}_j = \delta^i_j$.

Following considerable algebraic manipulation, the non-zero components of the strain tensor e_{ij} can be obtained, through use of Eqs. (4.26), (4.28), (4.29), (4.31), (4.32), in the following form:

$$2\sqrt{G}\, e_{13} = \alpha\left(\sqrt{G}\,\frac{\partial w}{\partial \theta_1} + \varphi \varkappa_1 - \theta_2\right) ,$$

$$2\sqrt{G}\, e_{23} = \alpha\left(\sqrt{G}\,\frac{\partial w}{\partial \theta_2} + \varphi \varkappa_2 + \theta_1\right) , \tag{4.33a}$$

$$G\, e_{33} = G\,\epsilon + \sqrt{G}\,\alpha'\,\varphi + \sqrt{G}\,\alpha\,\varkappa_3^{(0)}\left[\frac{\partial w}{\partial \theta_1}\,\theta_2 - \frac{\partial w}{\partial \theta_2}\,\theta_1\right]$$

$$- \theta_1\,\Delta\varkappa_1\,\sqrt{G} - \theta_2\,\Delta\varkappa_2\,\sqrt{G} - \tfrac{1}{2}\left(\theta_1\,\Delta\varkappa_1 + \theta_2\,\Delta\varkappa_2\right)^2$$

where

$$\sqrt{G} = 1 - \theta_1\varkappa_1 - \theta_2\varkappa_2 , \tag{4.33b}$$

$$\Delta\varkappa_i = \varkappa_i - \varkappa_i^{(0)} .$$

In the derivation of (4.33), it was assumed that ϵ, $b\alpha$, $b\,\Delta\varkappa_3$, $b^2\alpha'$, $\gamma_{ij} << 1$, where $b = \max(\theta_1, \theta_2)$; this follows from the hypothesis that $e_{ij} << 1$. Consequently, terms of order ϵ, $b\alpha$, $b^2\alpha'$, $b\Delta\varkappa_3$ were neglected compared to unity in the general expressions for e_{ij}, and only linear terms in α, α', $\Delta\varkappa_3$ were retained.

If the rod is "thin," i.e., if $b\varkappa_\alpha << 1$, then $G \approx 1$, and Eqs. (4.33a) can be further simplified as follows:

$$2\, e_{13} = \alpha\left(\frac{\partial w}{\partial \theta_1} + \varphi \varkappa_1 - \theta_2\right)$$

$$2\, e_{23} = \alpha\left(\frac{\partial w}{\partial \theta_2} + \varphi \varkappa_2 + \theta_1\right) \tag{4.34}$$

$$e_{33} = \epsilon + \alpha'\varphi + \alpha\,\varkappa_3^{(0)}\left[\frac{\partial w}{\partial \theta_1}\theta_2 - \frac{\partial w}{\partial \theta_2}\theta_1\right] - \theta_1\,\Delta\varkappa_1 - \theta_2\,\Delta\varkappa_2 .$$

$\Delta\kappa_i$, α , ϵ -Displacement Relations

To complete the geometric description of our rod, it will be necessary to express $\Delta\kappa_\beta$, α, ϵ in terms of suitable components of the displacement vector. Expressions for these quantities which are valid for arbitrarily large displacements are very complex. We shall therefore restrict the discussion to a small strain-moderate rotation theory. The latter is compatible with the approximations inherent in the shallow-shell theory employed in Chapter II.

Consider ϵ first. Suppose we represent the position vector $\underset{\sim}{r}(\theta_3)$ by

$$\underset{\sim}{r}(\theta_3) = \underset{\sim}{r}_0(\theta_3) + u_i(\theta_3)\, \underset{\sim}{a}_i(\theta_3) \quad . \tag{4.35}$$

Then, with use of (4.16), we obtain

$$\underset{\sim}{r}'(\theta_3) = \underset{\sim}{a}_1(u_1' - \kappa_3^{(0)} u_2 + \kappa_1^{(0)} u_3) + \underset{\sim}{a}_2(u_2' + \kappa_3^{(0)} u_1 + \kappa_2^{(0)} u_3) + \underset{\sim}{a}_3(1 - \kappa_1^{(0)} u_1 - \kappa_2^{(0)} u_2 + u_3') \quad . \tag{4.36}$$

Equations (4.36) and (4.3a) yield

$$1+2\epsilon = (1 + u_3' - \kappa_1^{(0)} u_1 - \kappa_2^{(0)} u_2)^2 + (u_1' - \kappa_3^{(0)} u_2 + \kappa_1^{(0)} u_3)^2 + (u_2' + \kappa_3^{(0)} u_1 + \kappa_2^{(0)} u_3)^2 \tag{4.37}$$

If we define

$$\cos \omega_{33} = \frac{1 + u_3' - \kappa_1^{(0)} u_1 - \kappa_2^{(0)} u_2}{(1+2\epsilon)^{\frac{1}{2}}} \quad ,$$

$$- \sin \beta_{31} = \frac{u_1' - \kappa_3^{(0)} u_2 + \kappa_1^{(0)} u_3}{(1+2\epsilon)^{\frac{1}{2}}} \quad , \tag{4.38a}$$

$$- \sin \beta_{32} = \frac{u_2' + \kappa_3^{(0)} u_1 + \kappa_2^{(0)} u_3}{(1+2\epsilon)^{\frac{1}{2}}} \quad ,$$

then (4.37) becomes simply

$$\cos^2 \psi_{33} + \sin^2 \beta_{31} + \sin^2 \beta_{32} = 1 \quad . \tag{4.38b}$$

Now, the tangent vector $\underset{\sim}{A}_3$ to C is given by

$$\underset{\sim}{A}_3 = d\underset{\sim}{r}/ds = (1+2\epsilon)^{-\frac{1}{2}} r' \quad . \tag{4.39}$$

Therefore Eqs. (4.36), (4.38) imply that

$$\underset{\sim}{A}_3 = - \sin \beta_{31} \underset{\sim}{a}_1 - \sin \beta_{32} \underset{\sim}{a}_2 + \cos \varphi_{33} \underset{\sim}{a}_3 \quad . \tag{4.40}$$

With reference to Fig. 4.2, let us introduce the angles φ, ψ_1, ψ_2 by

$$- \tan \psi_1 = \frac{d\underset{\sim}{r} \cdot \underset{\sim}{a}_2}{d\underset{\sim}{r} \cdot \underset{\sim}{a}_3} = \frac{\underset{\sim}{A}_3 \cdot \underset{\sim}{a}_2}{\underset{\sim}{A}_3 \cdot \underset{\sim}{a}_3} \quad ,$$

$$\tan \psi_2 = \frac{\underset{\sim}{A}_3 \cdot \underset{\sim}{a}_1}{\underset{\sim}{A}_3 \cdot \underset{\sim}{a}_3} \quad , \quad \cos \varphi = \underset{\sim}{A}_3 \cdot \underset{\sim}{a}_3 \quad . \tag{4.41}$$

These angles represent rotations of a differential element $d\underset{\sim}{r}$. With the aid of (4.41), (4.37) can be rewritten as

$$1 + 2\epsilon = (1+e)^2 (1+\tan^2 \psi_1 + \tan^2 \psi_2) \tag{4.42}$$

where

$$\epsilon = u_3' - \mathcal{K}_1^{(0)} u_1 - \mathcal{K}_2^{(0)} u_2 \quad . \tag{4.43}$$

Let us now simplify (4.42) under the restriction that

$$1)\ \epsilon << 1 \quad , \qquad 2)\ \varphi^2 << 1 \quad . \tag{4.44}$$

According to the definition of φ,

$$\cos \varphi = \cos \psi_{33} = (1+e)\,(1+2\epsilon)^{-\frac{1}{2}} \quad . \tag{4.45}$$

Expanding the radical of (4.45) in a binomial series and retaining only first order terms in ϵ, we have

$$\epsilon - e \approx \varphi^2/2 \quad . \tag{4.46}$$

Therefore e differs from ϵ only by terms of $O(\varphi^2)$ and e can be neglected compared to unity. Thus, (4.42) can be simplified under (4.44) to

$$\epsilon \approx e + \tfrac{1}{2} \tan^2 \psi_1 + \tfrac{1}{2} \tan^2 \psi_2 \quad . \tag{4.47}$$

Noting that (4.44) implies $\cos \psi_{33} \approx 1$, (4.47) can thus be written in terms of the displacements u_i as

$$\epsilon \approx (u_3'' - \mathcal{K}_1^{(0)} u_1 - \mathcal{K}_2^{(0)} u_2) + \tfrac{1}{2}(u_2' + \mathcal{K}_3^{(0)} u_1 + \mathcal{K}_2^{(0)} u_3)^2 + \tfrac{1}{2}(u_1' - \mathcal{K}_3^{(0)} u_2 + \mathcal{K}_1^{(0)} u_3)^2 \quad . \tag{4.48}$$

Consider now the curvature-displacement relations. Let

$$\underset{\sim}{A}_i \cdot \underset{\sim}{a}_j = \cos \psi_{ij} \quad ,$$
$$\cos \psi_{ij} = \cos (\pi/2 + \beta_{ij}) = - \sin \beta_{ij} \quad , \quad i \neq j \quad . \tag{4.49}$$

Then the directors $\underset{\sim}{a}_i$, $\underset{\sim}{A}_i$ can be related by

$$\begin{aligned}
\underset{\sim}{A}_1 &= \cos \psi_{11}\, \underset{\sim}{a}_1 - \sin \beta_{12}\, \underset{\sim}{a}_2 - \sin \beta_{13}\, \underset{\sim}{a}_3 \quad , \\
\underset{\sim}{A}_2 &= -\sin \beta_{21}\, \underset{\sim}{a}_1 + \cos \psi_{22}\, \underset{\sim}{a}_2 - \sin \beta_{23}\, \underset{\sim}{a}_3 \quad , \\
\underset{\sim}{A}_3 &= -\sin \beta_{31}\, \underset{\sim}{a}_1 - \sin \beta_{32}\, \underset{\sim}{a}_2 + \cos \psi_{33}\, \underset{\sim}{a}_3 \quad .
\end{aligned} \tag{4.50}$$

The quantities β_{31} , β_{32} , ψ_{33} are given in terms of displacements u_i through (4.38). The remaining unknowns in (4.50), namely β_{12} , β_{21} , β_{13} , β_{23} , ψ_{11} , ψ_{22} , can be determined as a function of the four quantities u_i , $i = 1, 2, 3$ and β_{12} through application of the constraints:* $\underset{\sim}{A}_1 \cdot \underset{\sim}{A}_1 = \underset{\sim}{A}_2 \cdot \underset{\sim}{A}_2 = 1$ and $\underset{\sim}{A}_1 \times \underset{\sim}{A}_2 = \underset{\sim}{A}_3$. With use of (4.50), these furnish

$$\begin{aligned}
\cos^2 \psi_{11} + \sin^2 \beta_{12} + \sin^2 \beta_{13} &= 1 \quad , \\
\cos^2 \psi_{22} + \sin^2 \beta_{21} + \sin^2 \beta_{23} &= 1 \quad , \\
-\sin \beta_{31} &= \sin \beta_{12} \sin \beta_{23} + \sin \beta_{13} \cos \psi_{22} \quad , \\
-\sin \beta_{32} &= \sin \beta_{21} \sin \beta_{13} + \sin \beta_{23} \cos \psi_{11} \quad , \\
\cos \psi_{33} &= \cos \psi_{11} \cos \psi_{22} - \sin \beta_{12} \sin \beta_{21} \quad .
\end{aligned} \tag{4.51}$$

Equations (4.51) constitute five equations for the five unknowns β_{21} , β_{13} , β_{23} , ψ_{11} , ψ_{22} .

In addition to the assumption $\varphi^2 = \psi_{33}^2 << 1$ of the preceding paragraphs, let us assume that <u>all</u> angles are moderately small (squares

* The remaining constraint $\underset{\sim}{A}_3 \cdot \underset{\sim}{A}_3 = 1$ is already satisfied by (4.38b).

of the angles are small compared to unity). Then, an expansion of all trigonometric terms in (4.5.), and a subsequent neglect of squares of angles in comparison to unity, yields

$$\beta_{13} \approx -\beta_{31} \quad , \quad \beta_{23} \approx -\beta_{32} \quad , \quad \beta_{21} \approx -\beta_{12} \quad ,$$
$$\cos \psi_{11} \approx 1 \quad , \quad \cos \psi_{22} \approx 1 \quad . \tag{4.52}$$

Thus, Eqs. (4.50) can be written

$$\begin{aligned} \underset{\sim}{A}_1 &\approx \underset{\sim}{a}_1 - \beta_{12}\, \underset{\sim}{a}_2 + \beta_{31}\, \underset{\sim}{a}_3 \\ \underset{\sim}{A}_2 &\approx +\beta_{21}\, \underset{\sim}{a}_1 + \underset{\sim}{a}_2 + \beta_{32}\, \underset{\sim}{a}_3 \\ \underset{\sim}{A}_3 &\approx -\beta_{31}\, \underset{\sim}{a}_1 - \beta_{32}\, \underset{\sim}{a}_2 + \underset{\sim}{a}_3 \end{aligned} \tag{4.53}$$

The curvatures $\mathcal{K}_i$ can now be computed in terms of u_i and β_{12} from (4.53) as follows:

$$\begin{aligned} \mathcal{K}_\alpha &= (1+2\epsilon)^{-\frac{1}{2}}\, \underset{\sim}{A}_\alpha \cdot \underset{\sim}{A}_3' \\ \mathcal{K}_3 &= (1+2\epsilon)^{-\frac{1}{2}}\, \underset{\sim}{A}_2 \cdot \underset{\sim}{A}_1' \end{aligned} \tag{4.54a}$$

which implies

$$\begin{aligned} \Delta\mathcal{K}_1 &\approx -\epsilon\, \mathcal{K}_1^{(0)} + \omega_2 \\ \Delta\mathcal{K}_2 &\approx -\epsilon\, \mathcal{K}_2^{(0)} - \omega_1 \\ \alpha &\approx \omega_3 \end{aligned} \tag{4.54b}$$

where

$$-\omega_1 = \beta_{32}' + \mathcal{K}_3^{(0)}\, \beta_{31} - \beta_{12}\, \mathcal{K}_1^{(0)} \quad ,$$

$$- \omega_2 = \beta'_{31} + \beta_{12} \kappa_2^{(0)} - \beta_{32} \kappa_3^{(0)} \quad , \tag{4.54c}$$

$$\omega_3 = \beta'_{12} + \kappa_1^{(0)} \beta_{32} - \kappa_2^{(0)} \beta_{31} \quad .$$

Equations (4.34), (4.48), (4.54) furnish a complete geometrical description of the rod under the restriction that squares of all angles are small compared to unity.

4.4 Stress Resultants and Constitutive Relations

Let the components of the stress tensor σ^{ij} be referred to the coordinates (Y_1, Y_2, Y_3). Since the latter are rectangular cartesian, the position of the indices is immaterial, and we shall simply write σ_{ij}. For a linear elastic, isotropic and homogeneous material, the stress tensor is given in terms of the strain tensor e_{ij} by

$$e_{ij} = \frac{1+\nu}{E}\,\sigma_{ij} - \frac{\nu}{E}\,\sigma_{kk}\,\delta_{ij} \tag{4.55}$$

where E is Young's modulus and ν is Poisson's ratio.

We now introduce an approximation: we assume that the stresses σ_{11} and σ_{22} can be neglected in comparison to σ_{33} in (4.55). As a result, the following relations are obtained:

$$\sigma_{33} \approx E\,e_{33} \quad , \quad \sigma_{3\alpha} = 2G\,e_{3\alpha} \tag{4.56}$$

where $G = E/2(1+\nu)$ is the shear modulus.

Let us now define the quantities N_i, M_i by

$$\begin{aligned} N_i &= \int\!\!\int_G \sigma_{3i}\, d\theta^1\, d\theta^2 \quad , \quad i = 1,2,3 \\ M_1 &= \int\!\!\int_G \theta_2\, \sigma_{33}\, d\theta^1\, d\theta^2 \quad , \\ M_2 &= \int\!\!\int_G -\theta_1\, \sigma_{33}\, d\theta^1\, d\theta^2 \quad , \\ M_3 &= \int\!\!\int_G (\sigma_{32}\,\theta_1 - \sigma_{31}\,\theta_2)\, d\theta^1\, d\theta^2 \quad . \end{aligned} \tag{4.57}$$

According to (4.57), N_i represent resultant forces on the rod cross section, and M_i are first moments of the stress field.

Sutstitution of (4.56) into (4.57), with use of (4.34), furnishes the following "constitutive" relations between. N_3 , M_i , V_α , ϵ , $\Delta\mathcal{K}_\beta$:

$$\begin{aligned} N_3 &= EG\,\epsilon \quad , \\ M_1 &= -\,EI_{22}\,\Delta\mathcal{K}_2 \quad , \\ M_2 &= EI_{11}\,\Delta\mathcal{K}_1 \quad , \\ M_3 &= GJ\,\alpha \quad , \end{aligned} \tag{4.58a}$$

where G = rod cross sectional area,

$$\begin{aligned} I_{\alpha\alpha} &= \int\int_G \theta_\alpha^2\, d\theta^1\, d\theta^2 \quad , \text{ (no sum in } \alpha) \\ J &= \int\int_G \left[\theta_1 \frac{\partial \varphi}{\partial \theta_2} - \theta_2 \frac{\partial \varphi}{\partial \theta_1} + \theta_1^2 + \theta_2^2\right] d\theta^1\, d\theta^2 \quad . \end{aligned} \tag{4.58b}$$

In the derivation of (4.58), the rod cross section was assumed to be symmetric about <u>both</u> principal axes.

It should be noted that the second and third of Eqs. (4.58a) can be written in the alternate form (see 4.54b)

$$M_1 = EI_{22}\,\omega_1 \quad , \quad M_2 = EI_{11}\,\omega_2 \quad . \tag{4.59}$$

This can be seen as follows: If the expressions for $\Delta\mathcal{K}_\alpha$ are substituted into Eq.(4.34) for e_{33} , then the resulting terms $\epsilon\mathcal{K}_\alpha^{(0)}\theta_\alpha$ (no sum on α) can be grouped with ϵ . However, the thin rod assumption implies that $\mathcal{K}_\alpha^{(0)}\theta_\alpha << 1$ (no sum in α), and therefore the latter can be neglected

compared to unity. The result is (4.59).

Finally, let us define external resultant force and moment vectors $\underset{\sim}{f}$, $\underset{\sim}{m}$ in terms of the traction vector $\overset{n}{T}$ on the lateral surface of the cable by

$$\underset{\sim}{f} = \oint_b \overset{n}{\underset{\sim}{T}}\, db \quad , \quad \underset{\sim}{m} = \oint_b (\theta_\alpha \underset{\sim}{A}_\alpha \times \overset{n}{\underset{\sim}{T}})\, db \tag{4.60}$$

where b denotes the boundary of the rod cross section.

4.5 Equilibrium Equations

According to our averaging procedure, an element ds of the cable is subjected to resultant forces and moments as indicated in Fig. 4.3. We now require that these force and moment fields satisfy equilibrium, which yields

$$\partial \underset{\sim}{N}/\partial s + \underset{\sim}{f} = 0 \quad ,$$

$$\partial \underset{\sim}{M}/\partial s + \underset{\sim}{m} + (\underset{\sim}{A}_3 \times \underset{\sim}{N}) = 0 \quad . \tag{4.61}$$

If the vectors $\underset{\sim}{N}$, $\underset{\sim}{M}$, $\underset{\sim}{f}$, $\underset{\sim}{m}$ are decomposed into components N_i, M_i, f_i, m_i along the A_i axes, respectively, Eqs. (4.61) become (with use of (4.16))

$$dN_1/ds - \mathcal{K}_3 N_2 + \mathcal{K}_1 N_3 + f_1 = 0 \quad ,$$

$$dN_2/ds + \mathcal{K}_3 N_1 + \mathcal{K}_2 N_3 + f_2 = 0 \quad , \tag{4.62a}$$

$$dN_3/ds - \mathcal{K}_1 N_1 - \mathcal{K}_2 N_2 + f_3 = 0 \quad ,$$

$$dM_1/ds - \mathcal{K}_3 M_2 + \mathcal{K}_1 M_3 - N_2 + m_1 = 0 \quad , \tag{4.62b}$$

$$dM_2/ds + \mathcal{K}_3 M_1 + \mathcal{K}_2 M_3 + N_1 + m_2 = 0 \quad ,$$

$$dM_3/ds - \mathcal{K}_1 M_1 - \mathcal{K}_2 M_2 + m_3 = 0 \quad .$$

Since

$$d(\,)/ds = (1+2\epsilon)^{-\frac{1}{2}} d(\,)/d\theta^3$$

and $\epsilon << 1$ by assumption, all derivatives with respect to s in (4.17) can be replaced with derivatives with respect to θ^3.

4.6 Summary of Equations

Equations (4.62), (4.58), (4.54b), (4.48) are fourteen equations for the fourteen unknowns: u_i, N_i, M_i, ω_i, β_{21}, ϵ. They are the basic rod differential equations. We summarize them below:

Equilibrium

$$\begin{aligned} &N_1' - \mathcal{K}_3 N_2 + \mathcal{K}_1 N_3 + f_1 = 0 \quad , \\ &N_2' + \mathcal{K}_3 N_1 + \mathcal{K}_2 N_3 + f_2 = 0 \quad , \\ &N_3' - \mathcal{K}_1 N_1 - \mathcal{K}_2 N_2 + f_3 = 0 \quad , \\ &M_1' - \mathcal{K}_3 M_2 + \mathcal{K}_1 M_3 - N_2 + m_1 = 0 \quad , \\ &M_2' + \mathcal{K}_3 M_1 + \mathcal{K}_2 M_3 + N_1 + m_2 = 0 \quad , \\ &M_3' - \mathcal{K}_1 M_1 - \mathcal{K}_2 M_2 + m_3 = 0 \quad . \end{aligned} \tag{4.62}$$

Constitutive

$$\begin{aligned} &N_3 = EA\,\epsilon \quad , \quad M_1 = EI_{22}\,\omega_1 \\ &M_2 = EI_{11}\,\omega_2 \quad , \quad M_3 = GJ\,\omega_3 \quad . \end{aligned} \tag{4.63}$$

Strain ϵ-displ.

$$\epsilon = (u_3' - \mathcal{K}_1^{(0)} u_1 - \mathcal{K}_2^{(0)} u_2) + \left(\frac{\beta_{32}}{2}\right)^2 + \left(\frac{\beta_{31}}{2}\right)^2 \quad . \tag{4.64}$$

Geometric

$$-\omega_1 = \beta_{32}' + \mathcal{K}_3^{(0)} \beta_{31} + \mathcal{K}_1^{(0)} \beta_{21} \quad ,$$

$$-\omega_2 = \beta'_{31} - \kappa_2^{(0)}\beta_{21} - \kappa_3^{(0)}\beta_{32} \quad , \tag{4.65a}$$

$$\omega_3 = \beta'_{21} - \kappa_1^{(0)}\beta_{32} + \kappa_2^{(0)}\beta_{31} \quad ,$$

$$-\beta_{31} = u'_1 - \kappa_3^{(0)}u_2 + \kappa_1^{(0)}u_3 \quad ,$$

$$-\beta_{32} = u'_2 + \kappa_3^{(0)}u_1 + \kappa_2^{(0)}u_3 \quad . \tag{4.65b}$$

4.7 Equations for Rings

Let us now specialize the results of the preceeding sections to rods that are circular rings in the undeformed state. Accordingly, we must set

$$\varkappa_1^{(0)} = -1/r_0 \quad , \quad \varkappa_2^{(0)} = \varkappa_3^{(0)} = 0 \tag{4.66}$$

in Eqs. (4.62), (4.64), (4.65), where r_0 denotes the ring radius in the undeformed configuration. The coordinate system selected is illustrated in Fig.

Prebuckled Configuration

Consider the prebuckled state. Here all quantities are independent of θ_3 (or s_0), and

$$\begin{aligned}
&u_3 = 0 \quad , \quad u_2 = \text{constant} \quad , \quad f_3 = 0 \quad , \\
&N_3 = \text{constant} \quad , \quad \beta_{21} = \text{constant} \quad , \quad \beta_{32} = \beta_{31} = 0 \quad , \\
&\omega_2 = \omega_3 = 0 \quad , \quad \omega_1 = -\varkappa_1^{(0)} \beta_{21} = \beta_{21} r_0 \quad , \\
&\varkappa_2 = 0 \quad , \quad -\varkappa_1^{-1} = r_0 + u_1 \, , \quad \varkappa_3 = 0 \quad , \\
&\epsilon = -\varkappa_1^{(0)} u_1 = u_1/r_0
\end{aligned} \tag{4.67}$$

Equations (4.63) and (4.67) imply that

$$N_3 = \frac{E A u_1}{r_0} \quad , \quad M_1 = \frac{\beta_{21} E I_{22}}{r_0}$$
$$M_2 = M_3 = 0 \quad . \tag{4.68}$$

With use of Eqs. (4.67) and (4.68) the following additional relations are obtained from (4.62):

$$\begin{aligned} &\mathcal{K}_1 M_1 = m_3 = \text{constant} \quad , \\ &N_1 = - m_2 = \text{constant} \quad , \\ &N_2 = - m_1 = \text{constant} \quad , \\ &\mathcal{K}_1 N_3 = - f_1 = \text{constant} \quad , \\ &f_2 = N_1 = 0 \quad . \end{aligned} \tag{4.69}$$

The dependent variables of the prebuckled state can therefore be written in terms of the assumed known functions f_1 , m_1 , m_2 , m_3 as follows:

$$\begin{aligned} &N_3 = f_1 \, r_0 \, (1 + \frac{u_1}{r_0}) \approx f_1 \, r_0 \quad , \\ &u_1 = \frac{N_3 \, r_0}{E \, A} = \frac{r_0^2 \, f_1}{E \, A} \quad , \\ &M_1 = - m_3 \, r_0 \, (1 + \frac{u_1}{r_0}) \approx - m_3 \, r_0 \quad , \\ &\beta_{21} = \frac{r_0 \, M_1}{E \, I_{22}} = - \frac{m_3 \, r_0^2}{E \, I_{22}} \quad , \\ &N_1 = - m_2 \quad , \quad N_2 = - m_1 \quad , \quad M_2 = M_3 = 0 \quad , \\ &u_3 = 0 \quad , \quad u_2 = \text{constant} \quad , \quad \epsilon = u_1 / r_0 \quad , \quad \omega_2 = \omega_3 = 0 \quad , \end{aligned} \tag{4.70}$$

$$\omega_1 = \beta_{21}/r_0 \quad .$$

The loads f_1, m_i and the constant u_2 in (4.70) are determined by proper matching of ring and shell displacements and forces.

Perturbation Equations

The stability analysis of Chapter II requires differential equations describing small ring deformations about the prebuckled configuration. These can be derived by perturbing the prebuckled variables as follows:

$$(u_i, N_i, M_i, \omega_i, \epsilon, \beta_{21}) = (\bar{u}_i, \bar{N}_i, \bar{M}_i, \bar{\omega}_i, \bar{\epsilon}, \bar{\beta}_{21}) + (u_i^*, N_i^*, M_i^*, \omega_i^*, \epsilon^*, \beta_{21}^*) \qquad (4.71)$$

where $(\bar{\ })$ denotes prebuckled state and $(\ )^*$ denote perturbations. Substitution of (4.71) into Eqs. (4.62), (4.63), (4.64), (4.65), with use of (4.70), yields:

Equilibrium

$$\begin{aligned}
&N_1^{*\prime} - \kappa_3^* \bar{N}_2 - N_3^*/r_0 + \kappa_1^* \bar{N}_3 + f_1^* = 0 \quad , \\
&N_2^{*\prime} + \kappa_3^* \bar{N}_1 + \kappa_2^* \bar{N}_3 + f_2^* = 0 \quad , \\
&N_3^{*\prime} + N_1^*/r_0 - \kappa_1^* \bar{N}_1 - \kappa_2^* \bar{N}_2 + f_3^* = 0 \quad , \\
&M_1^{*\prime} - M_3^*/r_0 - N_2^* + m_1^* = 0 \quad , \\
&M_2^{*\prime} + \kappa_3^* \bar{M}_1 + \bar{N}_1 + m_2^* = 0 \quad , \\
&M_3^{*\prime} + M_1^*/r_0 - \kappa_1^* \bar{M}_1 + m_3^* = 0 \quad .
\end{aligned} \qquad (4.72)$$

Constitutive

$$N_3^* = EA\left(u_3^{*\prime} + \frac{u_1^*}{r_0}\right) ,$$

$$M_1^* = EI_{22}\left(u_2^{*\prime\prime} - \frac{\beta_{21}}{r_0}\right) ,$$

$$M_2^* = EI_{11}\left(u_1^{*\prime\prime} - \frac{u_3^{*\prime}}{r_0}\right) \qquad (4.73)$$

$$M_3^* = GJ\left(\beta_{21}^{*\prime} - \frac{u_2^{*\prime}}{r_0}\right) .$$

This completes our formulation of the relevant differential equations governing the reinforcing rods.

REFERENCES TO CHAPTER IV

1. Green, A. E., and Ferna, W., Theoretical Elasticity, Oxford, 1960.

2. McConnell, A. J., Application of Tensor Analysis, Dover, 1937.

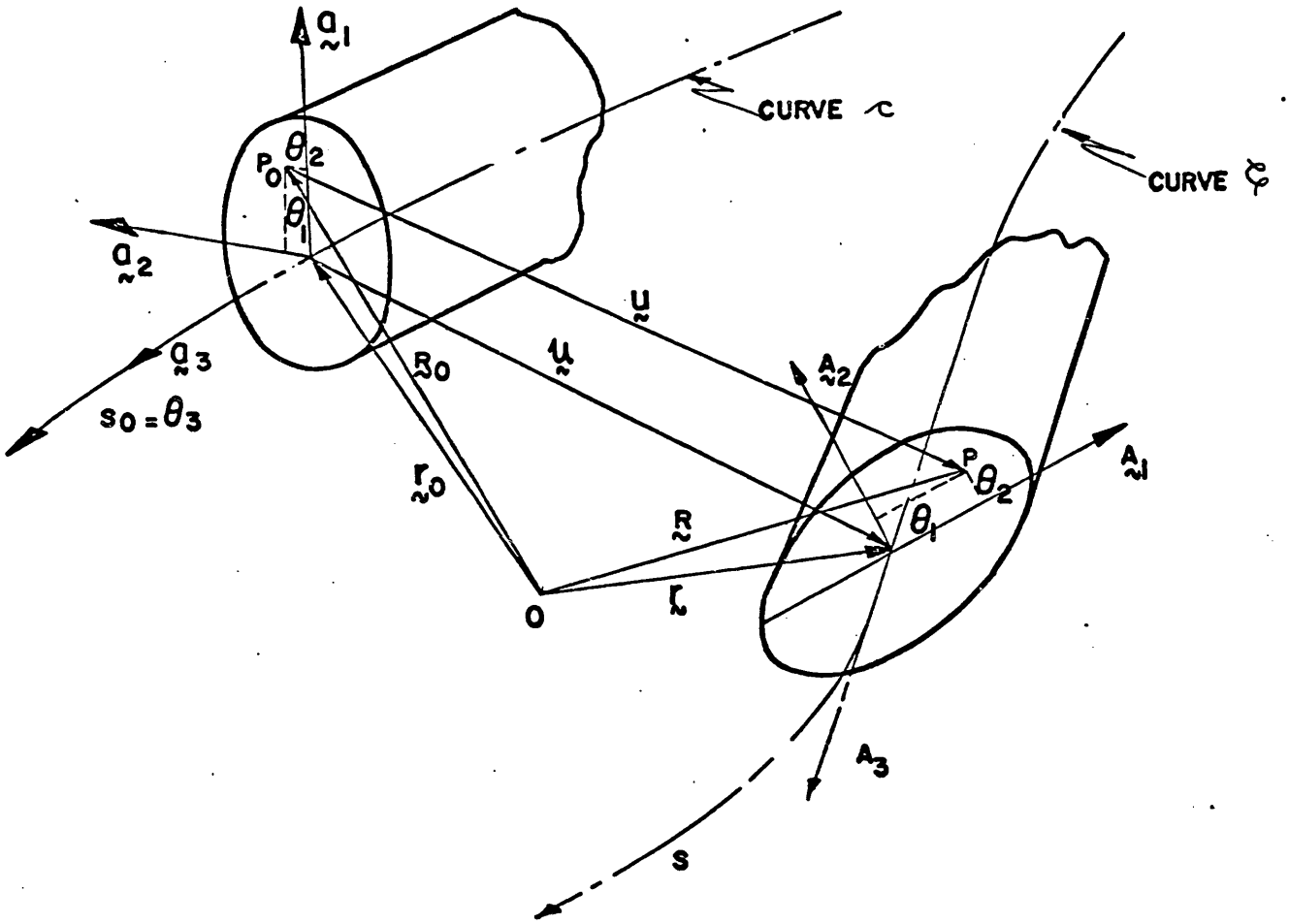

Fig. 4.1

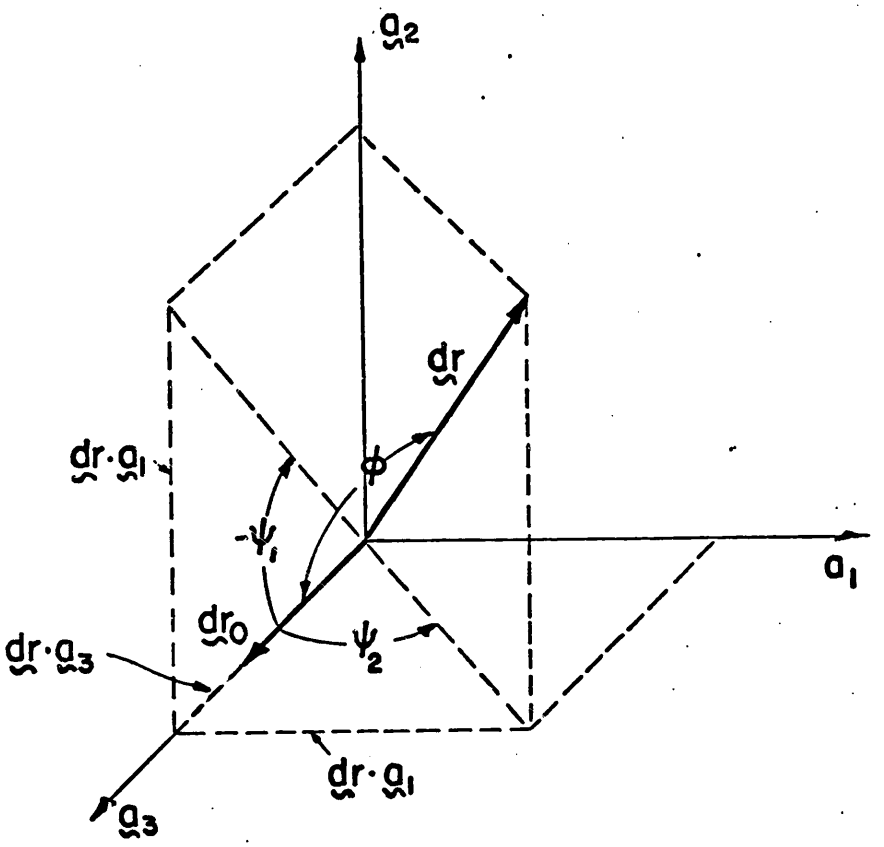

Fig. 4.2

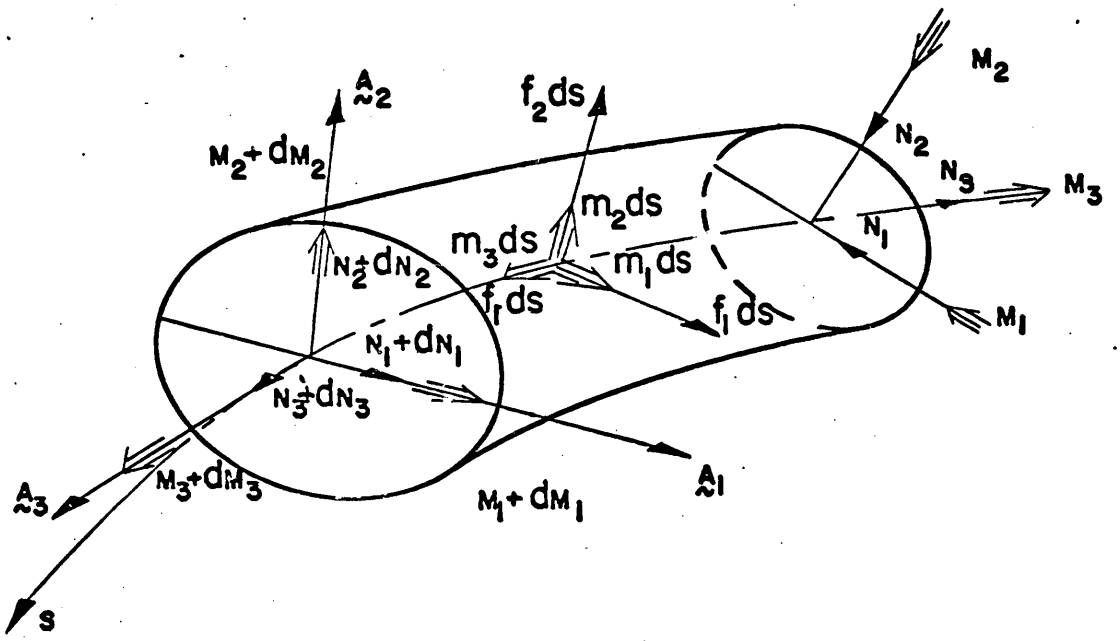
$\underset{\sim}{A}_2$
$f_2 ds$
M_2
$M_2 + dM_2$
N_2
N_3
M_3
$m_2 ds$
$m_3 ds$
N_1
$N_2 + dN_2$
$m_1 ds$
$f_1 ds$
$f_1 ds$
M_1
$N_1 + dN_1$
$N_3 + dN_3$
$\underset{\sim}{A}_3$
$M_3 + dM_3$
$M_1 + dM_1$
$\underset{\sim}{A}_1$
s

Fig. 4.3